Exploring the Structure Activity Relationship of Antiplasmodial Compounds Identified from the MMV Pathogen Box

A thesis submitted in fulfilment of the academic requirements for the

Degree of Master of Science

School of Chemistry and Physics

College of Agriculture, Engineering and Science (Pietermaritzburg)

Sean M. Mafuleka

Supervisor : Dr S. Sithebe (UKZN)

Co-supervisor : Prof. Clinton G. L. Veale (UCT)

February 2024

DECLARATION

I declare that the work presented in this thesis was carried out exclusively by me under the supervision of Dr. S. Sithebe and Prof. Clinton G. L. Veale. It is being submitted for the degree of Master of Science in Chemistry at the University of KwaZulu-Natal, Pietermaritzburg. It has not been submitted before for any degree or examination in any other University.

Signed [redacted]……

Sean Manqoba Mafuleka

I hereby certify that this statement is correct

Signed [redacted] ……..

Dr. S. Sithebe (**Supervisor**)

Signed……..

Prof. Clinton G. L. Veale (**Co-supervisor**)

ABSTRACT

Over 200 million new infections are caused by malaria-causing plasmodium species. This results in over 500 000 annual deaths. These deaths are mostly young children under the age of five years. As there is an emergence of resistance to primitive first-line treatments, there is an increasing need for the development of new targets with novel scaffolds. For such advancements, we have to consider the structure-activity of antiplasmodial compounds.

The Pathogen Box is a concept modelled on the Malaria Box, except the 400 drug-like compounds it contains are a diverse range of compounds which are active against numerous neglected diseases of interest, and is readily accessible. It unpacks 125 compounds of antiplasmodial activity, a lot of which have been identified from phenotypic screening of the GSK Tres Cantos Anti-Malarial Set (TCAMS). Upon request, select researchers around the globe receive a set of compounds from the Pathogen Box to help in the advancements towards neglected disease drug discovery. In turn, the researchers are requested to present, in the public domain, any data they will have generated in their work within two years. This presents an opportunity for a collaborative space for neglected disease drug research.

In this project, compound MMV023227 was found to have promising antiplasmodial activity. We have therefore designed and synthesized some analogues of the hit compound with the purpose of identifying an SAR.

We initiated the synthesis of the designed analogues of compound MMV023227 by successfully synthesising the three imidazole compounds that are 2-(3-bromophenyl)-4,5-dimethyl-1*H*-imidazole (**3.1**), 2-(3-bromophenyl)-4-methyl-1*H*-imidazole (**3.2**), and 2-(3-bromophenyl)-1*H*-imidazole (**3.3**) in yields between 33 – 42 %. We moved these compounds towards the desired final compounds through several stages, but we could only go as far as producing compounds *N*-(2-chlorobenzyl)-3-(1-(ethoxymethyl)-1*H*-imidazol-2-yl)aniline (**3.9**), *N*-(2-chlorobenzyl)-3-(1-(ethoxymethyl)-4-methyl-1*H*-imidazol-2-yl)aniline (**3.10**) and *N*-(2-chlorobenzyl)-3-(1-(ethoxymethyl)-5-methyl-1*H*-imidazol-2-yl)aniline (**3.11**) in yields between 7 – 41 %.

ACKNOWLEDGEMENTS

First and foremost, I would like to give glory to God for granting me the strength to wake up every morning and see this through, challenging as it was. By His grace, I've made it this far.

To my supervisors, Dr Siphamandla Sithebe and Prof Clinton Veale, I am forever grateful to have worked under your supervision. None of this would be possible without you.

To my mentor, Dr Shivani Naidoo, thank you for helping me find my feet when this was all new to me. With your gentle guidance, my faith in taking this on was restored. I will never forget that.

To the technical staff;

- Mr Craig Grimmer, thank you for never getting tired of me coming to pick your brain for your NMR expertise.
- Mr Shaun Ball, thank you for all your assistance with lab supplies and your words of wisdom during our spontaneous conversations.
- Mr Leigh Hunter, thank you for all your assistance with XRD analysis and advice on crystal growing.
- Mrs Caryl Janse van Rensburg, thank you for the HRMS analysis.

To Dr Gciniwe Mathenjwa, Dr Sbonelo Hlengwa and Dr Mncedisi Mazibuko, thank you all so much for your guidance through my writing journey. Your time was very much appreciated.

To my postgraduate colleagues, thank you for being the best support system to me and to one another. Venting to someone who knows firsthand what you're going through is so comforting.

To my entire family and friends, thank you all for always holding me down when it was rough. You all are truly amazing. My partner, Maxine Chetty, thank you for always being there for me in ways I never knew I needed, your love and support is immensely appreciated.

To my sister, Melissa Mafuleka, and my mother, Gloria McKerson, thank you for always understanding when I had to leave you two and go do what I had to do. I love you guys so much.

Lastly, but certainly not least, I would like to extend my gratitude to The Royal Society of Chemistry for the FLAIR scholarship through Prof Veale.

TABLE OF CONTENTS

LIST OF ABBREVIATIONS

AcOH	acetic acid
CDC	Centers for Disease Control and Prevention
COX	cyclooxygenase
DCM	dichloromethane
DMF	*N,N*-dimethylformamide
DMSO	dimethyl sulfoxide
DNDi	Drugs for Neglected Diseases Initiative
DPPF	1,1'-bis(diphenylphosphino)ferrocene
HAT	Human African Trypanosomiasis
HBV	Hepatitis B virus
HCMV	human cytomegalovirus
HMBC	heteronuclear multiple bond correlation
HRMS	high resolution mass spectroscopy
HSQC	heteronuclear single quantum correlation
HTS	high-throughput screening methods
IL-1β	interleukin-1 beta
IL-6	interleukin 6
IR	infrared
LTMP	lithium tetramethylpiperidide
MDR	multidrug-resistant
MeCN	acetonitrile
MMV	Medicines for Malaria Venture

MtGS	Mycobacterium tuberculosis glutamine synthetase
m/z	mass to charge ratio
NAA	nucleic acid amplification
NaH	sodium hydride
NFSI	*N*-Fluorobenzenesulfonimide
NMR	nuclear magnetic resonance
NNRTIs	non-nucleoside reverse transcriptase inhibitors
NOESY	Nuclear Overhauser Effect Spectroscopy
NOx	NADPH oxidase
NSAID	nonsteroidal anti-inflammatory drugs
NTDs	neglected tropical diseases
n-BuLi	n-Butyllithium
PfPKG	*Plasmodium falciparum* cGMP-dependent protein kinase
ppm	parts per million
R_f	retardation factor
r.t.	room temperature
RTDs	rapid diagnostic tests
SAR	structure-activity relationship
SEM	[2-(trimethylsilyl)ethoxy]methyl
SLEV	St. Louis encephalitis virus
SSA	Sub-Saharan Africa
Tb	tuberculosis
TCAMS	GSK Tres Cantos Anti-Malarial Set

TEA	triethylamine
TFA	trifluoroacetic acid
THF	tetrahydrofuran
TLC	thin layer chromatography
TMP	2,2,6,6-tetramethylpiperidine
TNF-α	tumor necrosis factor alpha
UV	ultraviolet
WHO	World Health Organisation

LIST OF SCHEMES

LIST OF FIGURES

LIST OF TABLES

1. CHAPTER ONE: INTRODUCTION

1.1 General Background: Malaria

Malaria, a zoonotic haemoparasitic disease spread by mosquitoes which continues to be a major cause of morbidity and mortality in many parts of Sub-Saharan Africa (SSA), primarily affecting children younger than five years of age.[1] It is reported that over 200 million new infections are caused by malaria-causing plasmodium species annually, resulting in over 500 000 annual deaths.[2] In the face of all efforts that have been directed towards protecting and educating people about malaria infection, about 93 percent of global malaria deaths in 2020 were in the SSA region.[3] The prevalence of malarial transmission has been significantly decreased by a number of orthogonal techniques such as insecticide-treated mosquito nets and indoor residual spraying.[2] However, these developments are continuously hampered by the devastating rise of resistance to first-line chemotherapy.[4]

The main cause of malaria are protozoan parasites of the *Plasmodium* genus.[5] These parasites that infect humans and other vertebrates are limited to five, namely *P. falciparum, P. vivax, P. malariae, P. ovale and P. knowlesi.*[5, 6] However, human infections are predominantly due to *Plasmodium falciparum* in the WHO regions of Africa, South-East Asia, Western Pacific and Eastern Mediterranean and *Plasmodium vivax*, in the WHO Regions of the Americas.[7]

A number of parasitic infections, including malaria, tend to be associated with environments more likely to experience wars and migration, poor sanitary conditions, poor education and poor animal disease control.[8] The prevalence of malaria in SSA, along with the increase in resistance to first-line treatment, encourages the quest for the discovery of potential targets with anti-plasmodial activity.

1.2 The life cycle of the parasite

The life cycle of the plasmodium parasite is complex with two reproductive processes taking place. There is an asexual reproductive process which takes place in the human host, and a sexual reproductive process which takes place in the vector. The life cycle has multiple stages within both the vector and the host. As illustrated in **Figure 1.1**, the cycle begins with the mosquito (vector) injecting sporozoites into the human (host) during a blood meal. Within 30-60 min of injection, the sporozoites then traverse through the bloodstream to the liver where they infect and rupture the hepatocyte. The parasite then replicates inside the hepatocyte, producing multiple merozoites. These merozoites are then released when the hepatocyte bursts and go on to infect the erythrocytes. Here, the merozoites will mature and replicate within the erythrocytes, releasing more merozoites as they depart. It is at this stage when symptoms of infections begin to show. Some merozoites differentiate into sexual forms (male and female) known as gametocytes which will then be absorbed by the *Anopheles* mosquito during the next bloodmeal. The gametocytes further differentiate in the mosquito into microgametes and macrogametes, after which a zygote will be produced as a result of fertilization. This zygote matures to an ookinete and crosses the stomach wall of the mosquito and becomes a round oocyst. The sporozoite-filled oocyst then bursts, releasing these sporozoites to migrate to salivary glands of the mosquito, completing the life cycle. These sporozoites are ready to infect the next human host during the *Anopheles* mosquito's next blood meal.[9-11]

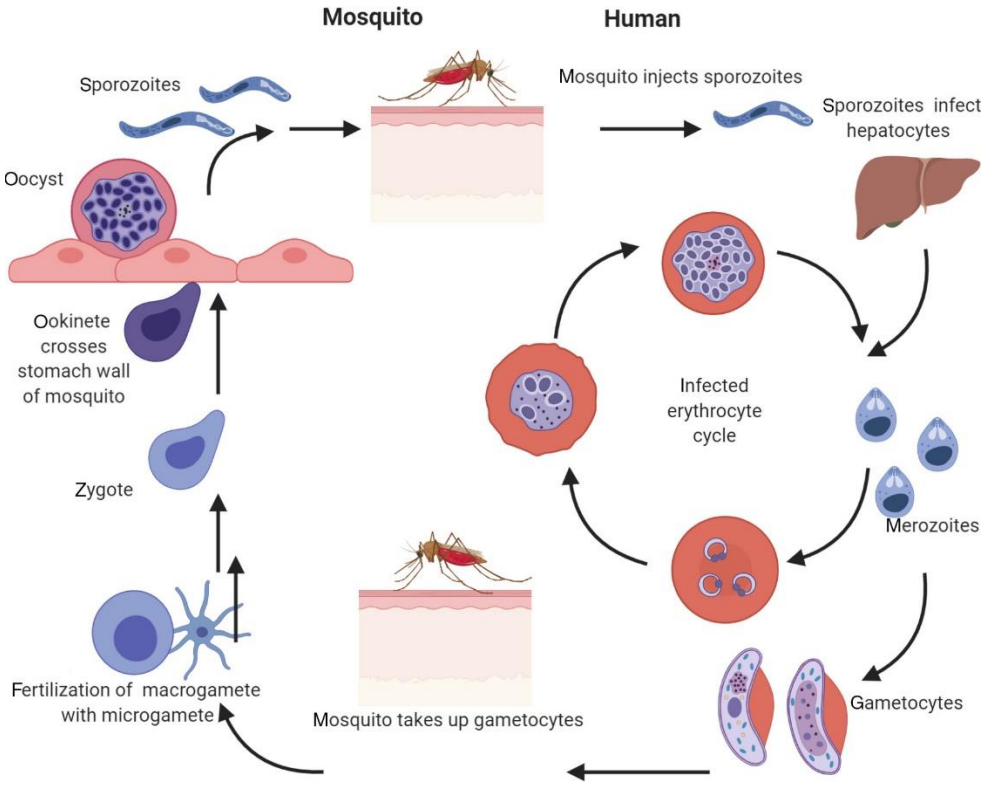

Figure 1.1: Life cycle of the *Plasmodium* parasite.[9]

1.3 Malaria diagnosis

Replacing aging antimalarial drugs with costly novel alternatives over the years has resulted in a gap in the effective management of malaria. This gap reflects a rising demand for accurate and reliable disease diagnosis that traditional microscopy techniques are unable to meet.[12] Early diagnosis may regulate the spread of malaria infection as it serves as the foundation for an early malaria treatment strategy.[13]

Several techniques may be regarded as accurate and reliable for diagnosing malaria, but microscopic examination remains the benchmark of laboratory confirmation of *Plasmodium* species. According to the CDC (Centers for Disease Control and Prevention)[14], the microscopic examination of a blood smear of a patient's blood remains by far the gold standard for the

confirmation of malaria parasites.[14] However, other methods such as antigen-based rapid diagnostic tests (RDTs) and nucleic acid amplification (NAA) tests can be used for the detection of antigens possibly derived from the malaria parasites. These techniques should be used in instances where microscopic diagnosis is not possible as they come at the cost of compromised quality results.[14, 15] Some complications experienced with RDTs are false-positive and false-negative results being captured.[16, 17] Any future advances in malaria diagnosis technologies should aim to surpass the exceptional sensitivity of known NAA methods.[15]

1.4 Phenotypic malaria drug discovery

With the emergence of resistance to primitive first-line treatments, there has been an increasing need to develop novel scaffolds to fill the antimalarial drug-discovery pipeline. The Medicines for Malaria Venture (MMV) along with the Drugs for Neglected Diseases Initiative (DNDi) has played a key role in coordinating these establishments.[18] At this stage, the pharmaceutical industry has relied more on two main high-throughput screening methods (HTS). Phenotypic screening methods look for changes that result from whole cells being exposed to prospective drug candidates. Contrarily, target-based screens pertain the screening of a collective of compounds against a protein in order to enhance their selectivity, potency against the enzyme, pharmacokinetic properties, and their cellular activity.[18, 19]

Phenotypic screens allow for the identification of drugs that show activity against the whole cell. This means that these screens concurrently address some concerns relating to cell uptake and cell efflux, making them a staple of HTS methods.[18, 20] Amongst other key advantages, most importantly, phenotypic screens do not require previous knowledge of the drug target for screen execution.[19] Phenotypic approaches have played a major role in neglected disease drug discovery, more specifically in the fields of malaria and trypanosomiasis (HAT), where notable successes have been reported in literature.[18, 21, 22] Antimalarial hit MMV390048 was studied by

Paquet *et al.*[23] and was found to have inhibitory activity against all life cycle stages of *Plasmodium* species, except for liver hypnozoites in their late stages.[23] These findings encouraged further development of this compound.[23] In the malaria field, MMV have numerous compounds discovered through phenotypic screening undergoing their preclinical and clinical trials. A study conducted by Nwaka *et al.*[24] expands on some *Plasmodium falciparum*-protein farnesyltransferase inhibitors emerging from the MMV catalogue. These candidates are now in their preclinical trials for efficacy *via in*-vivo animal work and are also studied for their adverse effects.[24] Current studies are aimed at understanding these compounds' mode of action and identifying their molecular targets.[18]

1.5 The MMV Pathogen Box

The most common infections among people in sub-Saharan Africa are neglected tropical diseases (NTDs), which account for hundreds of millions of cases worldwide and have an unbreakable link to extreme poverty.[25, 26] These regions also have high-prevalence of malaria, HIV/AIDS and tuberculosis (Tb).[26] Clinical records indicate that these NTD infections tend to increase a patient's susceptibility to HIV/AIDS, malaria or Tb, or perhaps worsen the course for a patient who is already infected by one of these diseases.[27] The need to fill the drug-discovery pipeline for controlling these diseases is undoubtedly a pressing matter.

The Pathogen Box (**Figure 1.2**) is a concept modelled on the Malaria Box, except that the 400 drug-like compounds it contains are a diverse range of compounds which are active against numerous neglected diseases of interest. This library shows great potential as a tool to provide means for the development of new chemotherapeutics for these neglected diseases. Numerous drug discovery programmes have started using this tool as a basis of remodeling promising scaffolds to produce new targets. [28-31]

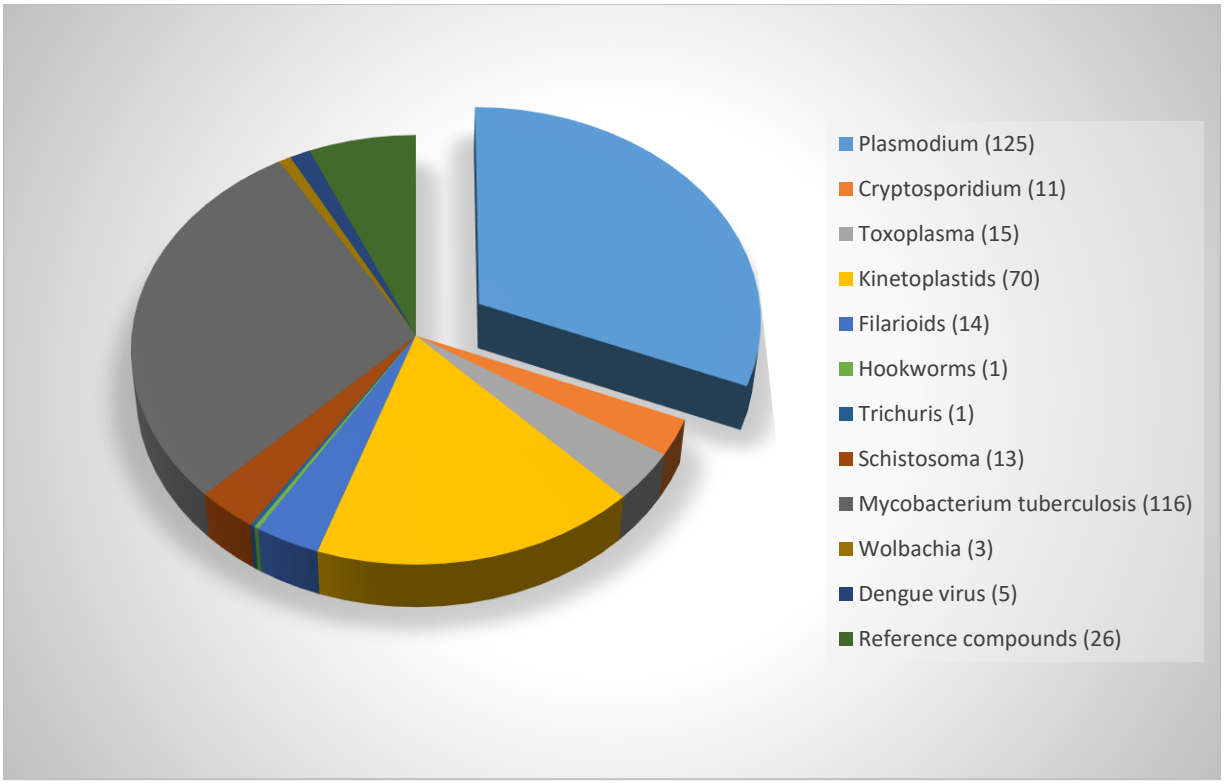

Figure 1.2: The MMV Pathogen Box containing 400 drug-like compounds with confirmed activity against several key pathogens.[32]

The MMV Pathogen Box has had some major successes in the fight against the neglected diseases it was intended for. This library has a number of compounds that have been identified as hits which are in their preclinical stages. In 2022, the structure-activity relationship studies of hit compound MMV675968 revealed novel *Trypanosoma brucei* inhibitors.[33] The two promising analogues emerging from this study were found to have potent antitrypanosomal activity and to be highly selective towards Vero cells.[33]

This library unpacks 125 compounds of antiplasmodial activity, a lot of which have been identified from phenotypic screening of the GSK Tres Cantos Anti-Malarial Set (TCAMS). Determining the Structure–Activity Relationships (SAR) of a chemical scaffold is one of the most important steps in the process of discovering novel drugs. This step is then followed by structural modifications in order to enhance some of the biological activities at a specified target. Hit

compound MMV023227 is one of the compounds that were identified from the MMV Pathogen Box. Because of its promising antiplasmodial activity, some analogues were designed with the purpose of identifying its SAR.

2. CHAPTER TWO: THE IMIDAZOLE MOIETY IN DRUG DISCOVERY

2.1 Imidazoles in drug discovery

Heterocyclic moieties are of high importance to mankind as they play a massive role in biological sciences, chemical sciences, and material sciences for nonlinear optical applications and the synthesis of catalysts.[34-36] Imidazoles and benzimidazoles, are two such nitrogen-containing heterocycles, whose electron-rich environment and special structural features render them particularly important heterocycles in pharmaceutical drug discovery.[37] Drugs containing these moieties tend to bind to a wide range of therapeutic targets and as a result, tend to exhibit a diverse range of bioactivities.[38]

Imidazole is a planar, five-membered heterocyclic molecule consisting of two nitrogen atoms at the first and third positions and three in-ring carbon atoms (**Fig 2.1**). The first person to successfully synthesise imidazole **1** (**Fig. 2.1**) was Debus in 1858, isolating it from a three-component reaction consisting of dicarbonyl compounds, aldehydes, and ammonia or its salts (**Scheme 2.1**).[39, 40] This method is still very much in use in the preparation of five-membered heterocyclic molecules.

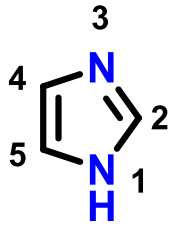

Figure 2.1: General structure of the imidazole scaffold.

The work reported by Debus in 1858[40] was further developed by Radziszewski in 1882[41] and later modified by Weidenhagen in 1935[42]. The reaction is the condensation of an α-dicarbonyl compound, an aldehyde and two equivalents of ammonia with an alcohol as the solvent[40, 41] (**Scheme 2.1**). As seen in **Scheme 2.1**, the reaction occurs in two steps where in the first step, the α-dicarbonyl condenses with the two molecules of ammonia *via* the carbonyl groups resulting in a diimine. In the second step, the diimine condenses with the aldehyde to form the imidazole ring. A detailed mechanistic scheme is shown in **Scheme 2.2.**

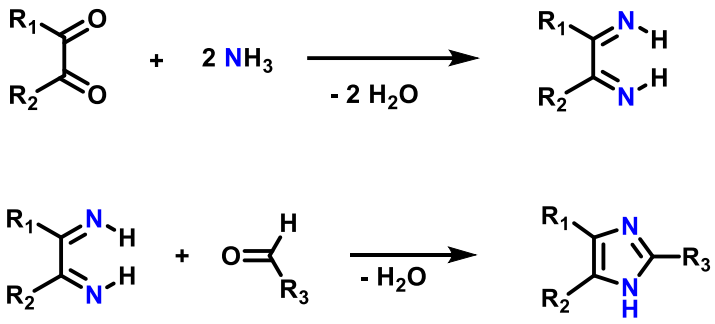

Scheme 2.1: The Debus–Radziszewski imidazole synthesis.

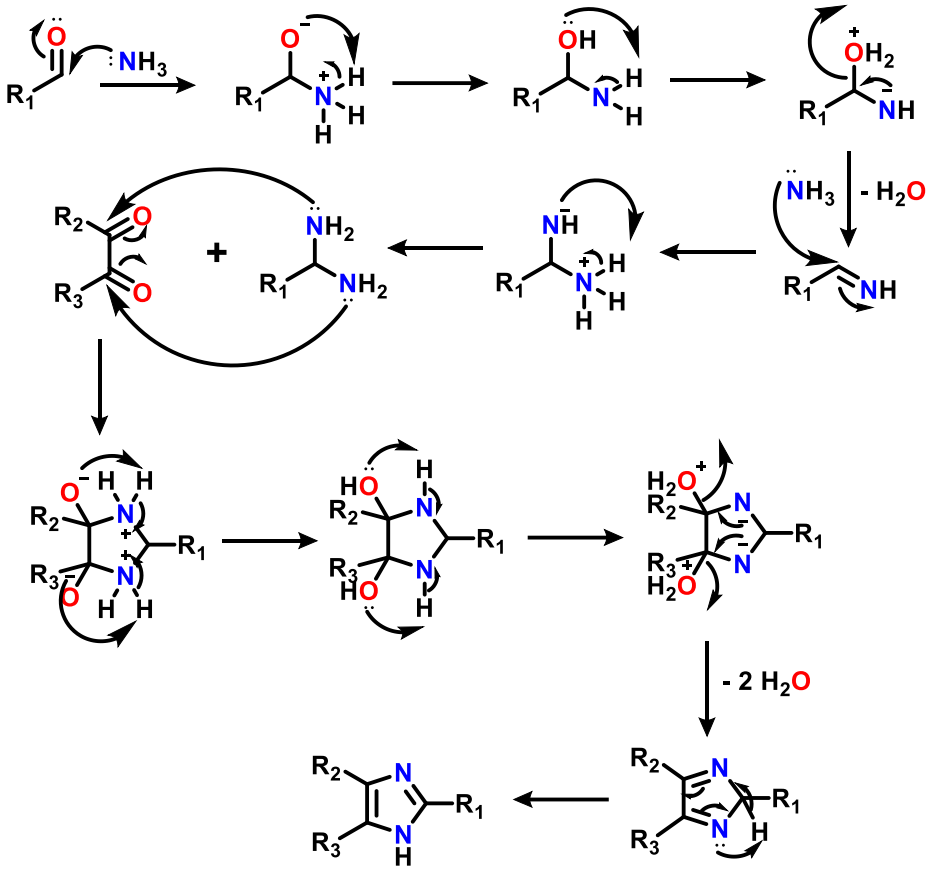

Scheme 2.2: Proposed mechanism for the formation of 2,4,5-trisubstituted imidazoles.

The imidazole nucleus and its derivates are constituents of a great range of natural products such as the amino-acid histidine, histamine, biotin, cyclooroidin, pilocarpine, agelastatin, naamidine A, to name but a few (**Fig 2.2**).[38, 43] This scaffold has been explored for developing therapeutic molecules with possible pharmaceutical or biological interests.[37]

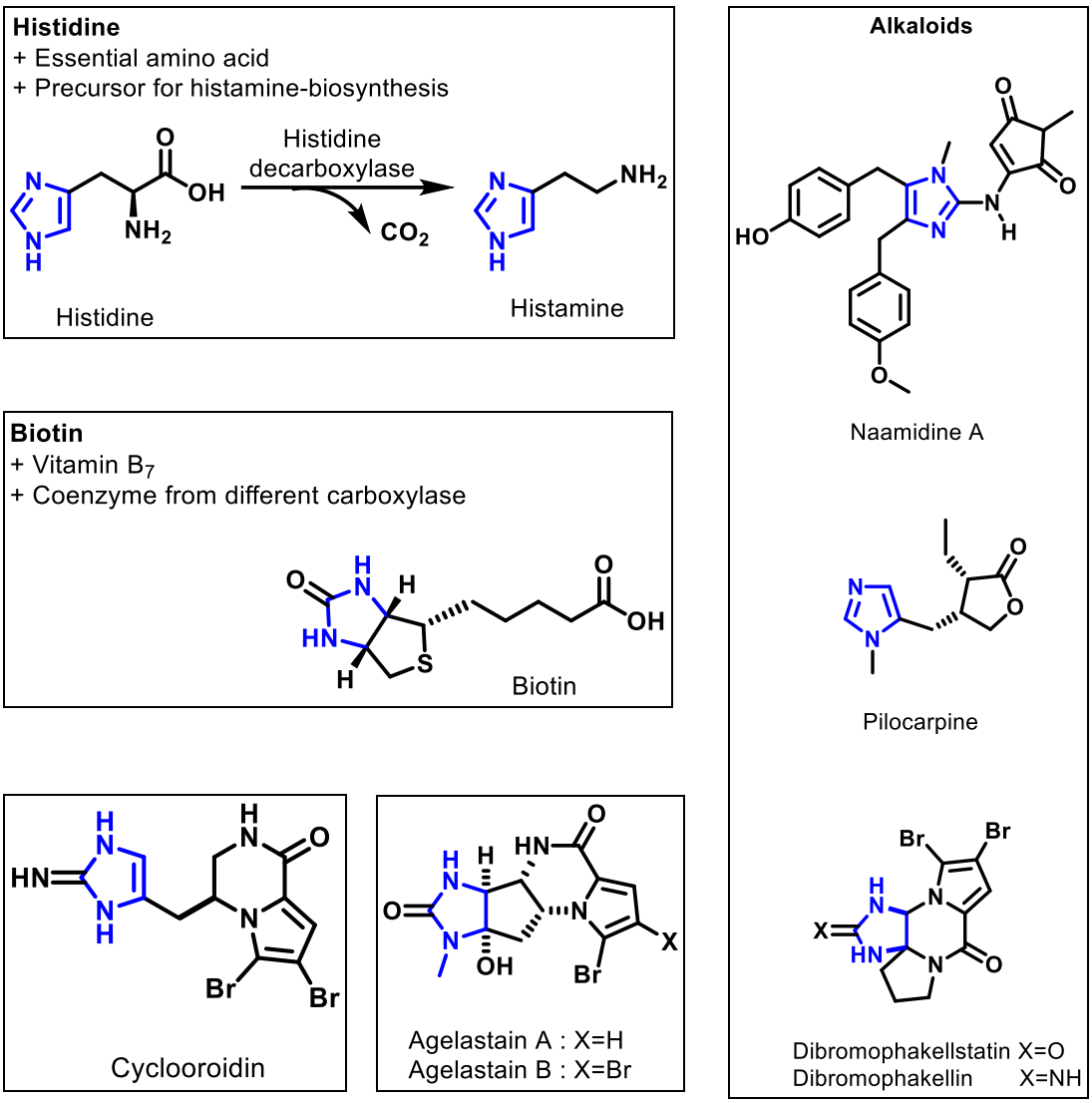

Figure 2.2: Natural products containing the imidazole derived scaffold.

2.2 Biological activity of imidazole-based compounds

Imidazole continues to be explored in pharmaceutical research due to its bioactivity against numerous diseases.[44] The imidazole scaffold is present in the structure of substances with antibacterial, anti-inflammatory, antiviral, anticancer, antitubercular and antimalarial activities,

among other biological activities (**Fig 2.3**). Metronidazole, ketoconazole and omeprazole are some of the most commonly known drugs containing the imidazole scaffold.[45-47] To date, there is a wide range of both natural and synthetic imidazole-containing molecules of biological activity.[44]

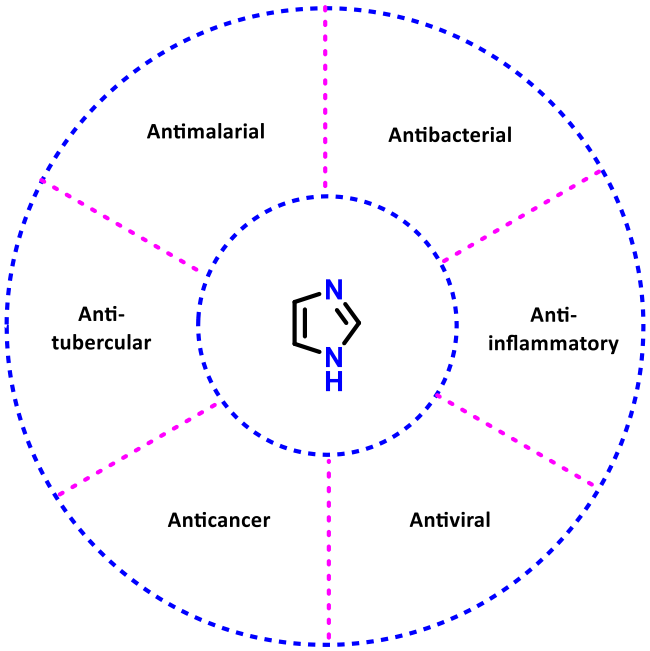

Figure 2.3: Biological profile of imidazole derivatives.

2.2.1 Antibacterial activity

One of the most significant advances in medicine over the past century has been the development of antibacterial drugs to treat various infections.[48-52] The widely recognised nitroimidazole drugs metronidazole (**2.1a**), secnidazole (**2.1b**), ornidazole (**2.1c**), tinidazole (**2.1d**), and nimorazole (**2.1e**) are used extensively in clinical practice to treat infections brought on by anaerobic bacteria and protozoa.

Vijesh *et al*. investigated the *in vitro* antibacterial activity of synthesised compounds **2.2a-d** and **2.3a-j**. The bacteria *Staphylococcus aureus*, *Escherichia coli*, *Bacillus subtilis*, *Clostridium perfringens*, *Salmonella typhimvrium*, and *Pseudomonas aeruginosa* were used to investigate their activity. The antibacterial screens showed that some of these compounds were highly active against numerous tested microbial strains. Compound **2.2c** reflected excellent inhibition against *C. perfringens* and *P. aeruginosa,* surpassing standard drug streptomycin.[53]

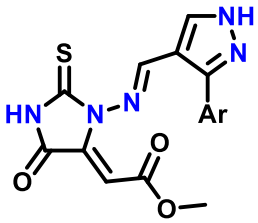

2.2a-d

	Ar
2.2a	2,4-Dichlorophenyl
2.2b	2,5-Dichlorothiophene
2.2c	4-SCH_3-C_6H_4
2.2d	4-CH_3-C_6H_4

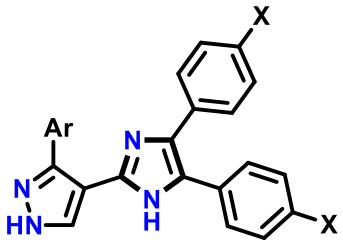

2.3a-j

	Ar	X
2.3a	4-SCH_3-C_6H_4	H
2.3b	2,4-Dichlorophenyl	H
2.3c	Biphenyl	H
2.3d	4-$CH_3C_6H_4$	H
2.3e	2,5-Dichlorothiophene	H
2.3f	4-SCH_3-C_6H_4	Br
2.3g	2,4-Dichlorophenyl	Br
2.3h	Biphenyl	Br
2.3i	4-CH_3-C_6H_4	Br
2.3h	2,5-Dichlorothiophene	Br

A series of 2-substituted-4,5-diphenyl-N-alkyl imidazole derivatives synthesised by Jain *et al*. were evaluated for their antibacterial activities. These compounds were evaluated for their activity against *E. coli, B. subtilis* and *S. aureus*. Only two (**2.4a** and **2.4b**) out of the five compounds (**2.4a-e**) reflected some sort of activity, but none had an activity that compares to that of the standard.[54]

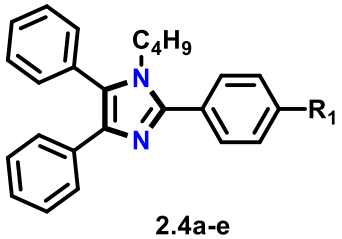

2.4a-e

	R_1
a	*p*-NO_2
b	*m*-NO_2
c	*p*-Cl
d	*o*-Cl
e	*m*-Br

Padmavathi *et al*. synthesised a series of amido-linked imidazole derivatives and screened them for their antibacterial activity. Two of these compounds (**2.5c** and **2.7c**) were highly active against *Pseudomonas aeruginosa*. The activity of these two compounds (**2.5c** and **2.7c**) particularly against *P. chrysogenum* was impressively high; it almost matched that of Ketoconazole, the standard drug. Amongst the bis heterocycles (**2.6** and **2.7**), aromatised bis heterocycle **2.7** demonstrated high efficiency compared to its non-aromatised bis heterocycle **2.6** counterpart. Of all the tested compounds, only one compound was found to be highly active against *B. subtilis*, and that was the chlorosubstituted imidazolyl cinnamamide **2.5c**.[55]

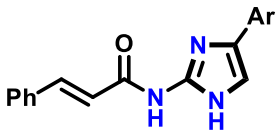

2.5a-c

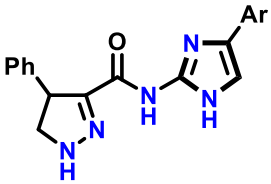

2.6a-c

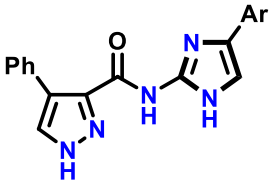

2.7a-c

	Ar
a	Ph
b	4-Me.Ph
c	4-Cl.Ph

Sharma *et al*. synthesised a series of 2-(substituted phenyl)-1H-imidazole and (substituted phenyl)-[2-(substituted phenyl)-imidazol-1-yl]-methanone derivatives for *in vitro* antimicrobial activity screening against Gram-positive bacteria (*B. subtilis* and *S. aureus*), Gram-negative bacterium (*E. coli*) and fungal strains (*A. niger* and *C. albicans*) using norfloxacin as a standard for antibacterial activity and fluconazole as the antifungal activity standard. The results showed that three compounds (**2.8**, **2.9** and **2.10**) had the highest antibacterial activity, which matched that of norfloxacin, the standard drug.[56]

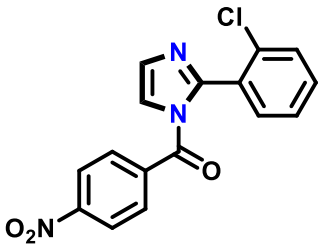

2.8

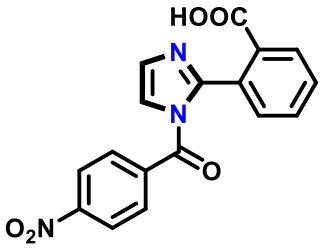

2.9

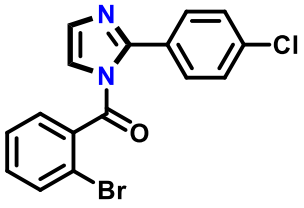

2.10

Brahmbhatt *et al*. synthesized a series of 3-(2,4-disubstituted phenyl)-1-(4-substituted phenyl)-4-(4,5-diphenyl-1H-imidazol-2-yl)-1H-pyrazole derivatives for antibacterial activity screening. Their antibacterial activity was tested against *E. coli, B. subtilis, P. aeruginosa* and *S. aureus* using ampicillin, chloramphenicol and amikacin sulfate as reference drugs. Compound **2.11h** proved to be the most potent among the rest. [57]

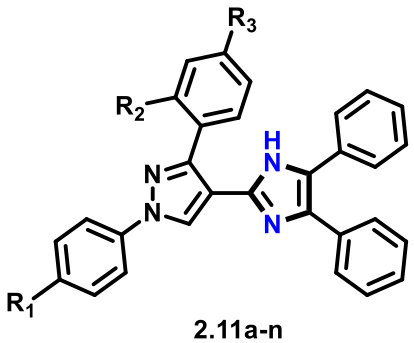

2.11a-n

	R_1	R_2	R_3		R_1	R_2	R_3
a	CH_3	H	CH_3	h	CH_3	Br	H
b	CH_3	H	OCH_3	i	CH_3	H	H
c	CH_3	H	F	j	Cl	H	CH_3
d	CH_3	H	Cl	k	Cl	H	Cl
e	CH_3	H	Br	l	Cl	H	Br
f	CH_3	H	I	m	Cl	H	NO_2
g	CH_3	H	NO_2	n	Cl	Br	F

2.2.2 Anti-inflammatory activity

The most common response to a disease or harmful stimuli is inflammation. Pro-inflammatory chemicals are released as a result of this response; these chemicals increase blood vessel permeability and cause fluid to leak into the tissues, causing pain, swelling, redness, and (in some instances) loss of function.[58] The most widely used inflammation treatments are nonsteroidal anti-inflammatory drugs (NSAID) and corticosteroids.[59] However, the use of NSAIDs usually results in some undesirable side effects.[60] For that reason, the pharmaceutical industry is investigating the imidazole moiety for its anti-inflammatory potential, and current reports reflect promising results.

Husain *et al*. synthesised two series of imidazole analogues 2,4-disubstituted-1*H*-imidazoles (**2.12a-m**) and 1,2,4-trisubstituted-1*H*-imidazoles (**2.13a-m**) with the hopes of discovering dual-acting agents, i.e. antifungal and anti-inflammatory agents. Six of these compounds (**2.12h, 2.12l, 2.13g, 2.13h, 2.13l, 2.13m**) displayed good anti-inflammatory action. The same compounds were screened for analgesic activity, exhibiting considerable protection against saline-induced writhing test. Two compounds (**2.13h** and **2.13l**) showed appreciable inhibition for antifungal activity.[61]

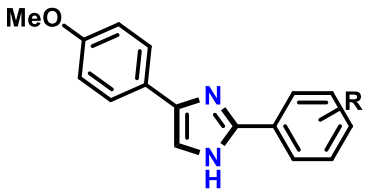

2.12a-m

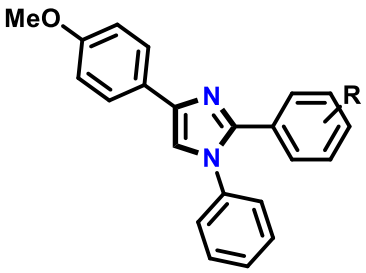

2.13a-m

a: R=H, **b:** R=2-Cl, **c:** R=3-Cl, **d:** R=4-Cl,
e: R=4-F, **f:** R=2-NO_2, **g:** R=3-NO_2,
h: R=4-NO_2, **i:** R=2-OH, **j:** R=3-OH,
k: R=4-OH, **l:** R=4-OCH_3,
m: R=3-OCH_3; 4-OH

A series of 1-(2-((18Z)-4-substituted benzylidene-4,5-dihydro-5-oxo-2-phenylimidazol-1-yl)ethyl)-1,2-dihydro-4methyl-2-oxoquinolin-7-yl imidazolo quinoline analogues synthesised by Raghavendra *et al*. were screened for their anti-inflammatory and ulecerogenicity action using *ibuprofen* as the standard drug. Compound **2.14** was found to have considerable inflammation inhibition compared to the control.[62]

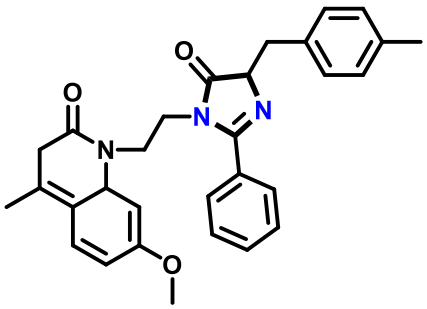

2.14

Achar *et al*. synthesised a library of 2-methylaminibenzimidazole derivatives and screened them for anti-inflammatory and analgesic activity. Compound **2.15** exhibited analgesic activity that compared to that of the standard, nimesulide.[63]

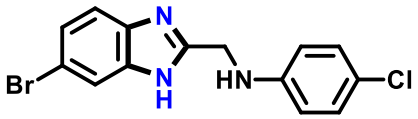

2.15

Shankar *et al*. synthesised and screened ten imidazole derivatives for their anti-inflammatory activity using cyclooxygenase-1 (COX-1) and cyclooxygenase-2 (COX-2) enzymes *in vitro*. Compound **2.16** exhibited high COX-2 inhibition potency (78.68%), surpassing the standard drug ibuprofen (29.67%). Furthermore, the findings from *in vitro* experiments translated very well to the *in-vivo* setting, demonstrating that compound **2.16** had good anti-inflammatory activity against the COX-2 enzyme. Specifically, it displayed an inhibition percentage of 54.314, surpassing that of ibuprofen (52.986).[64]

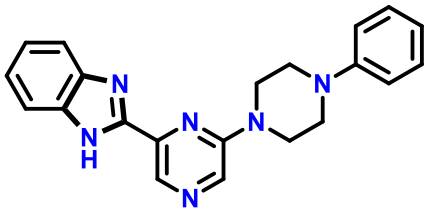

2.16

Katikireddy *et al*. synthesised and screened five imidazole derivatives for their anti-inflammatory action *in vivo*. The results for the selected compounds compared closely to the standard drug Indomethacine. Compound **2.17** had a percentage inhibition of 90.30 at 6 hours, proving to be the most effective anti-inflammatory candidate. This potent anti-inflammatory activity of

compound **2.17** was attributed to its dichloride substitution at *ortho* and *para* positions. It was also revealed in docking studies that compound **2.17** binded excellently to the active site of enzyme cyclooxygenase-2 (COX-2).[65]

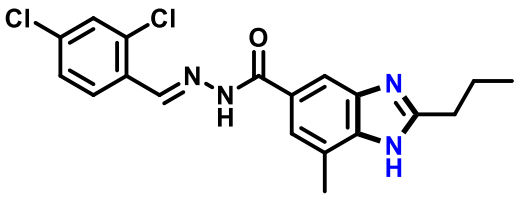

2.17

Eight novel imidazole derivatives were synthesised and screened for anti-inflammatory activity by Nascimento *et al*., employing *in vitro* and *in vivo* techniques. The data showed that all eight compounds performed fairly well, but compound **2.18** stood out. Compound **2.18** displayed high inhibition potency in the production of TNF-α, NOx, IL-1β, and IL-6.[66]

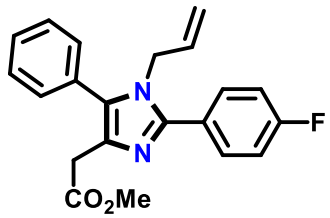

2.18

Shantharam *et al*. performed *in vitro* studies to evaluate the anti-inflammatory activity of some compounds they synthesised using aspirin and indomethacin as standard drugs. Compounds **2.19a-h** exhibited excellent anti-inflammatory activity, significantly surpassing the standards aspirin and Indomethacin. The results indicated that compounds with electron-withdrawing groups such as Cl, F, NO_2, and Br (**2.19a-h**) exhibited significant efficacy as anti-inflammatory drugs instead of those consisting of electron-donating (OH and OCH_3) groups.[67]

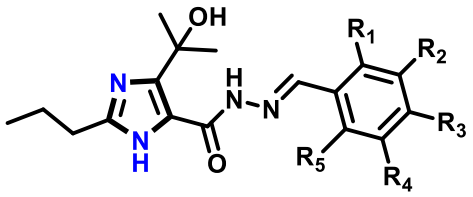

2.19a-h

	R_1	R_2	R_3	R_4	R_5
a	H	H	Cl	H	H
b	H	H	NO_2	H	H
c	H	H	F	H	H
d	H	H	Br	H	H
e	Cl	H	Cl	H	H
f	F	H	F	H	H
g	NO_2	H	NO_2	H	H
h	Cl	H	H	H	F

2.2.3 Antiviral activity

Viral infections are obligate parasites which commonly cause (but not limited to) respiratory and digestive illnesses. These parasites can also infect most other parts of their host's body, threatening the life thereof.[68] An antiviral drug's intended mode of action is to inhibit viral replication in the host's body. Imidazole-based antivirals are under development for the treatment of various common viruses such as human immunodeficiency virus (HIV), cytomegalovirus (HCMV), hepatitis B and C, and human herpes simplex virus.[37]

In the search for new antiviral compounds, a series of (substituted phenyl)-[2-(substituted phenyl)-imidazol-1-yl]-methanone derivatives synthesised by Sharma *et al*. underwent antiviral screening against a series of viral strains. Compounds **2.20** and **2.21** emerged as the only compounds with potential as antiviral agents and for the development of new drugs with activity against pox viruses.[56]

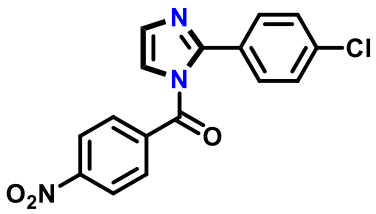

2.20

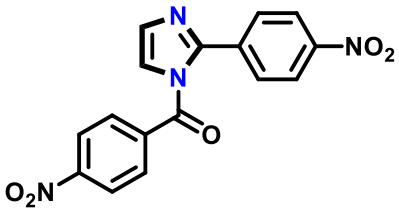

2.21

From a series of 2-(1-aryl-1H-imidazol-2-ylthio)acetamide [imidazole thioacetanilide (ITA)] derivatives synthesised and evaluated by Zhan *et al*. for human immunodeficiency virus type-1 (HIV-1) inhibition, two compounds (**2.22b** and **2.22e**) proved to be the best candidates as HIV-1 inhibitors in comparison to standard drugs nevirapine and delavirdine. A few other compounds from the series (**2.22a**, **2.22c**, **2.22d** and **2.23**) also demonstrated higher anti-HIV-1 potency than lead compound derivative **L1**. This suggested that the imidazole moiety can serve as a suitable isosteric substitute for the tetrazole, triazole, or 1,2,3-thiadiazole groups present in the lead compounds.[69]

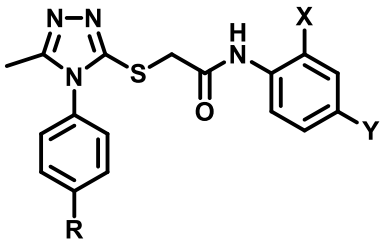

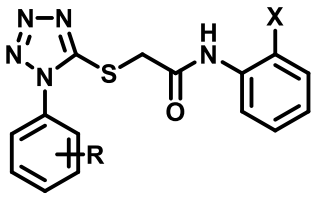

L1 R= CH_3, X=Y= H
L2 R= H, X= Br, Y= CH_3

L3 R= 2,4,6-TriMe, X= Cl
L4 R-Ph= 1-naphthalene, X= NO_2

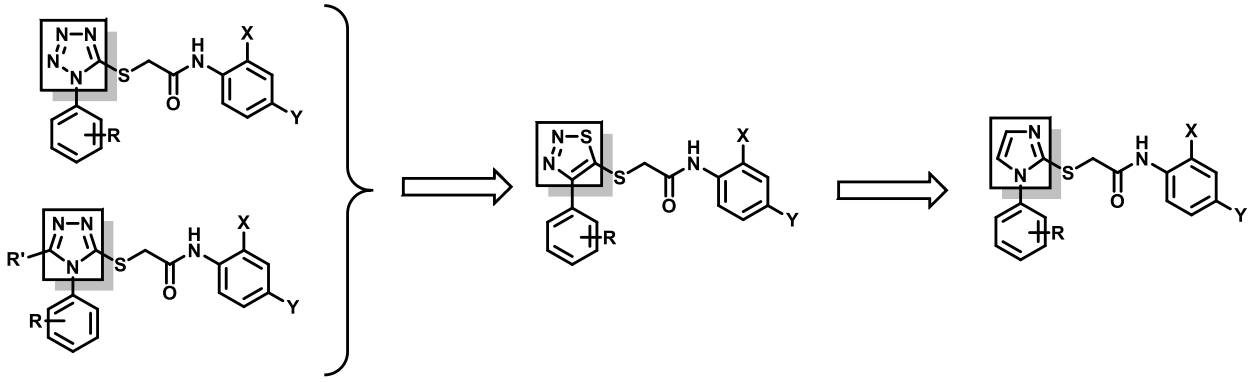

Original leads | Previously reported NNRTIs by authors | Newly designed ITA scaffold

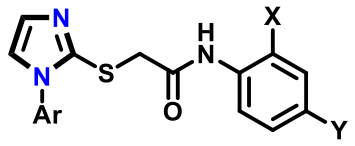

2.22a-e, 2.23

	Ar	X	Y
2.22a	Naphthalen-1-yl	F	H
2.22b	**Naphthalen-1-yl**	**Cl**	**H**
2.22c	Naphthalen-1-yl	Br	H
2.22d	Naphthalen-1-yl	Br	Me
2.22e	**Naphthalen-1-yl**	**NO_2**	**H**
2.23	*p*-Tolyl	NO_2	H

Bicyclic pyrimidine derivatives have shown significant potency as inhibitors of HIV integrase. This inhibitory effect is achieved by their ability to engage in coordinative interactions with metal ions, which play a crucial role in the enzyme's catalytic activity.[70] Le *et al*. synthesised a series of diverse azoles and explored their use as amide isosteres in the design of potential HIV integrase inhibitors. Imidazole-incorporated bicyclic pyrimidine compound **2.24** exhibited the highest efficacy in single-round HIV-1-based infective assays among the whole set of the azole derivatives.[71] Substituting the imidazole ring with a thiazole or oxazole moiety decreased inhibitory potency, clearly signifying the importance of the nitrogen atom (over oxygen or sulfur) for metal chelation. These results portrayed the significance of imidazoles as metal chelators in the exploration of highly effective HIV integrase inhibitors.[70, 71]

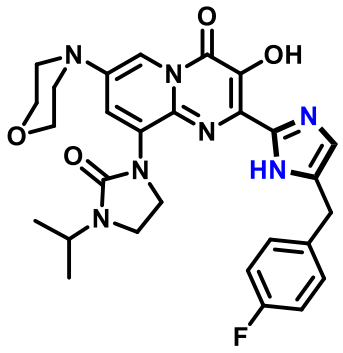

2.24

In the quest for new Hepatitis B virus (HBV) inhibitors, Jia *et al*. synthesised a series of 9-methoxy-6H-[1]benzothiopyrano[4,3-b]quinolin-10-ols with novel scaffolds and explored their anti-HBV activity. Compound **2.25** showed excellent anti-HBV activity and selectivity compared to the standard drug lamivudine. Further studies revealed that the imidazole scaffold did not only improve inhibitory efficacy but also decreased toxicity.[72]

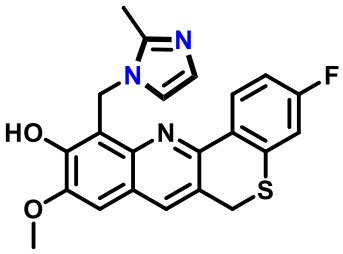

2.25

A set of ethyl 8-imidazolylmethyl-7-hydroxyquinoline-3-carboxylate derivatives synthesised by Liu *et al*. were evaluated for their anti-HBV activity and cytotoxicity. Compounds **2.26** , **2.27a** and **2.27b** proved to have higher inhibitory action against the replication of HBV DNA than the standard drug lamivudine.[73]

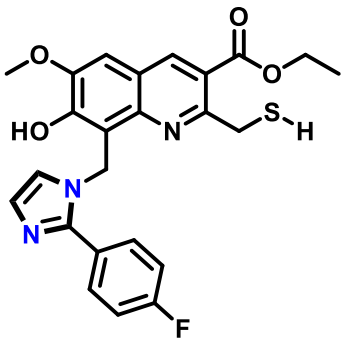

2.26

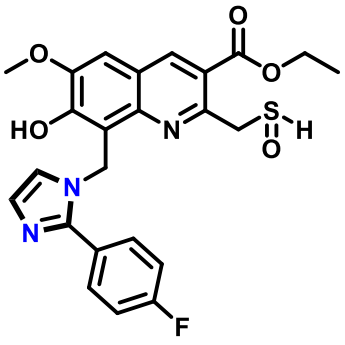

2.27a

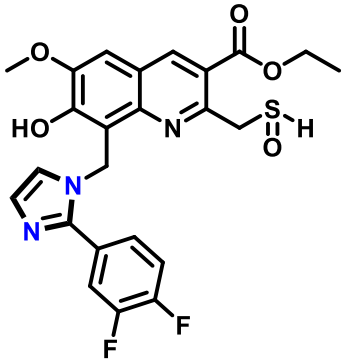

2.27b

De Martino *et al*. synthesised a set of 1-[2-(Diarylmethoxy)ethyl]-2-methyl-5-nitroimidazoles (DAMNIs) in the quest to discover new HIV-1 non-nucleoside reverse transcriptase inhibitors (NNRTIs). It was observed that introducing heterocyclic rings such as 3-pyridinyl or 2-thienyl resulted in novel DAMNIs of increased activity. Compounds **2.28** and **2.29** exhibited higher activity than the control drug efavirenz against the viral reverse transcriptase carrying the K103N mutation. These findings played a role in stimulating the development of novel DAMNIs.[74]

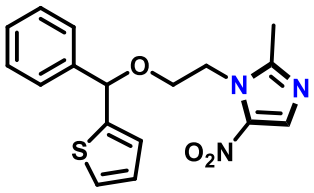

2.28

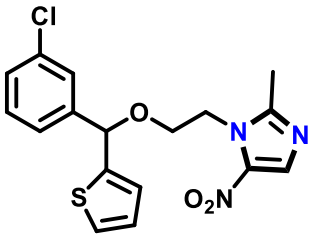

2.29

2.2.4 Anticancer activity

Cancerous diseases are among some of the biggest threats to human health. There is therefore an urgent need for the development of potent novel anticancer therapeutics. Some imidazole-based drugs such as dacarbazine (**2.30**), azathioprine (**2.31**), nilotinib (**2.32**), tipifarnib (**2.33**) and zoledronic acid (**2.34**) are already used as anticancer agents in medicine.[75-77]

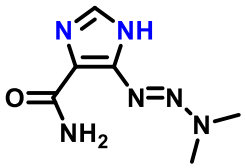

2.30. Dacarbazine

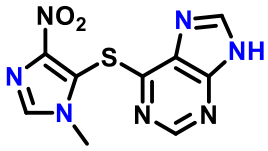

2.31. Azathioprine

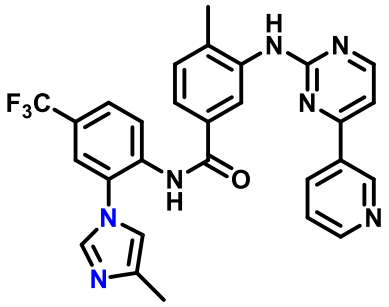

2.32. Nilotinib

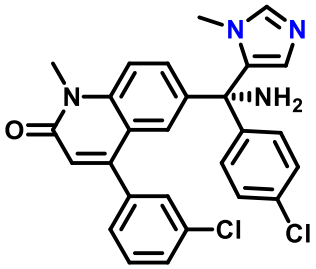

2.33. Tipifarnib

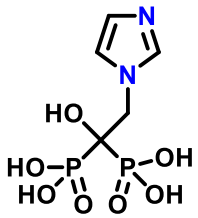

2.34. Zoledronic Acid

With the hopes of discovering new antitumour agents active against C6 and HepG2 tumour cells, Yurttas *et al*. synthesised a series of N-(6-substituted-benzothiazol-2-yl)-2-[[4,5-dimethyl1-((p-tolyl/4-nitrophenyl)amino)-1H-imidazol-2-yl]thio]acetamide derivatives and assessed their antitumour potential using cisplatin as the reference drug. From the set, compound **2.35** exhibited the best cytotoxic potential.[78]

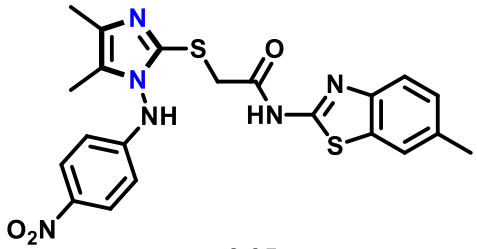

2.35

Romagnoli *et al*. designed a series of tubulin polymerisation inhibitors from the 1-(3',4',5'-trimethoxyphenyl)-2-aryl-1H-imidazole scaffold to assess their anticancer activity against various cancer cell lines with C-A4 as the reference drug. Amongst the set, compounds **2.36a**, **2.36b** and **2.36c** had significantly higher activities than the rest of the other derivatives. Of the three, compound **2.36c** was found to be the most active.[79]

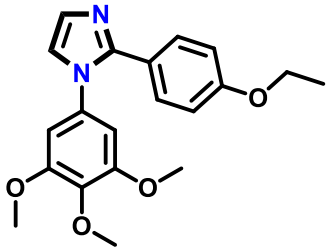

2.36a

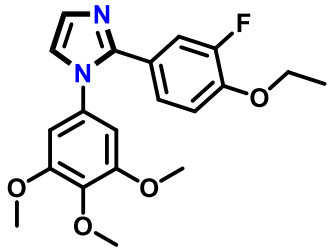

2.36b

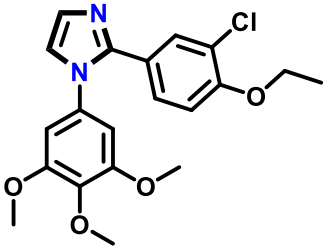

2.36c

Hsieh *et al*. synthesised 24 new N-substituted benzimidazole derivatives with a functional chalcone group to explore their anticancer activity through various biological studies. From the 24 synthesised compounds, compound **2.37** was the most active, with an *in vitro* cytotoxicity that surpassed that of cisplatin.[80]

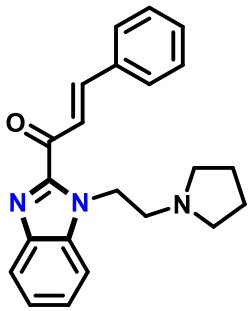

2.37

Roopashree *et al*. reported the synthesis of new *N*-substituted 2-(2-butyl-4-chloro-1H-imidazole-5-yl)-1H-benzo[d]imidazole derivatives to explore them as potential antitumor agents against HeLa cell lines. Compound **2.38** proved to be a potent *in vivo* antitumor agent against HeLa cell lines.[81]

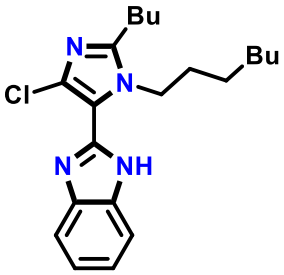

2.38

A set of benzimidazole derivatives synthesised by Rajendran *et al*. revealed that benzimidazole compounds containing the pyrimidine moiety (**2.39a-e**) and those holding the pyrazole moiety (**2.40a-d**) tend to have significantly enhanced activity against various cancer cell lines. From the set, compound **2.39a** exhibited exceptional antitumor potential against MCF-7 and CaCo-2 cell lines with Fluorouracil as the reference drug.[82]

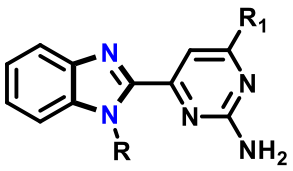

2.39a-e

	R	R_1
2.39a	**H**	**Ph**
2.39b	H	Pyridine
2.39c	H	3,4-dimethoxybenzene
2.39d	CH_3	Pyridine
2.39e	CH_3	3,4-dimethoxybenzene

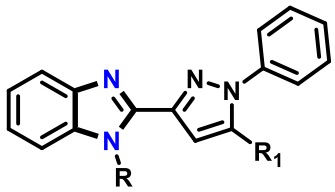

2.40a-d

	R	R_1
2.40a	H	Pyridine
2.40b	H	3,4-dimethoxybenzene
2.40c	CH_3	Pyridine
2.40d	CH_3	3,4-dimethoxybenzene

Meenakshisundaram *et al*. synthesised a series of bis-imidazole and bis-imidazo[1,2-a]pyridines with the intention of exploring their potential as anticancer agents. The screens were performed on three cancer lines: HeLa, MDA-MB-231, and ACHN, with Adriamycin as the reference drug. Compounds **2.41** and **2.42** exhibited the best anticancer activities across all three cell lines, surpassing the reference drug Adriamycin. These results suggested that the dimeric imidazo[1,2-a]pyridine scaffold posed as a potential lead in the advancement of anticancer therapeutics.[83]

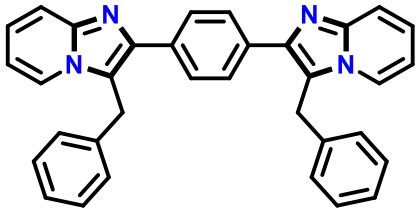

2.41

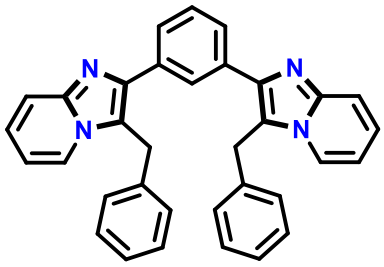

2.42

2.2.5 Antitubercular activity

Tuberculosis caused by *Mycobacterium tuberculosis* is one of the greatest threats to human health globally.[70] With the prevalence of drug-resistant TB and multidrug-resistant TB, the efficacy of renowned anti-TB agents such as rifampin and isoniazide has been compromised.[70, 84] This calls for the development of more potent antitubercular agents. Many imidazole derivatives have been studied over the years for their activity against drug-resistant and drug-sensitive *Mycobacterium tuberculosis* strains.[85, 86]

Prompted by drawbacks faced by antitubercular drug research, Nandha *et al*. synthesised a series of substituted fluorobenzimidazoles and evaluated their *in vitro* antitubercular activity against the Mycobacterium tuberculosis strain with Isoniazid as the reference drug. Of the fifteen synthesised compounds, compounds **2.43** and **2.44** were the most potent against the Mycobacterium tuberculosis strain. These results saw these two compounds as potential leads towards the development of antitubercular agents.[87]

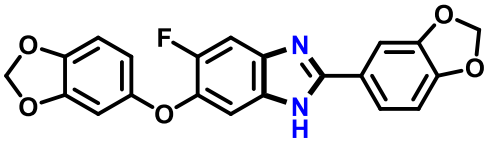

2.43

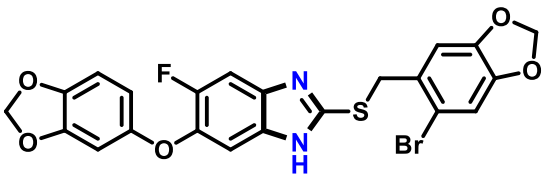

2.44

Gising *et al*. synthesised a class of 2-tert-butyl-4,5-diarylimidazoles with the hopes of identifying Mycobacterium tuberculosis glutamine synthetase (MtGS) inhibitors. After an X-ray structure of compound **2.45** bound to *Mt*GS was obtained, compound **2.45** emerged as the best Mycobacterium tuberculosis inhibitor on *Mt*GS, significantly surpassing the rest of the compounds in the set.[88]

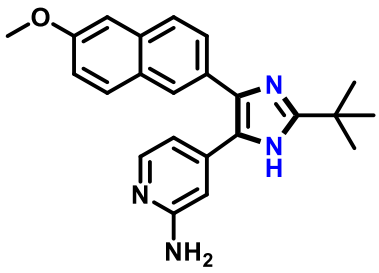

2.45

A series of 2,4-diphenyl-1H-imidazoles was synthesised by Pieroni *et al*. to be explored as potential antitubercular agents active against Mycobacterium tuberculosis in a whole cell phenotypic assay. Compound **2.46** greatly surpassed the rest of the compounds with exceptional inhibitory activity. Owing to its *m*-CF_3 substituted phenyl rings attached to the imidazole ring, compound **2.46** was 18 times more active than its counterparts.[89]

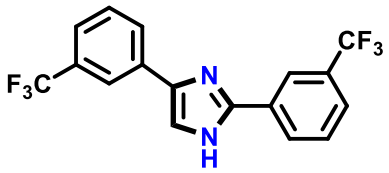

2.46

From three series of imidazole derivatives synthesised and screened against *M. tuberculosis* by Kishk *et al*., two compounds emerging from Series 3 (the isobutyl (**2.47a**) and tert-butyl (**2.47b**)

compounds) were found to be the most effective compounds of antitubercular activity. Through further studies, it was determined that increased lipophilicity maximised drug uptake in the *M. tuberculosis* lipid-rich cell wall, enhancing the antimycobacterial activity of the compound.[90] The Hansch analysis directly linked the lipophilicity and MIC of the compounds, proving the latter hypothesis to be true.[90]

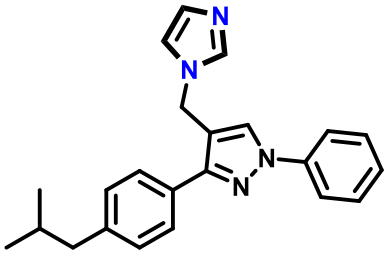

2.47a

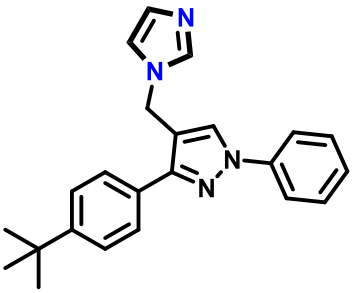

2.47b

Raghu and his group developed an effective synthesis of 2,4,5-trisubstituted imidazole analogues. The synthesised compounds underwent *in vitro* antitubercular screening against *M. tuberculosis* using pyrazinamide, ciprofloxacin, and ethambutol as reference drugs. The *in vitro* anti-TB activity results and the docking studies revealed that compounds **2.48a-e** had higher potency than the reference drugs, and had potential as future research lead compounds.[91]

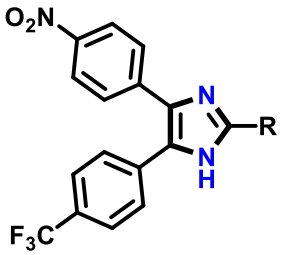

2.48a-e

	R		R
a	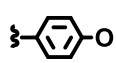	d	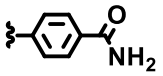
b	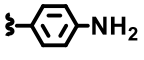	e	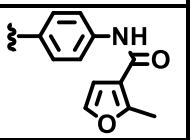
c	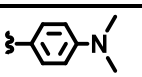		

2.2.6 Antimalarial activity

For many years, many of the drugs used in malaria chemotherapies were quinoline-based compounds. Chloroquine (**2.49**) would stand out as the most used of this class of drugs because of its high activity, low cost and good tolerability.[92] However, due to mutations occurring in parasite proteins, there has been an emergence of drug resistance to these quinoline-based drugs (including chloroquine) and many other classes of antimalarials.[92-94] Because of this, there is a need for the development of new antimalarial targets active against these drug-resistant parasites.[95]

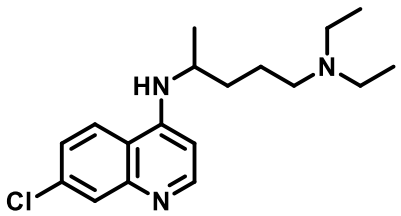

2.49. Chloroquine

In the quest for the development of new antimalarials, Casagrande *et al*. synthesised a set of 7-chloro-*N*-(heteroaryl)-methyl-4-aminoquinoline and 7-chloro-*N*-(heteroaryl)-4-aminoquinoline derivatives to investigate the effects of various heterocycles linked to the 4-aminoquinoline moiety on antimalarial activity against various *Plasmodium falciparum* strains. From the results, the thienyl derivative **2.50**, the arylimidazolyl derivative **2.51** and the *N*-methylimidazolyl derivative **2.52** displayed the most impressive antiplasmodial activity, surpassing the standard drug chloroquine. The results demonstrated the importance of constituting a heteroaryl nucleus to 7-chloro-4-aminoquinoline for the design of new potent antimalarial hits.[96]

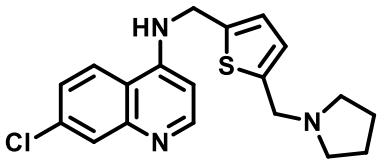

2.50

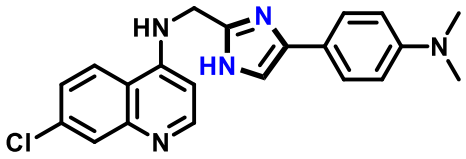

2.51

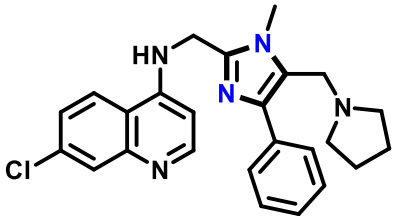

2.52

Kondaparla *et al*. also synthesised a series of 4-aminoquinoline-based imidazole derivatives to assess their antimalarial activity. The set was screened against chloroquine-resistant and chloroquine-sensitive strains of *P. falciparum*. The four compounds **2.53a-d** displayed antiplasmodial activity comparable to that of the reference drug chloroquine. These results confirmed that hydrophobic substitutions on the N-(2-(1H-imidazol1-yl)ethyl)-7-chloroquinolin-4-amine moiety greatly enhanced antiplasmodial activity.[95]

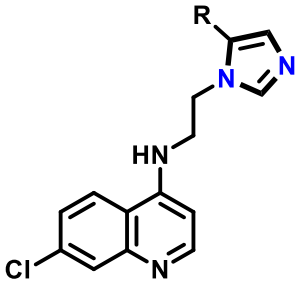

2.53a-d

	R		R
a	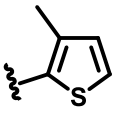	c	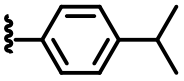
b	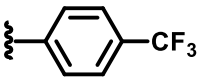	d	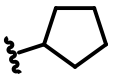

In the pursuit of discovering new potential antimalarials, Roy *et al*. synthesised a series of quinoline-imidazole hybrids and evaluated their blood-stage antimalarial activity in a range of

drug-sensitive and multidrug-resistant strains of *P. falciparum*. From the set, compound **2.54** exhibited impressive sub-micromolar activities *in-vitro* against both CQ-sensitive and MDR strains. This compound also proved to be highly selective with minimal cytotoxicity. A fascinating finding revealed through the enantiomeric separation of a racemic mixture of this compound that the (-)-**2.54** enantiomer displayed greater activity than its isomer.[94]

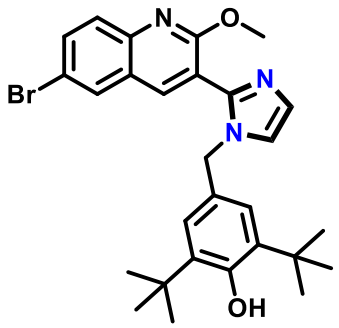

2.54

Over the years, more antimalarial research has been carried out based on more novel nuclei, moving away from the quinoline nucleus due to the rise in resistance to quinoline-based antimalarial agents. Driven by this kind of research, Roman *et al*. designed and synthesised a series of benzimidazole analogues structurally related to astemizole to screen them for their antiplasmodial activity. These compounds underwent *in vitro* antiplasmodial activity studies against the ItG strain. These studies showed that some of these compounds had IC_{50} values in the nanomolar range with high selectivity indices. Several compounds from the set had promising parasite proliferation inhibition, but only compound **2.55** exhibited higher potency than astemizole. It was also revealed that substituting chlorine at positions 4 and 5 in the benzimidazole scaffold is a key modification that led to potent and highly selective antimalarial agents.[97]

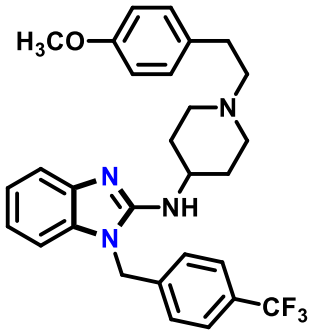

2.55

Also using the benzimidazole scaffold, Sharma *et al*. synthesised a series of 18 benzimidazole acrylonitriles and evaluated them for their antimalarial activity and cytotoxicity. From the results, it was found that compounds **2.56a-c** have inhibitory activity against the formation of falcipain-2 and hemozoin, with their cytotoxicity being within bearable limits.[98]

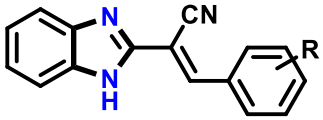

	R
a	3-OCH_3
b	3,5-OCH_3
c	3-OH, 4-OCH_3

2.56a-c

In most recent studies, much research is being carried out where the imidazole scaffold is being examined as a core antimalarial framework without the presence of the quinoline nucleus. This scaffold has been reported to have a broad range of antimalarial inhibition.[95, 99] In a lot of this research, researchers tended to evaluate the antimalarial activity of various imidazole derivatives with methoxy and hydroxy substitutions, as these groups have been found to enhance the antimalarial activity of benzimidazole[100], coumarin[101] and chalcone[98, 102] compounds.

To aid this line of research, Septiana *et al*. were encouraged by the rise of resistance against the chloroquine-sensitive *Plasmodium falciparum* 3D7 strain to synthesise a set of three 2-

(disubstituted)-4,5-diphenyl-*1H*-imidazole compounds and assess their *in vitro* antiplasmodial activity. Compounds **2.57a-c** exhibited good antimalarial activity, promising to be good potential leads in the development of antimalarial agents through further modification.[103]

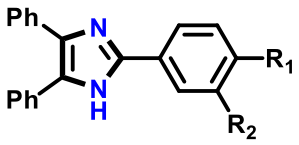

	R_1	R_2
a	OH	OCH_3
b	OCH_3	OCH_3
c	OCH_3	H

2.57a-c

To address the issue of the increase in artemisinin-resistant *Plasmodium falciparum* parasites, Bheemanaboina *et al*. presented a series of *Plasmodium falciparum* cGMP-dependent protein kinase (PfPKG) inhibitors of the imidazole scaffold with impressive *in vitro* PfPKG potency and cell-based antiparasitic activity against a wide variety of Plasmodium species. Out of the series, compound **2.58** stood out as the potential lead in this quest of PfPKG inhibitors, exhibiting exceptional selectivity against two kinases (human PKG and *P. falciparum* mutant T618Q).[104]

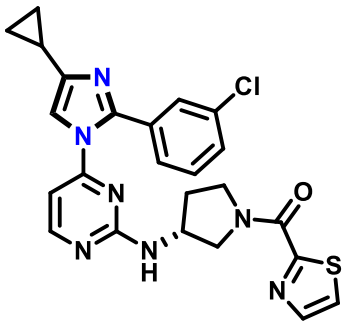

2.58

2.3 Aim and Objectives

This project aimed to explore the structure-activity relationship (SAR) of imidazole derivatives based on the lead compound MMV023227 identified from the MMV Pathogen Box as an antiplasmodial scaffold.

The objectives of this project were:

- To synthesise analogues of the hit compound (MMV023227)
- To characterise the analogues by spectroscopic techniques
- To assess the antiplasmodial activity of the analogues.

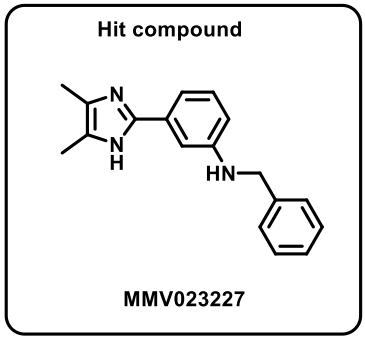

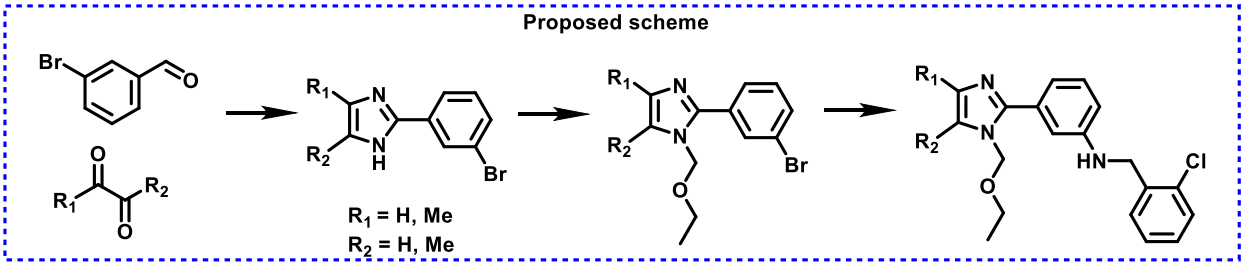

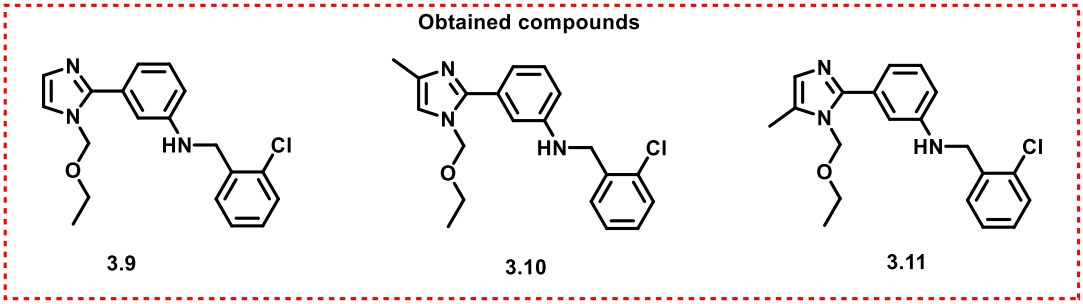

3. CHAPTER THREE: RESULTS AND DISCUSSION

3.1 Synthesis of imidazole derivatives

3.1.1 Synthesis of imidazole 3.1

The desired imidazole compound **3.1** was obtained from the condensation reaction between 3-bromobenzaldehyde and 2,3-butanedione adapted from a study performed by Eseola *et al*.[105] (**Scheme 3.1**). The product was obtained in low 34 % yield because aliphatic diketones such as 2,3-butanedione are electron-poor, thus less reactive compared to most aromatic diketones, therefore requiring harsh reaction conditions.[106]

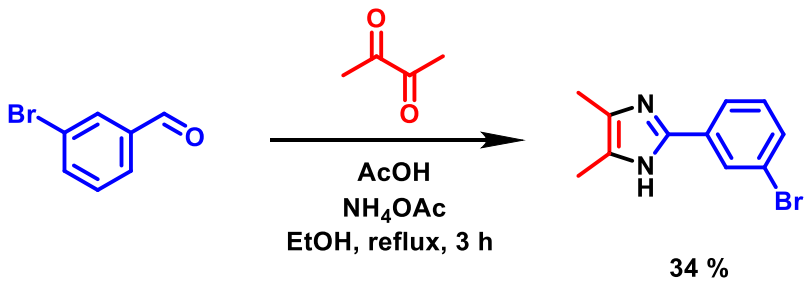

Scheme 3.1: Acetic acid-mediated imidazole synthesis of compound **3.1**.

The titled compound was obtained as a yellow powder and was confirmed by spectroscopic techniques. The ^{1}H NMR spectrum (**Figure 3.1**) shows a signal resonating at 2.11 ppm, which integrated for 6 protons, indicating an overlap of the two methyl groups. In this case, a single resonance is observed for both methyl groups of the two forms shown in the **Scheme 3.2**. Similarly, a single resonance at 12.11 ppm is observed for the N-H signal of both forms.

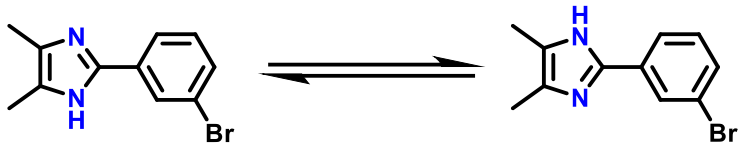

Scheme 3.2: Tautomeric forms of compound **3.1**.

Due to this tautomerisation, the methyl groups show up as one small bulge (from 13.13 to 8.65 ppm) on the ^{13}C NMR spectrum (**Figure 3.2**), also affecting the attached quaternary carbon atoms. This can be resolved by either heating up or cooling down the sample. If the sample is heated up, this speeds up the rate of the exchange to a point where the two states are indistinguishable, resulting in one time-averaged broadened singlet. Cooling down the sample does quite the opposite. This slows down the rate of the exchange, clearly distinguishing the two states and, therefore, yielding two sharpened singlets. The signal area is constant; a broad signal with a lower intensity and a sharp signal with a higher intensity.

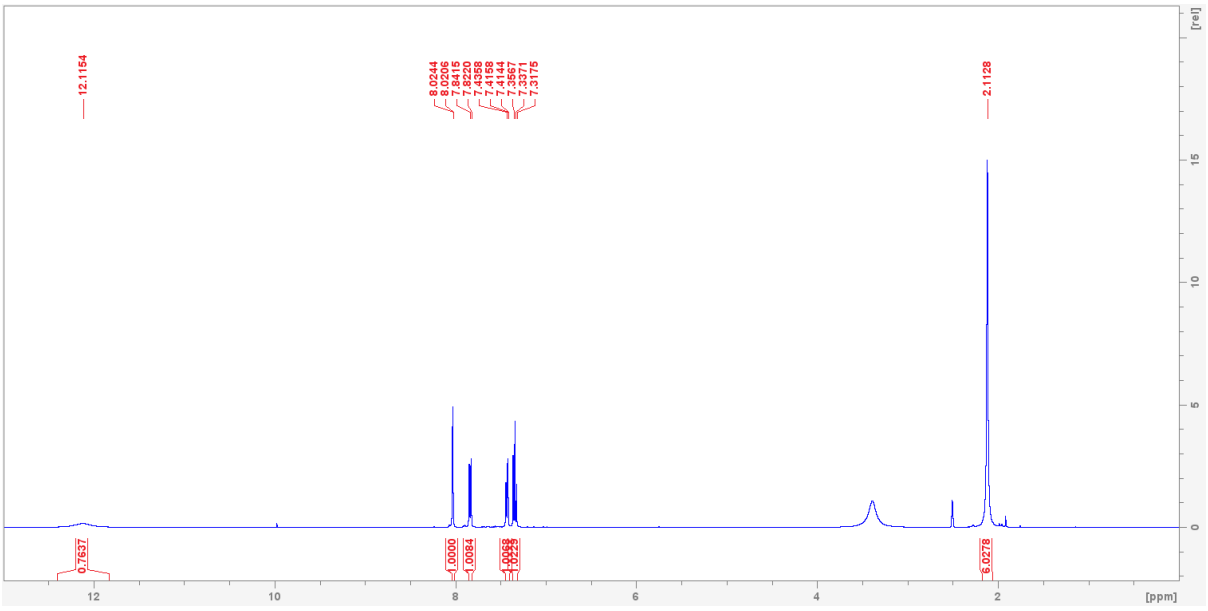

Figure 3.1: ^{1}H NMR spectrum of compound **3.1** (DMSO-d_6, 400 MHz).

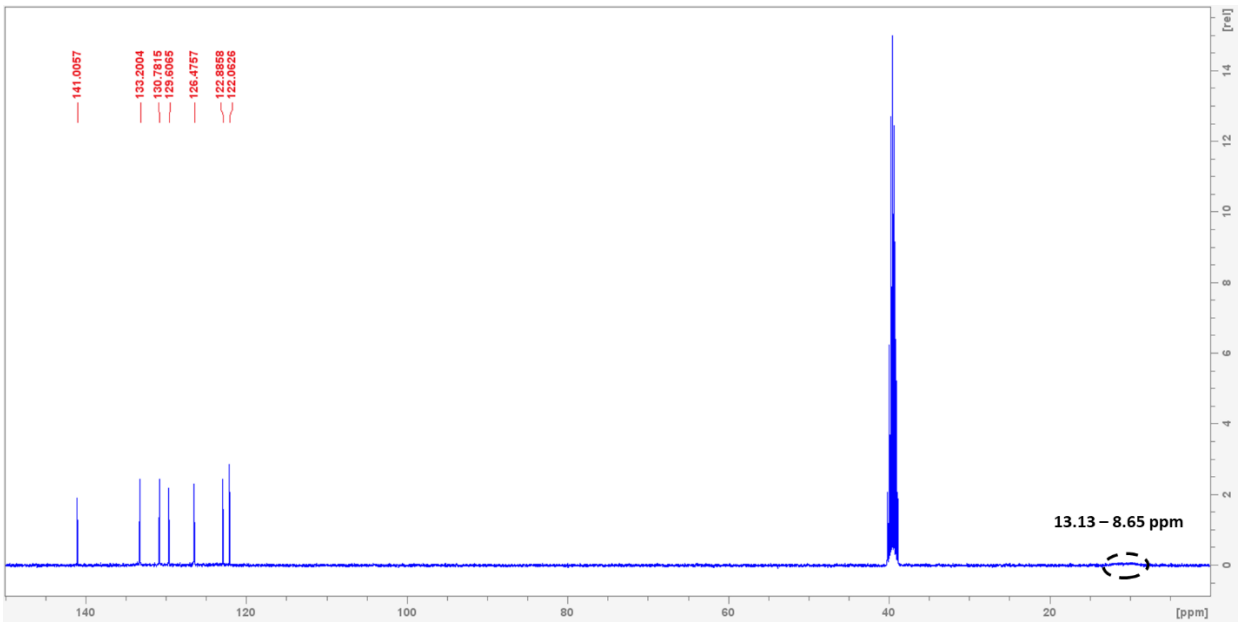

Figure 3.2: ^{13}C NMR spectrum of compound **3.1** (DMSO-d_6, 400 MHz).

3.1.2 Synthesis of imidazoles 3.2 and 3.3

Since the procedure for compound **3.1** did not work for compounds **3.2** and **3.3**, a new procedure had to be explored. The two most noticeable changes with this method adapted from Hedström *et al*.[107] (**Scheme 3.3**) are the absence of the acidic catalyst and the significantly lower reaction temperatures. Another change is the use of ammonium hydroxide instead of ammonium acetate as the nitrogen atom source.

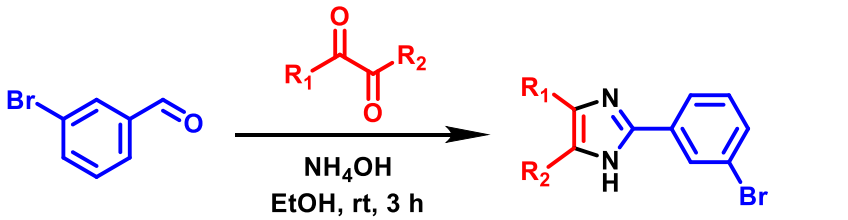

(3.2) R_1 = CH_3, R_2 = H, **33 %**
(3.3) R_1 = R_2 = H, **42 %**

Scheme 3.3: Catalyst-free synthesis of compounds **3.2** and **3.3**.

Comparing the ^{1}H NMR spectra of the two compounds (**Figure 3.3**), the key difference would be observed at the methyl (**R_1**) resonating at 2.19 ppm for compound **3.2,** which is not observed for compound **3.3**. Another observable difference is the singlet observed at 6.84 ppm, which integrates for one proton (**R_2**) in compound **3.2,** and the signal observed at 7.17 ppm, which integrates for two protons (**R_1** and **R_2**) in compound **3.3**. The four signals for the four aryl protons remain the same in both spectra, with very slight changes in chemical shift.

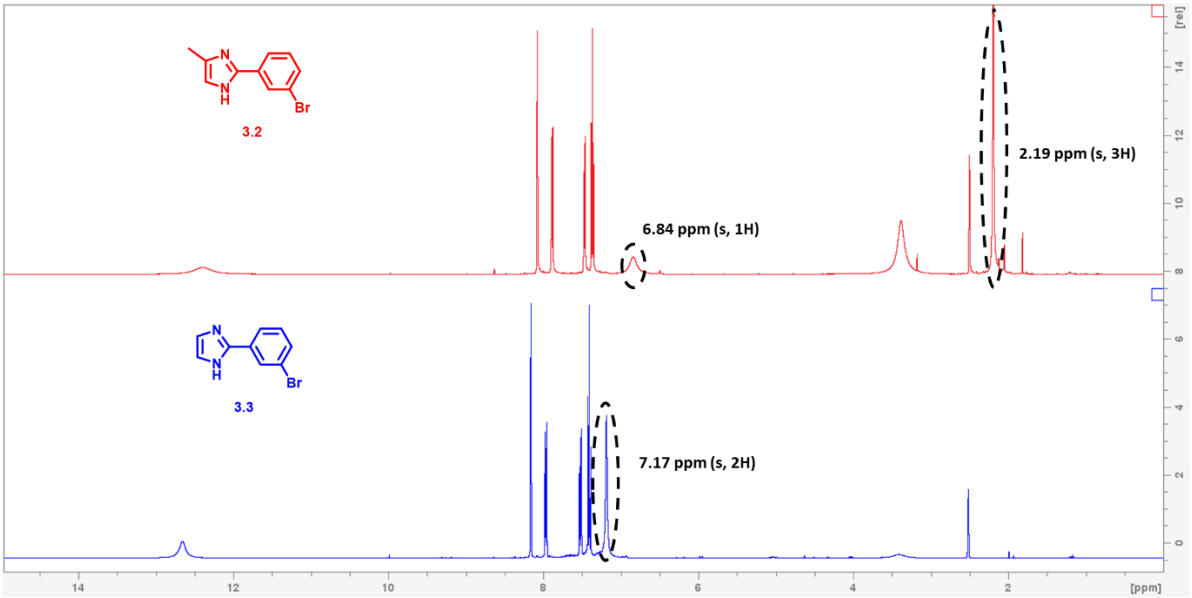

Figure 3.3: Stacked view of the ^{1}H NMR spectra of compound **3.2** (red) (DMSO-d_6, 500 MHz) and compound **3.3** (blue) (DMSO-d_6, 500 MHz).

The ^{13}C NMR spectra of these two compounds (**Figure 3.4**) also give the same idea, with the observable key change being the methyl signal observed at 13.7 ppm for compound **3.2**, which is the only difference between the two compounds. The methyl signal at 13.7 ppm appears very short. This is due to the tatumarization of the the two nitrogen atoms as previously discussed.

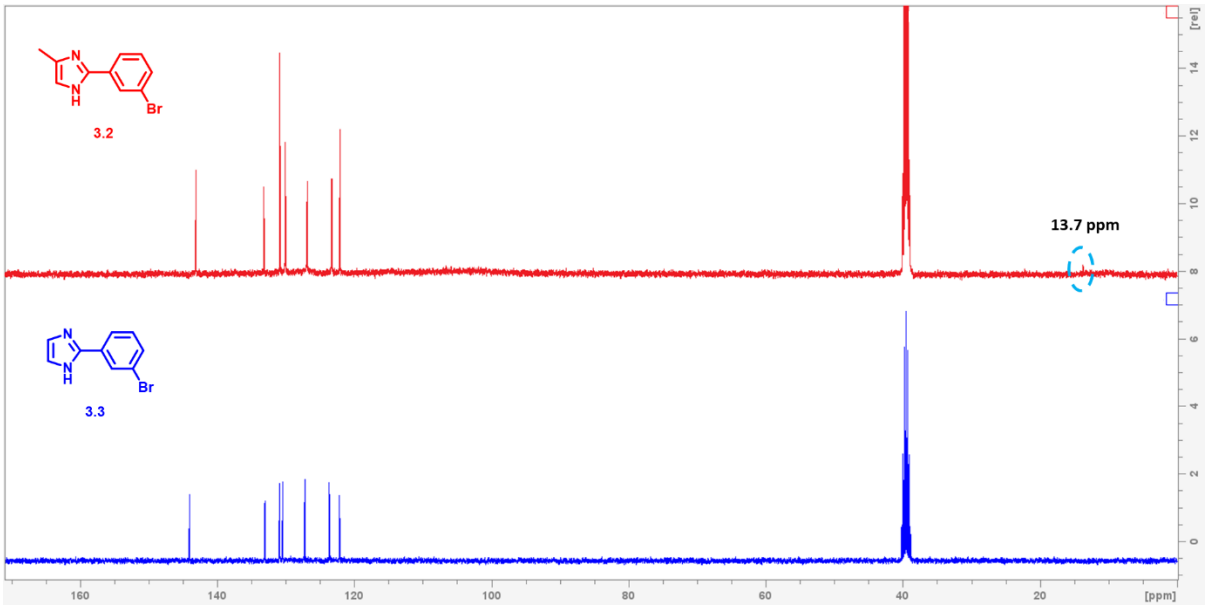

Figure 3.4: Stacked view of the ^{13}C NMR spectra of compound **3.2** (red) (DMSO-d_6, 500 MHz) and compound **3.3** (blue) (DMSO-d_6, 500 MHz).

Having succesfully synthesised compound **3.2** in substantial amounts, we then thought it would be a good idea to grow single X-Ray crystals to investigate the strcture of the synthesised imidazole. The X-ray structure of compound **3.2** is shown in **Figure 3.5**.

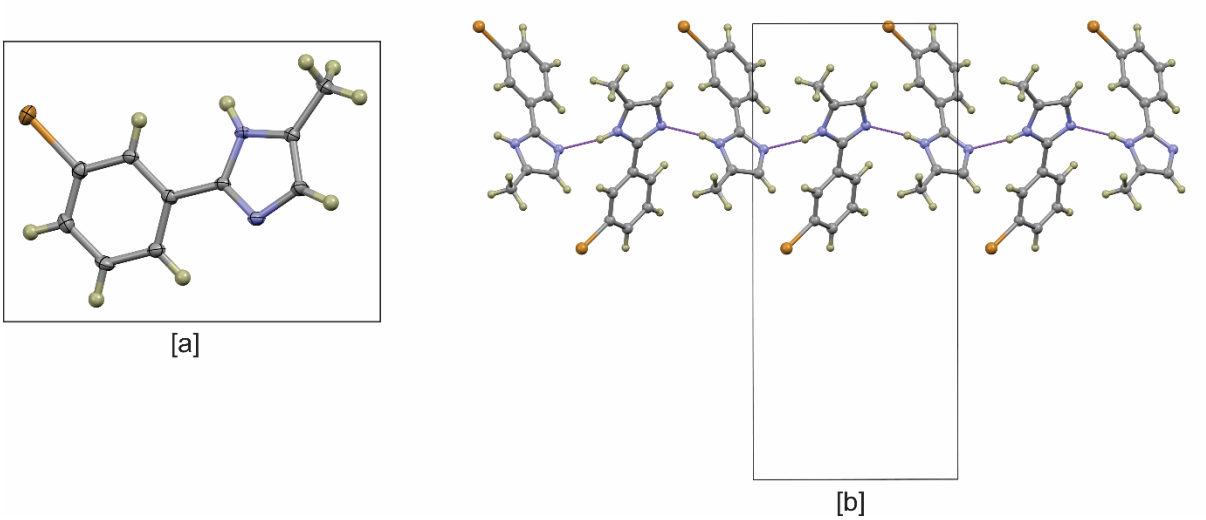

Figure 3.5: Thermal ellipsoid plot showing 50% probability surfaces for compound **3.2**. Hydrogen atoms are shown as spheres of arbitrary radius. Atom colours: grey = carbon, beige = hydrogen, blue = nitrogen and light brown = bromine.

The molecule crystallised in the monoclinic Space Group P21/n with a single molecule in the asymmetric unit and Z = 4 **[a]**. One-dimensional supramolecular structure (symmetry code: -1/2+x, 1.5-y, -1/2+z) supported by N–H···N hydrogen bonds between the imidazole rings of adjacent molecules. The H1···N distance measures 1.997 Å; this is significantly shorter than the sum of the van der Waals radii of the interacting atoms, hinting at it being a strong interaction **[b]**.

3.2 Synthesis of ether-protected imidazole derivatives 3.4, 3.5 and 3.6

The general procedure for the three ether-protected imidazole derivatives was adapted from Albertshofer and Mani[108], where the only reagent that differed from their work in each case was the imidazole used. All other reaction parameters were the same.

3.2.1 Synthesis of compound 3.4

For the synthesis of compound **3.4**, imidazole **3.3** was dissolved in THF and reacted with sodium hydride (60% dispersion in oil) and chloromethyl ethyl ether for 3 hours at room temperature (**Scheme 3.4**). The titled compound was obtained as a reddish-brown oil with a yield of 83%, which compared well to the 84% reported Albertshofer and Mani[108].

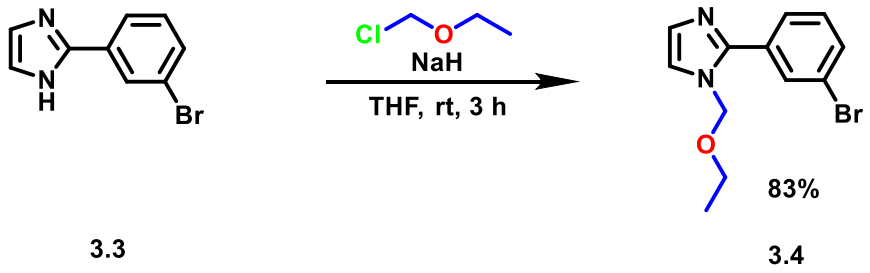

Scheme 3.4: Alkyloxymethyl ether protection of compound **3.3**.

On the ^{1}H NMR spectrum, the most significant indication of this reaction's success would be the disappearance of the N-H signal downfield and the appearance of the three expected signals from the ether group upfield. As expected, these signals show up as a singlet at 5.16 ppm integrating for two protons, a quartet at 3.47 ppm integrating for two protons and a triplet at 1.14 ppm integrating for three protons (**Figure 3.6**). These signals represent the methylene CH_2, ethylene CH_2 and the ethylene CH_3 respectively.

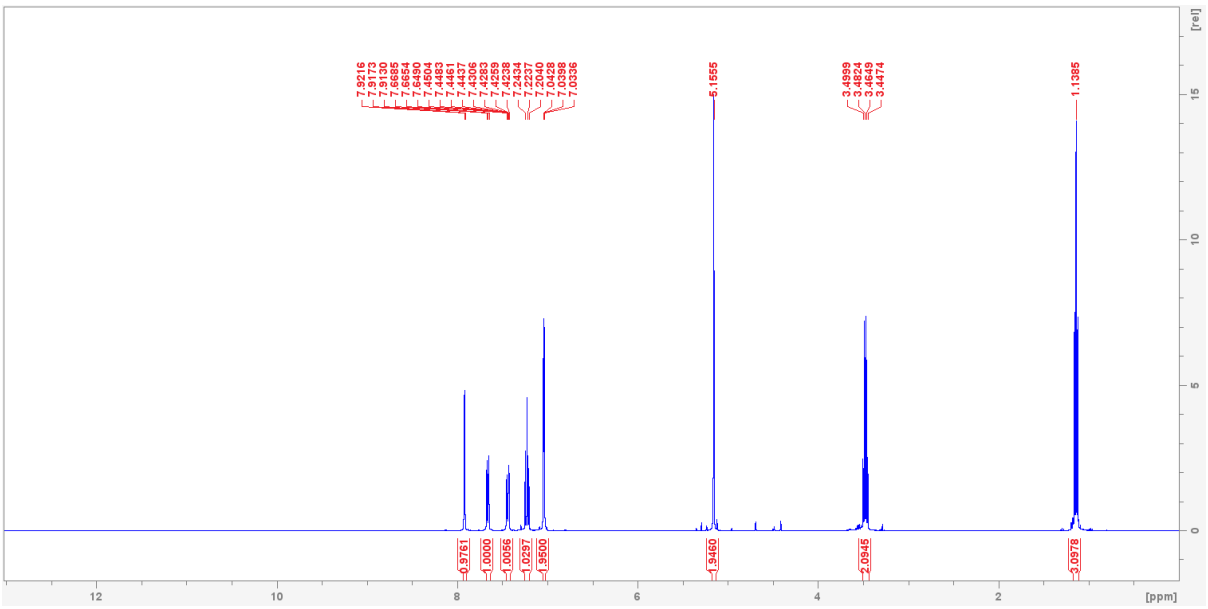

Figure 3.6: ^{1}H NMR spectrum of compound **3.4** ($CDCl_3$-*d*, 400 MHz).

3.2.2 Synthesis of compounds 3.5 and 3.6

The synthesis of these two compounds followed the general procedure mentioned above, starting with imidazole **3.2** in THF being reacted with sodium hydride (60 % dispersion in oil) and chloromethyl ethyl ether for 3 hours at room temperature (**Scheme 3.5**). Introducing the methyl group to imidazole **3.2**, which was not present in imidazole **3.3**, brought about the possibility of having two isomers as the products of this reaction. Compounds **3.5** and **3.6** were obtained in a mixture as a yellow oil (**Scheme 3.5**).

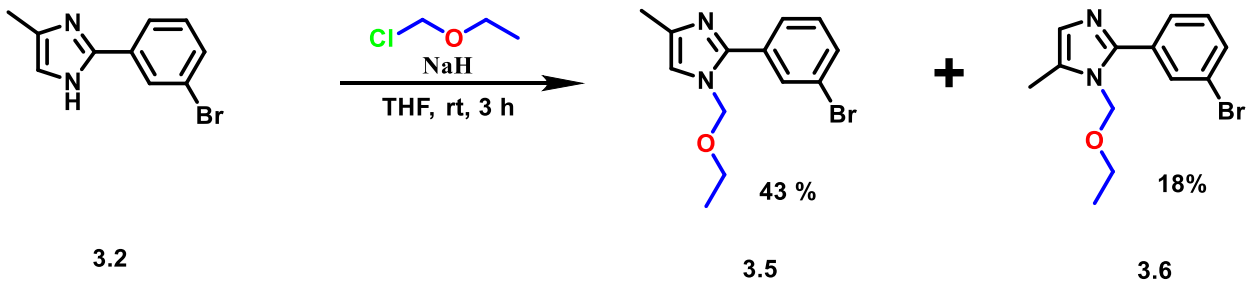

Scheme 3.5: Alkyloxymethyl ether protection of compound **3.2**.

The two isomers showed up as two super close spots on the TLC plate, making separating the two challenging. The two isomers were eventually isolated by column chromatography using a gradient system with gradual increments from 10 % to 40 % ethyl acetate in *n*-hexane, yielding both compounds **isomer A** and **isomer B** as yellow oils of 43 % and 18 % yields, respectively. (**Figure 3.7**). Evidently, the ^{1}H NMR spectra of the two compounds would essentially display the same information, with slight differences in the chemical shifts of the signals (**Figure 3.8**).

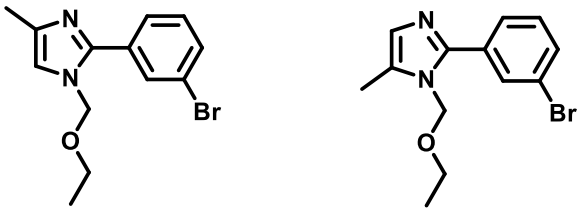

isomer A
43 % yield

isomer B
18 % yield

Figure 3.7: Two isomer products from the alkyloxymethyl ether protection reaction.

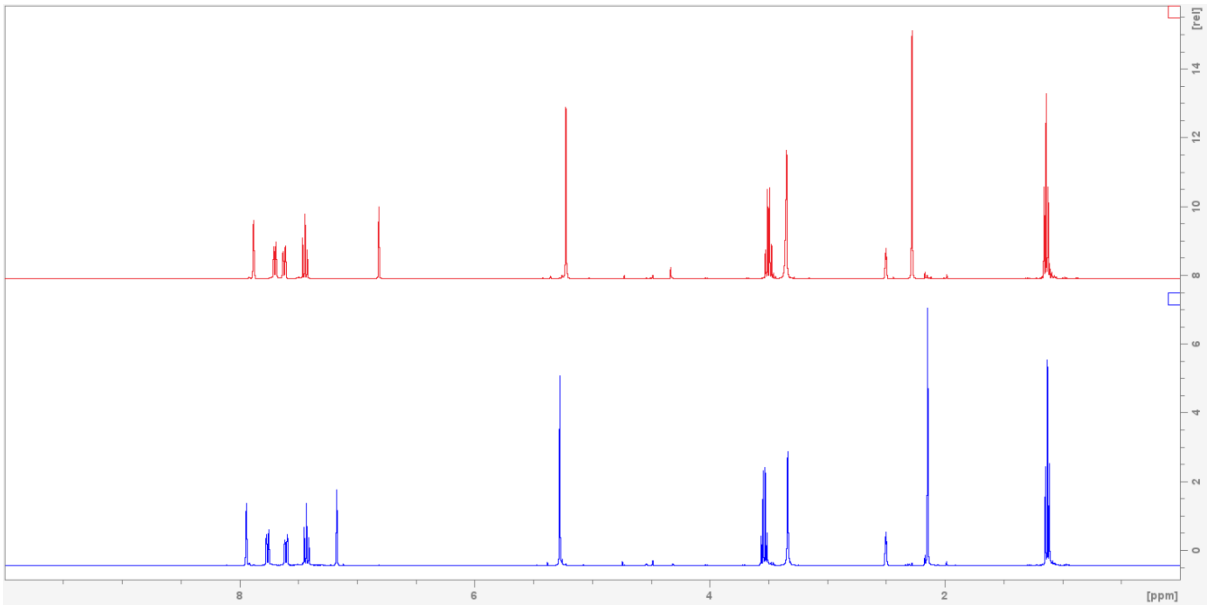

Figure 3.8: Stacked view of the ^{1}H NMR spectra of **isomers A** and **B** (DMSO-d_6, 400 MHz).

From these spectra, it can be seen that these are two very closely related species, but there is not enough evidence to assist in distinguishing one from the other. To make that possible, we performed a series of NOESY (Nuclear Overhauser Effect Spectroscopy) experiments. NOESY is a handy spectroscopic technique that shows through-space correlations within the molecule via spin-lattice relaxation (**Scheme 3.6**), as opposed to the through-bond correlations observed in other techniques.

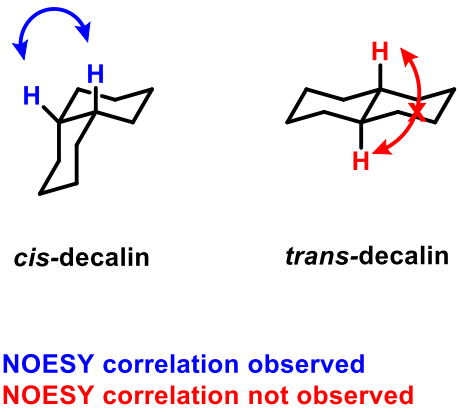

Scheme 3.6: Key NOESY correlations for the two conformations of decalin.

To run a successful NOESY experiment, it is rather pivotal to identify the best excitation site wisely. Irradiating the signal of interest should result in specific effects to provide relative stereochemical information about the molecule of concern. In the case of **isomers A** and **B**, the irradiated signals are the same in both cases. Two NOESY experiments were performed for each isomer (**Scheme 3.7**). This should help determine the methyl group's positioning in each isomer, making it easier to tell the two isomers apart.

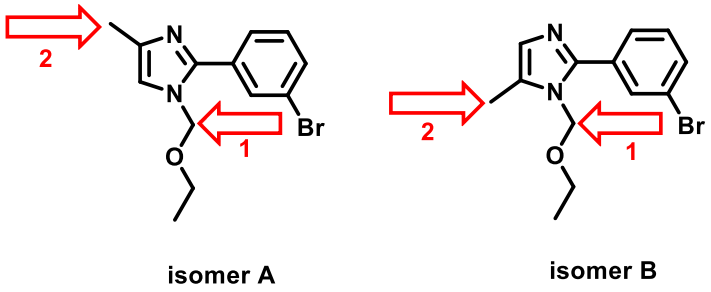

Scheme 3.7: Proposed NOESY experiment excitation sites.

Two NOESY NMR experiments were performed to determine the relative configuration of **isomer A**. In the first experiment, exciting position 1 labelled on **Scheme 3.7** resulted in five observed enhancements (**Figure 3.9**). This indicates that the five enhanced signals are of protons that are in close proximity to the excitation site. The methyl in the imidazole ring not being enhanced was indicative that it is not close in space to the excitation site, supposing it is two carbons away from the ether arm. The proton labelled H_c being enhanced further cemented that supposed fact. Protons H_a and H_b both getting enhanced suggests free rotation through the imidazole-aryl ring bond.

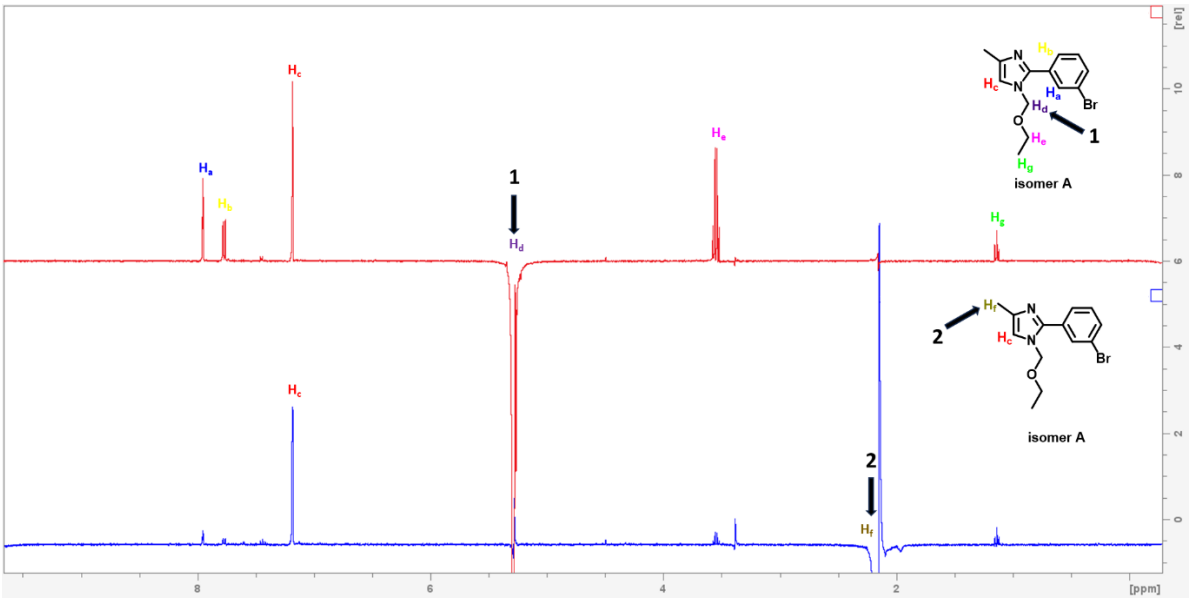

Figure 3.9: NOESY NMR spectrum of **isomer A** (DMSO-*d*$_6$, 400 MHz).

The second experiment, where the imidazole methyl signal was irradiated, resulted in a brief but conclusive outcome. The only enhancement observed was of the proton attached to the carbon next to it. No enhancements were observed on the signals belonging to the ether arm, proving there are no correlations to that region. **Isomer A** was therefore confirmed as compound **3.5**.

For **isomer B**, two NOESY NMR experiments similar to those for **isomer A** were also performed to determine the relative configuration of this compound. The results for the first experiment were the same, with the only change that separates the two being the enhancement of the methyl group in the imidazole ring instead of proton H_c, which is an indication that these two groups have switched positions between **isomer A** and **isomer B** (**Figure 3.10**).

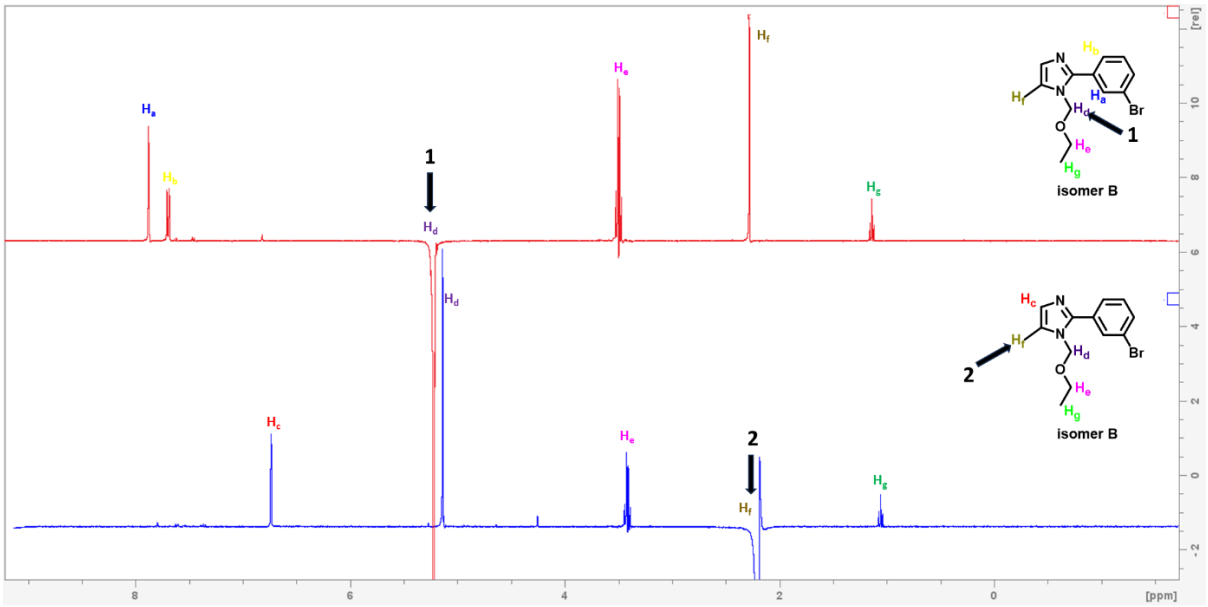

Figure 3.10: NOESY NMR spectrum of **isomer B** (DMSO-d_6, 400 MHz).

The second experiment was also helpful towards the elucidation of **isomer B**'s configuration. The irradiation of the imidazole methyl group confirmed all the protons around it in space. This established **isomer B** as compound **3.6**.

Compounds **3.5** and **3.6** were both confirmed by high-resolution mass spectrometry (**Figure 3.11**). Since both compounds have the same molecular formula, their calculated mass was the same. However, it is highly improbable that the exact value will be obtained experimentally due to experimental variation (with tolerance up to 5.0 PPM). In the case of compounds **3.5** and **3.6**, the experimental variation for both compounds fell within the range, confirming the two compounds are appropriately configured. The two peaks observed in both cases which are of almost the same intensity are as a result of the isotopic pattern of bromine. Bromine has two stable isotopes which are ^{79}Br and ^{81}Br, with mass abundances of 50.686% and 49.314%.[109-111] Since their mass abundances are so close, this results in their intensities being almost equal.[110, 111] The presence of these two peaks being two mass units apart indicates the presence of the bromine atom in the compound in each case.

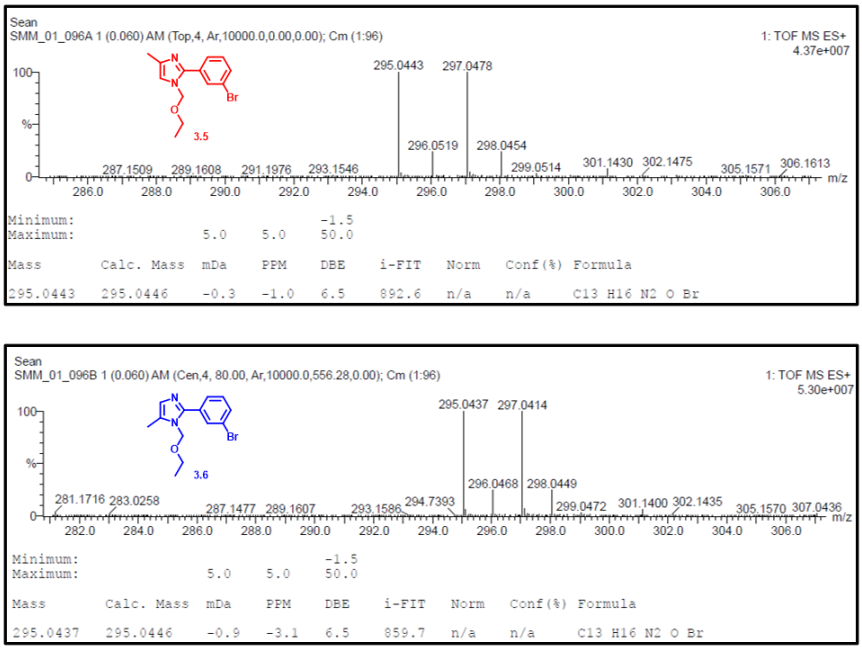

Figure 3.11: HRMS spectra of compounds **3.5** and **3.6**.

3.3 Buchwald-Hartwig amination of brominated imidazoles

The continuous emergence of C-N bond-forming reactions catalysed by transition metals pledges to be a powerful route for the formation of aryl amines. These palladium-mediated cross-coupling reactions of aryl halides and amines, through the highly impactful efforts contributed by the groups of Buchwald[112] and Hartwig[113], have been reckoned to be among some organic transformations of paramount significance.[114]

3.3.1 Synthesis of the palladium complex (DPPF)$PdCl_2$

Reaping the benefits of these advancements, we adopted the work done by Driver and Hartwig[113], where they produced secondary arylamines in impressive yields through the cross-coupling of aryl halides and primary amines. These reactions were mediated by the air-stable (DPPF)$PdCl_2$ complex. The preparation of (DPPF)$PdCl_2$ was through a procedure adapted from Davies *et al*.[115] (**Scheme 3.8**). Palladium chloride was dissolved in refluxing acetonitrile and stirred for 4 hours under nitrogen gas to form the intermediate complex palladium(II)chloride diacetonitrile (**3.7**). Subsequently, DPPF was added to the reaction mixture in a 1:1 stoichiometric ratio with the intermediate metal ion (**3.7**). After 1 hour of stirring, the solvent was evaporated, and the powder was filtered off and recrystallised from dimethylformamide. The complex (**3.8**) was obtained as a red solid in 98 % yield (**Scheme 3.8**).

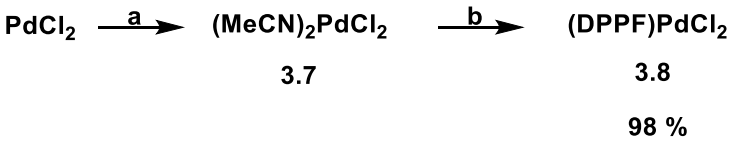

Scheme 3.8: Praparation of (DPPF)$PdCl_2$.

Reaction conditions: (a) MeCN, reflux, 4 h, $N_{2(g)}$; (b) DPPF, reflux, 1 h

The formation of (DPPF)$PdCl_2$ was confirmed by spectroscopic techniques. The stacked view of the ^{31}P NMR spectra of the DPPF ligand and the (DPPF)$PdCl_2$ complex clearly reflects the chemical shift that defines the transition from ligand to complex (**Figure 3.12**). These ^{31}P NMR results coincide with those reported by Guilbaud *et al*. in their study.[116]

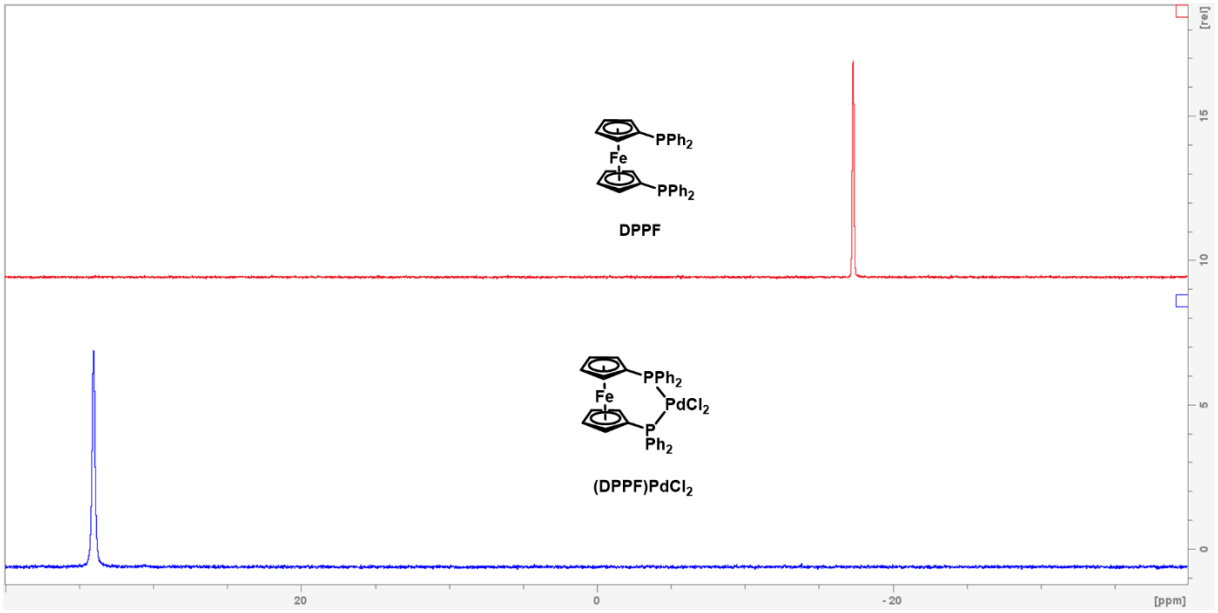

Figure 3.12: The ^{31}P NMR spectra of DPPF (red) and (DPPF)$PdCl_2$ (blue) (CD_2Cl_2-*d*2, 400MHz).

3.3.2 Synthesis of arylamines 3.9, 3.10 and 3.11

For the synthesis of compounds **3.9**, **3.10** and **3.11,** the procedure reported by Driver and Hartwig[113] was followed (**Scheme 3.9**). The aryl bromide (**3.9-3.11**) and sodium *tert*-butoxide were added to anhydrous tetrahydrofuran. Complex **3.8** and DPPF were then subsequently added to the suspension, followed by 2-chlorobenzylamine, which was added last. The reaction mixture was refluxed and monitored by TLC, indicating no significant changes up to 24 hours. The reaction was stopped after 24 hours and concentrated. The TLC reflected that many species were present in the reaction mixture, making it a little challenging to isolate the product by silica gel chromatography. For a good separation, these compounds were first isolated using column chromatography followed by radial chromatography (**Figure 3.13**).

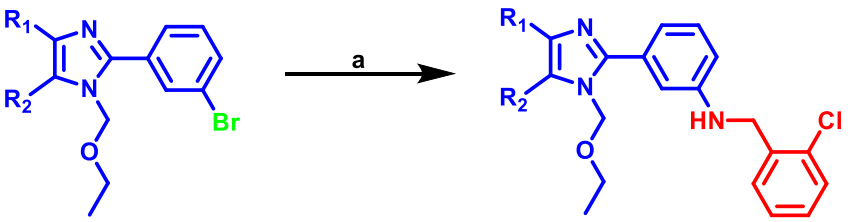

	R_1	R_2		R_1	R_2	
3.4	H	H	3.9	H	H	41 %
3.5	Me	H	3.10	Me	H	13 %
3.6	H	Me	3.11	H	Me	7 %

Scheme 3.9: Palladium-catalysed arylamine formation.

Reaction conditions: (a) 2-chlorobenzylamine, **3.8**, DPPF, NaO-*t*-Bu, THF, reflux, 24 h

Figure 3.13: Different coloured fractions collected from silica gel chromatography.

In an effort to isolate the desired compound, radial chromatography was explored as a potential technique for the separation of these compounds. The fractions collected from silica gel chromatography containing the product were mixed and loaded onto a chromatotron plate for further purification. We did not have much success with this technique either, but the most significant advantage of it is that one can track eluting bands under UV light as they move out (**Figure 3.14**). After several attempts trying to separate these compounds, eluting with a more non-polar solvent system of only 10 % ethyl acetate in *n*-hexane, we managed to isolate our desired arylamine in each case.

Figure 3.14: Radial chromatography under UV light.

The three compounds, **3.9**, **3.10** and **3.11,** were obtained and analysed by spectroscopic techniques. The compounds' molecular masses and chemical formulae were confirmed through high-resolution mass spectrometry. Looking at all three spectra, one noticed the possible chlorine isotopic pattern. Chlorine has two stable isotopes which are ^{35}Cl and ^{37}Cl with mass abundances of 75.77 % and 24.23 %.[117-119] The presence of the two prominent peaks (prominance relating to the respective mass abundance) that are two mass units apart confirmed the incorporation of a chlorine-containing group into the compound. That, along with the calculated masses of each of the compounds, confirm the compounds in each case. Compounds **3.10** and **3.11** stem from the Isomers **3.5** and **3.6,** and as a result, compounds **3.10** and **3.11** are also isomers with the same chemical formulae and molecular mass (**Figure 3.15**). After looking at all the spectroscopic analysis results, it was safe to confirm our attempts at cross-coupling reactions of aryl bromides and aryl amines were successful.

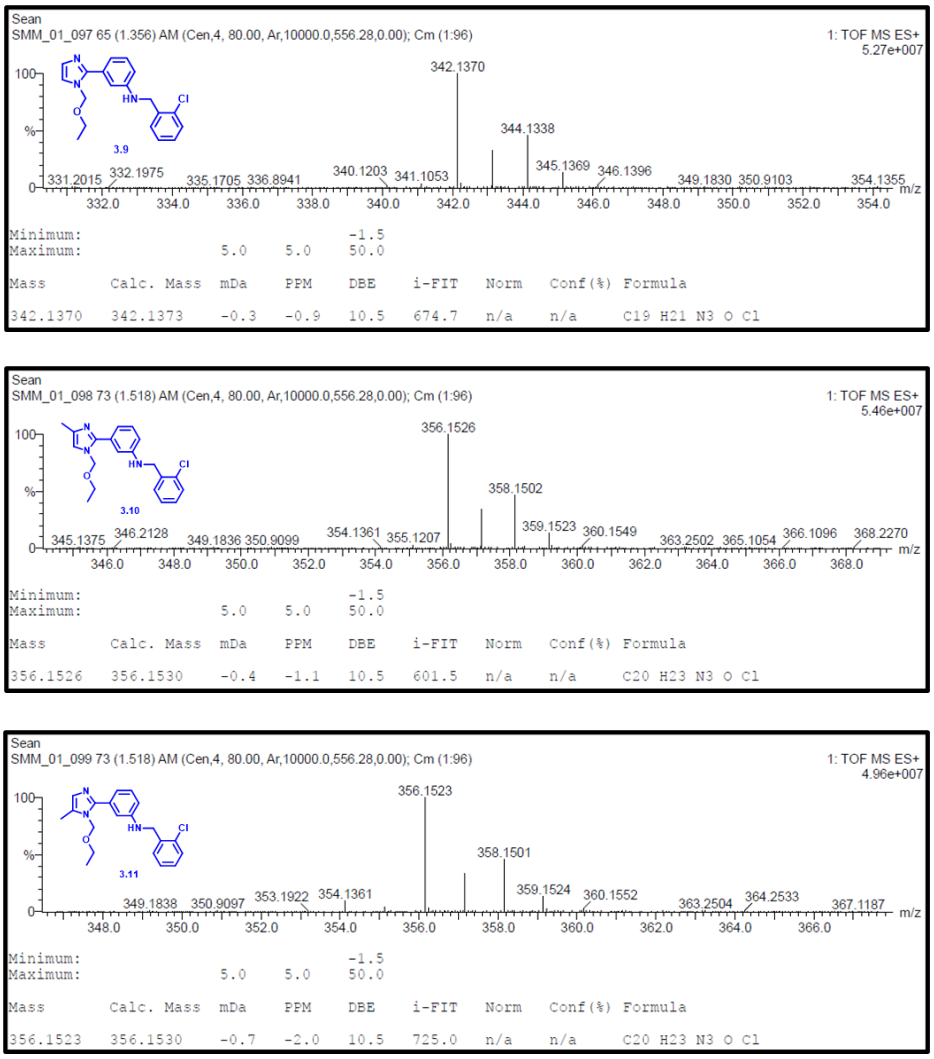

Figure 3.15: HRMS spectra of compounds **3.9**, **3.10** and **3.11**.

The progress made up to this point is somewhat gratifying. To complete our designed synthesis, the next step was to fluorinate our compounds at their respective desired positions, remove the ether arm, and restore the N-H functional group of the imidazole ring. The fluorination of these compounds was then explored.

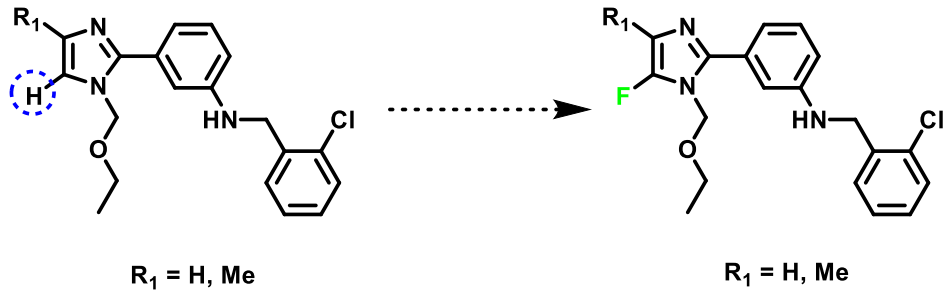

Scheme 3.10: Proposed regioselective fluorination.

3.4 Regioselective fluorination reactions

The introduction of fluorine at specific positions of pharmaceutically significant targets is of growing significance in modern pharmaceutical research and drug development.[120-122] A large pool of target molecules that contain fluoroimidazole demonstrate substantial biologically activity across various disease domains, such as dermatology, oncology, and infectious disorders.[123, 124] With this idea in mind, we adapted the work of Albertshofer and Mani[108] where they reported the electrophilic fluorination of some rationally designed Imidazoles using *N*-fluorobenzenesulfonimide as the fluorinating agent. This fluorination was facilitated by *in-situ* deprotonation using lithium 2,2,6,6-tetramethylpiperidine (LTMP).

From a study done by Chadwick and Ngochindo[125] in 1984, it was noted that imidazoles consisting of alkyloxymethyl ethers perform excellently in transformation reactions involving lithiation, and they also have high potential as *ortho*-directing groups.[125-127] Based on the findings of these two groups and many others, we were able to anticipate the possible fluorination sites for compounds **3.9**, **3.10** and **3.11** (**Figure 3.16**). We can then explore the potential of obtaining 5-fluoroimidazoles from the three mentioned compounds.

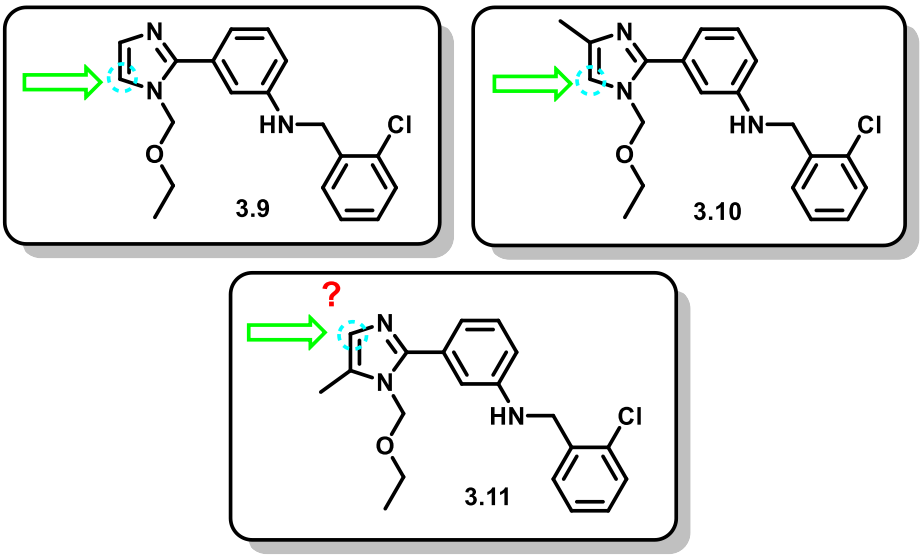

Figure 3.16: Anticipated fluorination sites for compounds **3.9**, **3.10** and **3.11**.

Since the ether was *ortho*-directing, the fluorination of compound **3.11** did not seem plausible. However, the flourination of compound **3.10** would result in compound **3.13** which when deprotected results in the desired fluorinated compound which exists in two forms; of which one of those forms is the expected final compound from the fluorination of compound **3.11.**

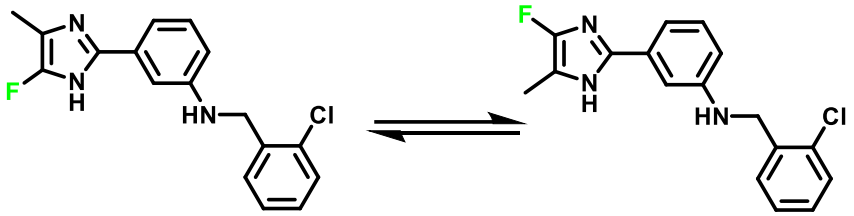

Scheme 3.11: Tautomeric forms of compound **3.13**.

Before attempting to fluorinate the three compounds, the procedure was tested on compound **3.4** (**Figure 3.17**) as it is a simpler compound and is easier to produce in good yields. Following the procedure, 2,2,6,6-tetramethylpiperidine was added to freshly dried THF under nitrogen gas at -78°C, followed by n-BuLi. The reaction mixture was stirred for 30 minutes at -78°C to achieve lithium tetramethylpiperidide. After 30 minutes of stirring, **3.4** dissolved in dry THF was added

and stirred for 10 minutes. After 10 minutes, *N*-Fluorobenzenesulfonimide precooled to -78°C was added and stirred for another 5 minutes. After 5 minutes, the reaction mixture was quenched at -78°C with ammonium chloride solution and then allowed to warm to room temperature. THF was removed *in vacuo,* followed by extraction with ethyl acetate from the aqueous solution of ammonium chloride. The organic layer was washed with brine and concentrated. The crude extract was dry-loaded into a column and purified by 100 % chloroform using column chromatography. The product **3.15** was obtained in a very low yield of 1 % and was characterised by spectroscopic techniques. Compound **3.4** was recovered from the column.

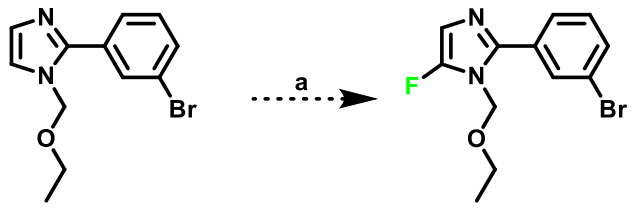

3.4 **3.15**

Scheme 3.12: Fluorination of compound **3.4**.

Reaction conditions: (a) LTMP, n-BuLi, **3.4**, NFSI, THF, -78°C, 5 min

The results obtained from ^{19}F NMR (**Figure 3.17**) coincided with those obtained by Albertshofer and Mani[108], suggesting the success of the reaction. After receiving these results, our confidence in the success of this reaction was boosted. However, the issue of the low yields is still very concerning.

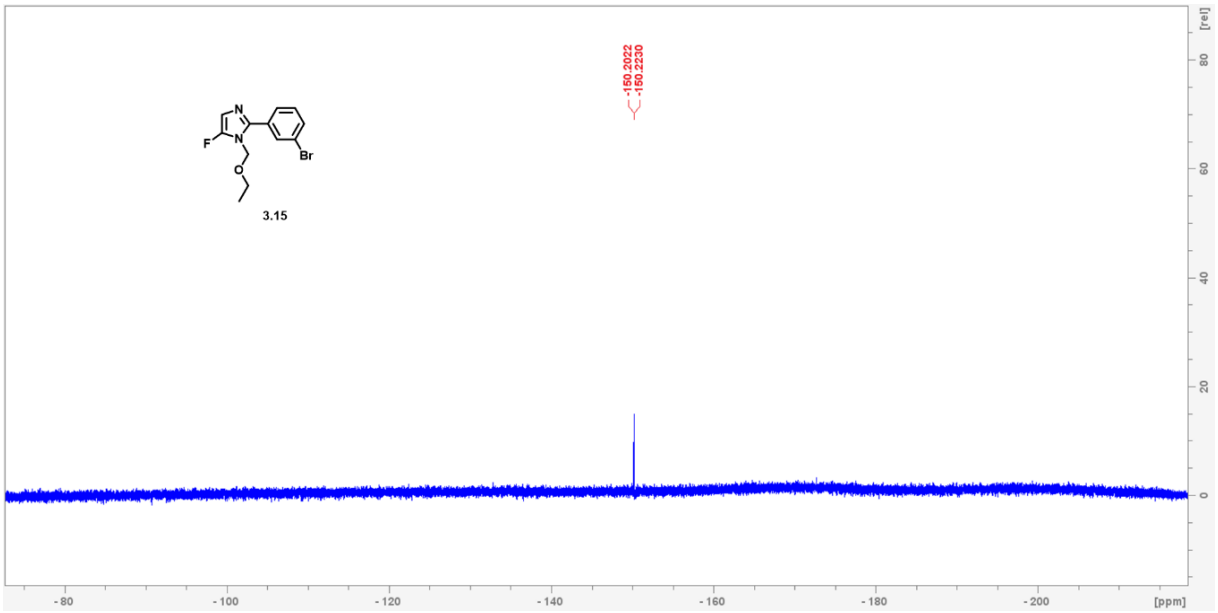

Figure 3.17: ^{19}F NMR spectrum of compound **3.15** ($CDCl_3$-*d*, 400MHz).

Albertshofer and Mani[108] investigated the effects of various functional groups at position C2. From their findings, they observed that a simple electron-neutral phenyl could only produce the product in low yields, whereas the tolerance of fluorine or chlorine in the *para* position in the same phenyl ring would result in fluorinated products converted in good yields (**Figure 3.18**). It would have been interesting to look at the mechanism to better understand the reasons behind the outcomes, but unfortunately, the authors did not provide the mechanism in their work. When they investigated the products functionalised at position C4, they observed that electronegative substituents are detrimental. After reviewing all this conflicting information, it was only safe to assume that reaction outcomes are rather analogue-specific, irrespective of electronic factors. From all this information, we gathered that the 1 % yield could be attributed to having bromine in the phenyl ring's *meta* position.

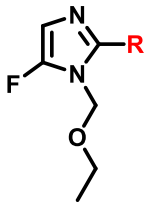

R = Cl	**55 %**
R = phenyl	**20 %**
R = 4-Cl-phenyl	**71 %**
R = 4-F-phenyl	**62 %**

Figure 3.18: The influence of the functionalisation of C2.

We then had to face the challenge of performing the fluorination on our compounds **3.9**, **3.10** and **3.11** amid all the disadvantages experienced up to this point. Compound **3.9** was the first candidate as it was the closest to compound **3.4**. The same reaction protocols (**Scheme 3.12**) were followed as for compound **3.4**. The same workup procedure was also observed, with the only difference being that the solvent system used to purify the isolated compound was 30 % ethyl acetate in chloroform instead of 100 % chloroform. The isolated compound was characterised by spectroscopic techniques.

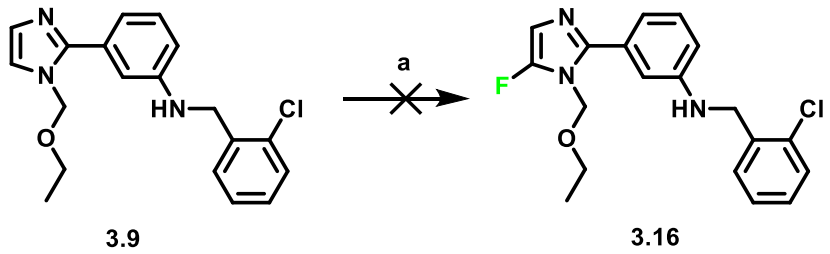

Scheme 3.13: Attempted fluorination of compound **3.9**.

Reaction conditions: (a) LTMP, n-BuLi, **3.9**, NFSI, THF, -78°C, 5 min

The results obtained from ^{19}F NMR indicated that the reaction was unsuccessful. Instead of getting a ^{19}F NMR spectrum with one signal for the expected product, we observed nine signals

on the spectrum (**Figure 3.19**). The nine fluorine signals observed in Figure **3.19** suggested that multiple fluorination reactions may have occurred.

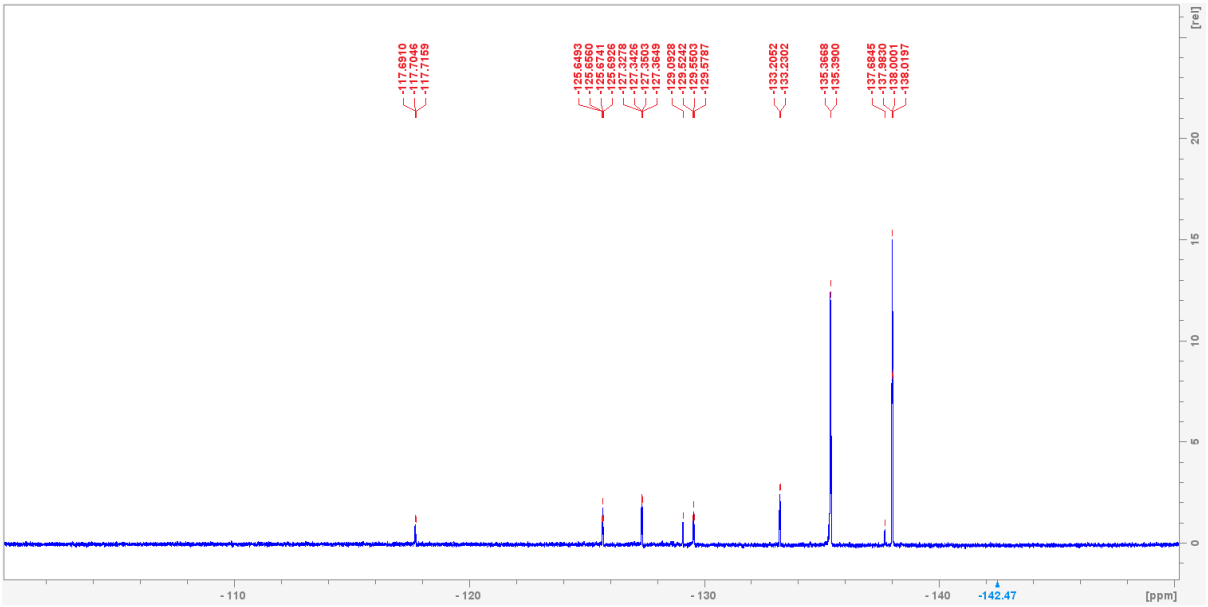

Figure 3.19: ^{19}F NMR spectrum of the failed fluorination of compound **3.9** ($CDCl_3$-*d*, 400MHz).

3.5 Exploration of other potential protecting groups

Albertshofer and Mani referred to chloromethyl ethyl ether as a removable protecting group[108], but they never provided the procedure for the removal thereof, nor did they present their attempts at trying to remove it, presumably because they did not wish to do so. However, in our work, we only needed the protecting group as a director for fluorinating our compounds.[108, 128]

We wished to perform a successful fluorination on all of our compounds directed by the ethoxymethyl group and thereafter remove the protecting group to restore the N-H bond in the imidazole ring. At an early stage, looking into the future, we opted to find a procedure for

removing the protecting group we would employ on our compounds upon successfully fluorinating them.

A study adapted from Cerezo *et al*.[129], where they dealt with an ether that attaches itself similarly to the ethoxymethyl group, was explored (**Figure 3.20**). Their work presents the removal of the protecting group [2-(trimethylsilyl)ethoxy]methyl, commonly referred to as SEM, in yields ranging from 70 – 99 %.

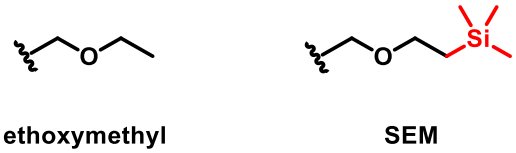

Figure 3.20: Comparison of the functionalisation of ethoxymethyl and [2-(trimethylsilyl)ethoxy]methyl.

The procedure entailed dissolving compound **3.4** in TFA/CH_2Cl_2 (2:1) and stirring at room temperature (**Scheme 3.18**). After monitoring by TLC, the reaction was stopped after 24 hours. The solvent was evaporated, and the products were separated by column chromatography.

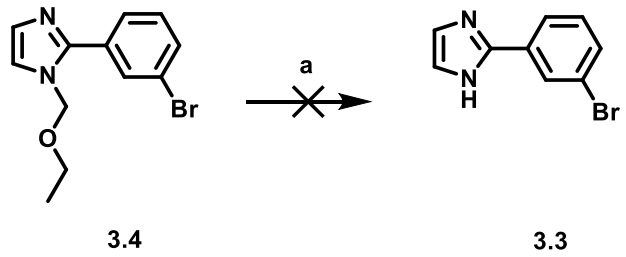

Scheme 3.14: Attempted removal of ethoxymethyl.

Unfortunately, the reaction was unsuccessful, as it was seen on the ^1H NMR spectrum that the two CH_2 and the CH_3 signals were still present (**Figure 3.21**). The expected outcome was the disappearance of the latter-mentioned signals and the appearance of the

N-H signal between 12 and 13 ppm. From the spectrum, there is no visible trace of the expected N-H signal, signifying the failure of the deprotection reaction.

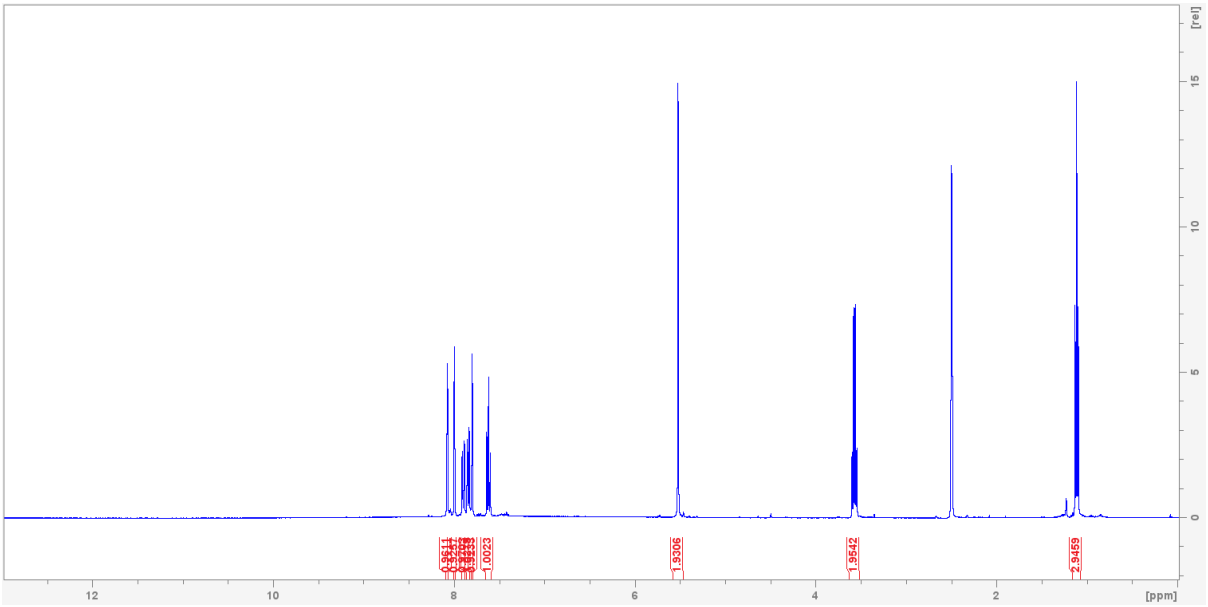

Figure 3.21: ^{1}H NMR spectrum of attempted deprotection of **3.4** (DMSO-d_6, 400MHz).

Foreseeing the challenge we would face with the detachment of this protecting group, we sought to explore other protecting groups that may not be as tedious to remove as the ethoxymethyl group. The best candidate would be a group that can be easily attached, correctly direct the fluorination, and detach easily from the final compound. The three compounds we investigated as possible protecting groups are benzyl bromide, trityl chloride and di-*tert*-butyl dicarbonate (**Figure 3.22**).

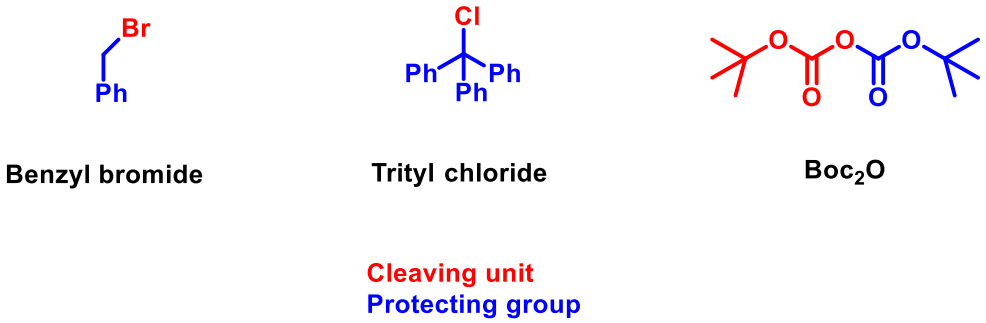

Figure 3.22: Investigated possible protecting groups.

3.5.1 Synthesis of 1-benzyl-2-(3-bromophenyl)-1H-imidazole (3.17)

Compound **3.17** was afforded by exploring a study done by Park[130] and his group, where they investigated the capabilities of benzyl bromide as a protecting group *via* its debromination. The benzyl group has previously been reported as a robust protecting group. The procedure written by Park *et al*.[130] works effortlessly with good yields in a short amount of time. Following the procedure, we dissolved compound **3.3** in DMF and added sodium *tert*-butoxide and benzyl bromide. The mixture was then stirred for an hour at 60 °C. The mixture was extracted with DCM and washed twice with brine. The organic layer was dried with anhydrous magnesium sulphate and concentrated. Compound **3.17** was obtained through column chromatography isolation, eluting with 5% methanol in DCM (**Scheme 3.19**).

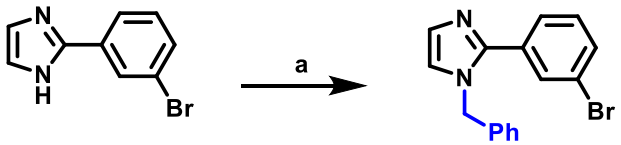

75 %

3.3 **3.17**

Scheme 3.15: Imidazole protection by benzyl group.

Reaction conditions: (a) **3.4**, sodium tert-butoxide, benzyl bromide, DMF, 60°C, 1 h

This reaction afforded compound **3.17** in a good yield of 75 %, and the ^{1}H NMR spectrum reveals the success of the reaction by the total number of proton integrations adding up to the expected value of 13 protons. The most apparent giveaway would be the signal integrating for two protons at 5.36 ppm, belonging to the benzyl CH_2 (**Figure 3.23**). The successful synthesis of the compound was also confirmed by mass spectrometry.

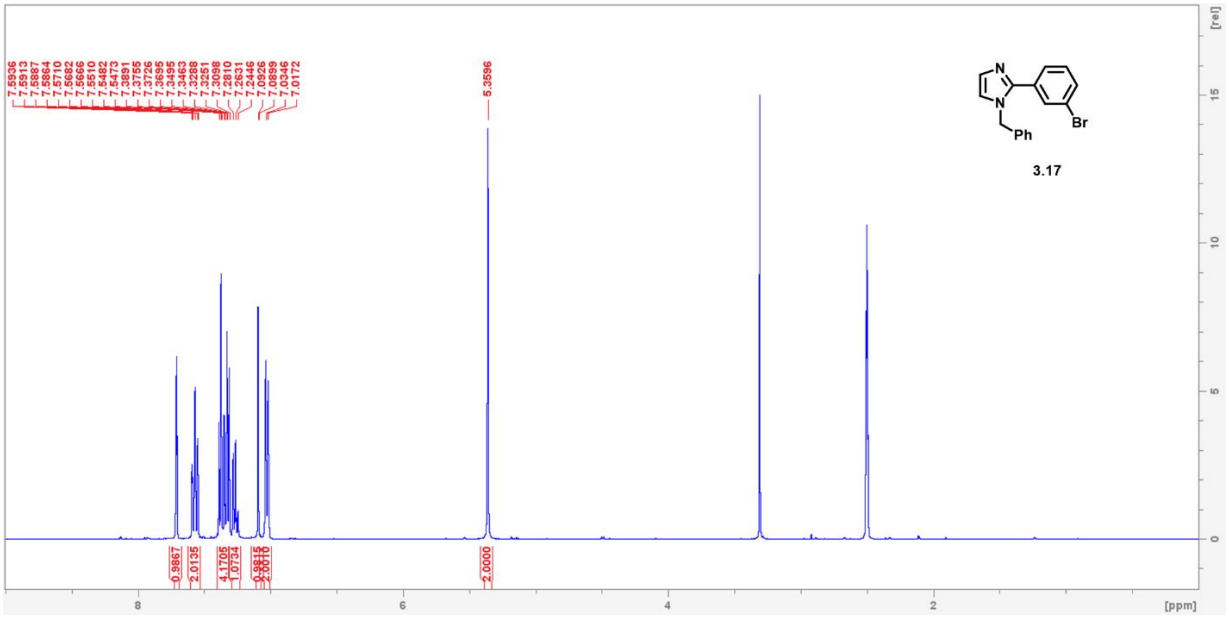

Figure 3.23: ^{1}H NMR spectrum of compound **3.17** ($CDCl_3$-*d*, 400MHz).

The success of this reaction was very pleasing. However, the main issue here is that the protecting group itself is very similar to the benzylamine group that would have to be coupled to the compound in the subsequent reaction (**Scheme 3.20**). There is a selectivity concern regarding the selective removal of the correct benzyl group. We wish to perform a selective deprotection later, so using a benzyl group as a protecting group in the presence of a 2-chlorobenzyl group in the same substrate hinders that possibility. For that reason, this method was aborted and other avenues had to be explored.

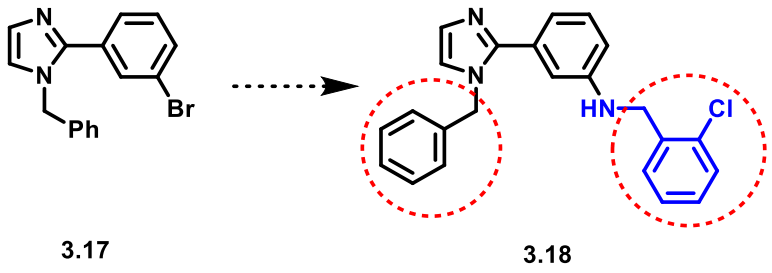

3.17 3.18

Scheme 3.16: Anticipated Buchwald-Hartwig amination of compound **3.17**.

3.5.2 Synthesis of compound 3.19

Compound **3.19** was obtained following a procedure adapted from Okano *et al*.[131], where they performed *N*-Boc protection. In their work, they applied this procedure to primary amines and the yields were satisfying. However, in the case of our secondary amine, the reaction was a success, but the yields were low. Following the procedure, we added sodium bicarbonate and di-*tert*-butyl dicarbonate to a solution of **3.3** dissolved in acetone/water (1:1) and stirred the mixture at room temperature overnight (**Scheme 3.21**). Upon stopping the reaction, acetone was evaporated, and the remaining solvent was acidified to pH = 7 with 32 % HCl. The product was extracted from water with ethyl acetate. Thereafter, the organic layer was washed with brine and concentrated. The product was purified by column chromatography using ethyl acetate/*n*-hexane (1:1) to afford a brown oil in a very low 14 % yield. The compound was characterised by spectroscopic techniques.

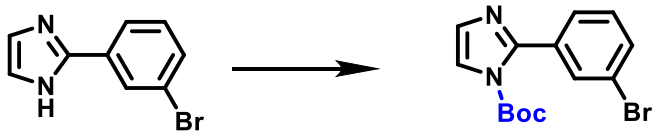

3.3 3.19

14 %

Scheme 3.17: *N*-Boc protection of the secondary amine group of the imidazole.

Reaction conditions: (a) **3.3**, $NaHCO_3$, BOC_2O, acetone/water (1:1), rt, overnight

The ^{1}H NMR spectrum indicated the success of this conversion. There were six aromatic protons, as expected, and the most significant change was the appearance of the nine protons upfield, which belong to the *tert*-butyl of the Boc protecting group (**Figure 3.24**).

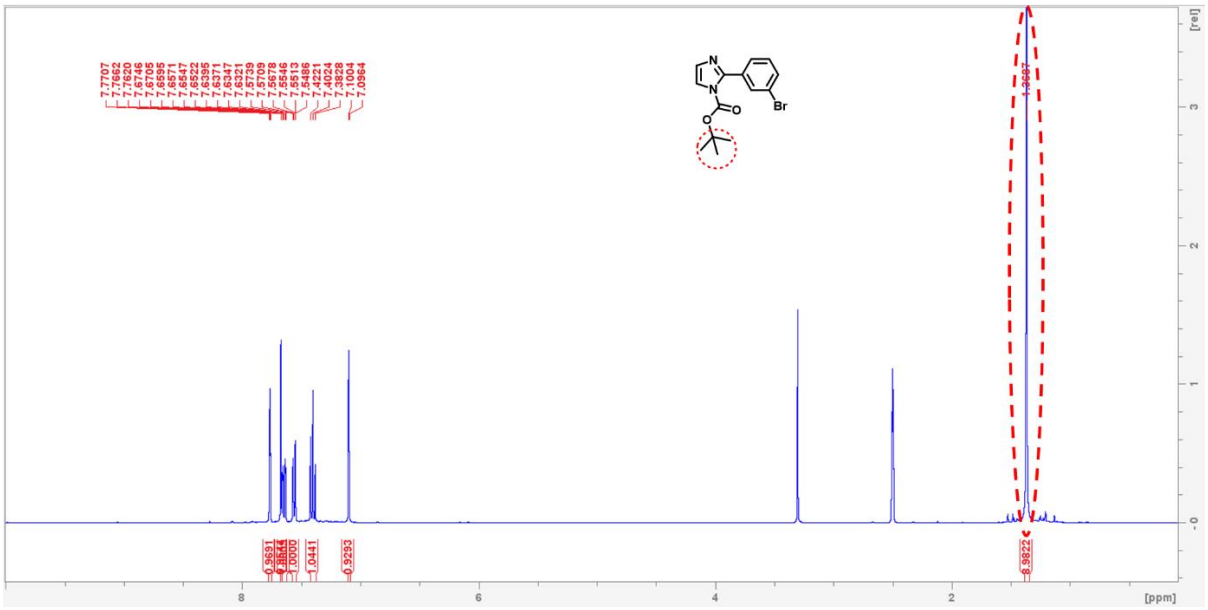

Figure 3.24: ^{1}H NMR spectrum of compound **3.19** (DMSO-d_6, 400MHz).

We spotted a few indications confirming our compound on the FTIR spectrum. We can focus on four significant functional groups to confirm this compound (**Figure 3.25**). The weak band observed at 2979 cm^{-1} is attributed to the C=C-H bonds of the imidazole ring (red). The strong band observed at 1752 cm^{-1} is ascribed to the carbonyl group (magenta). The strong band observed at 1287 cm^{-1} is attributed to the C-N bond of the *N*-Boc bonding (blue). The strong band observed at 1142 cm^{-1} is of the carboxylate group (green). The band observed at 704 cm^{-1} is attributed to the C-Br bond of the aryl ring (yellow).

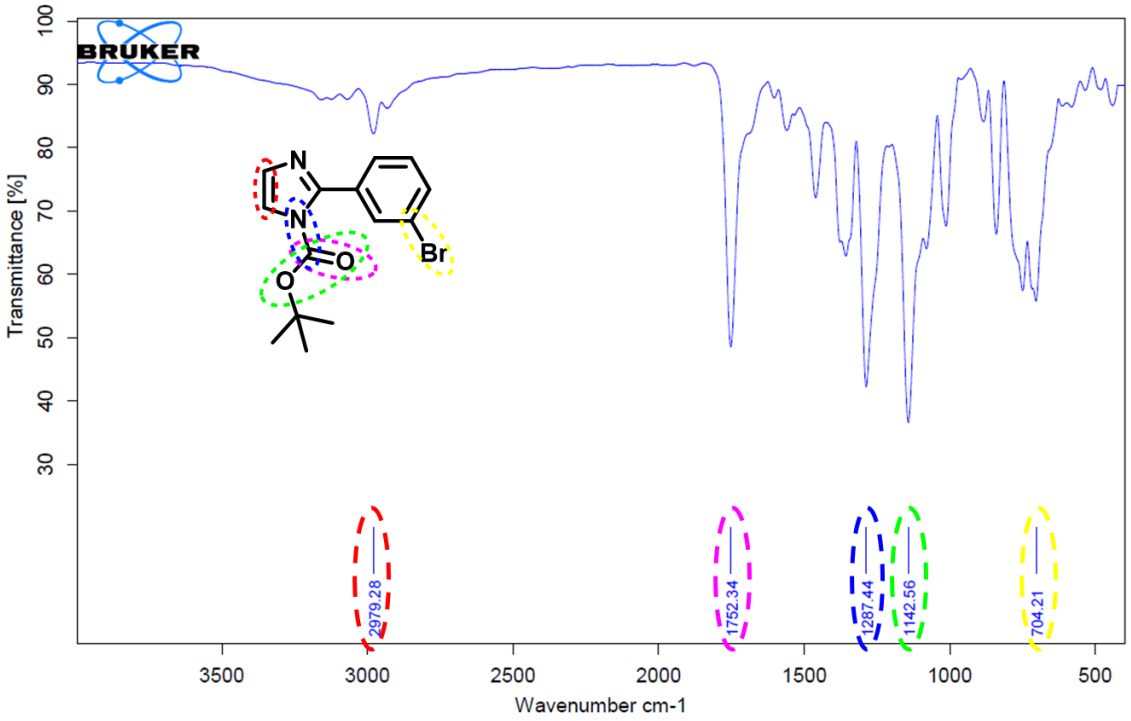

Figure 3.25: FTIR spectrum of compound **3.19**.

Having confirmed the compound, all that was left to do was to couple it to the benzylamine, try fluorinating it, and then deprotect it to remove the Boc protecting group. Before this, we proceeded to investigate one more protecting group.

3.5.3 Synthesis of compound 3.20

The trityl group was the last protecting group to be explored. Compound **3.20** was afforded by following a procedure adapted from Zhang *et al.*[132] where triethylamine was added dropwise below 0 °C to a solution of compound **3.3** in DCM, with trityl chloride added last (**Scheme 3.22**). The reaction mixture was stirred at room temperature for three hours and concentrated thereafter. Compound **3.20** was isolated using column chromatography, eluting 30% ethyl acetate in *n*-hexane and obtained as a white powder in 53% yield. This powder was crystallised in DCM

to produce clear glacial crystals. This compound was, therefore, characterised by spectroscopic techniques and single X-ray crystallography.

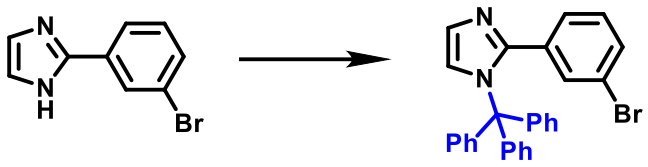

3.3 **3.20**

53 %

Scheme 3.18: Protection of the imidazole N-H bond by trityl chloride.

Reaction conditions: **3.3**, TEA, trityl chloride, DCM, rt, 3 h.

The compound's molecular formula and molecular weight were confirmed by high-resolution mass spectrometry and X-ray crystallography. The results obtained from both methods coincided with the expected outcome. The HRMS spectrum shows the exact (465.0973 m/z) and calculated (465.0966 m/z) masses for compound **3.20** (**Figure 3.26**).

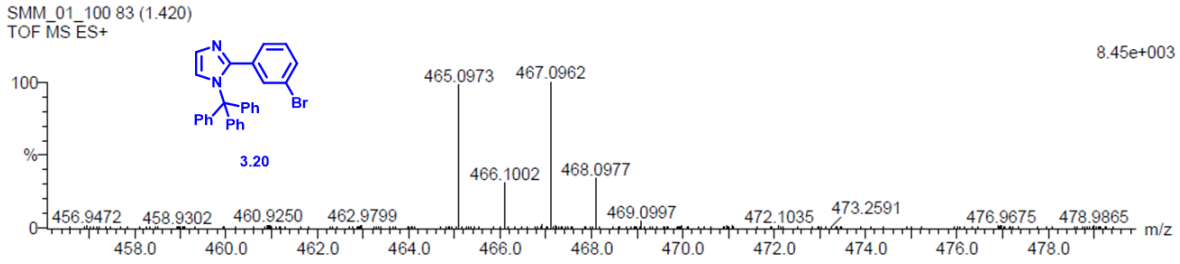

Minimum:			-1.5				
Maximum:		5.0	5.0	50.0			
Mass	Calc. Mass	mDa	PPM	DBE	i-FIT	Norm	Conf(%) Formula
465.0973	465.0966	0.7	1.5	18.5	193.6	n/a	n/a C28 H22 N2 Br

Figure 3.26: HRMS spectrum of compound **3.20**.

The X-ray structure of compound **3.20** is shown in **Figure 3.27**. In the figure, hydrogen atoms have been omitted for clarity.

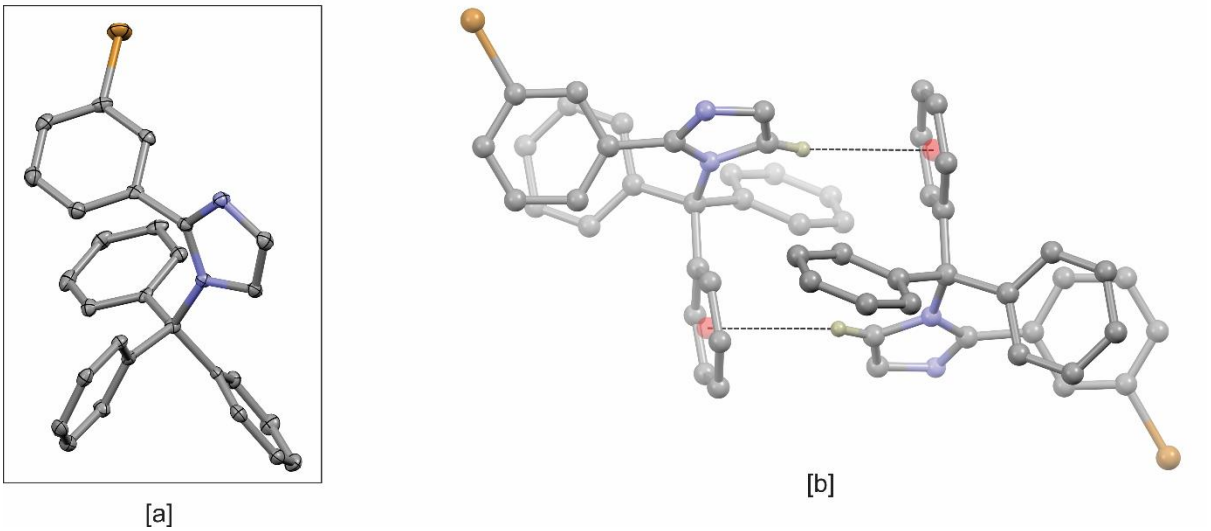

Figure 3.27: [a] Thermal ellipsoid plot showing 50% probability surfaces for compound **3.18**. Hydrogen atoms have been omitted for clarity. Atom colours: grey = carbon, beige = hydrogen, blue = nitrogen and light brown = bromine.

The compound crystallised in the monoclinic Space Group P21/n with a single molecule in the asymmetric unit, i.e. Z = 4 **[a]**. In the absence of any H-bond donors, the structure does not show any significant intermolecular interactions. The molecules are, however, weakly associated through C–H···π interactions between the imidazole C–H and phenyl ring of an adjacent molecule. These weak interactions link the molecules to form dimers. The distance from the C–H to the centroid of the phenyl ring measures 3.165 Å **[b]**.

Zhang *et al*.[132] had also successfully performed a deprotection of this trityl group. We also adopted that procedure to explore the removal of this group. Sodium hydroxide (1.0 M) was added dropwise to a solution of compound **3.20** dissolved in methanol. The reaction mixture was stirred overnight at reflux (**Scheme 3.23**). The solvent was then evaporated, and the remaining reaction mixture was diluted with distilled water. The mixture was acidified to a pH of between 4

and 5 with 3.0 M HCl and extracted with DCM. The organic layer was dried, concentrated, and purified by column chromatography, eluting ethyl acetate/*n*-hexane (5.5:4.5). A light-brown precipitate was obtained as expected but at a very low yield of 13 %.

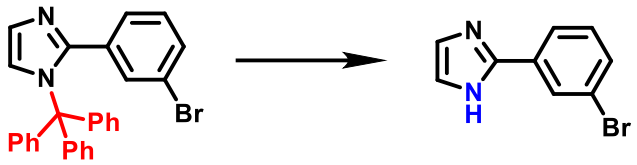

3.20 **3.3**

13 %

Scheme 3.19: Removal of trityl protecting group.

Reaction conditions: **3.20**, 1.0 M NaOH, MeOH, reflux, overnight.

The obtained compound was confirmed through spectroscopy. The HRMS spectrum confirmed the molecular formula and the molecular weight of the expected compound. The spectrum of the obtained product (top) was compared with the spectrum of compound **3.3** (bottom) as a reference (**Figure 3.28**). The obtained sample was run in positive mode (TOF MS ES+), whereas sample 3.3 was run in negative mode (TOF MS ES-), both agreeing to the same molecular formula.

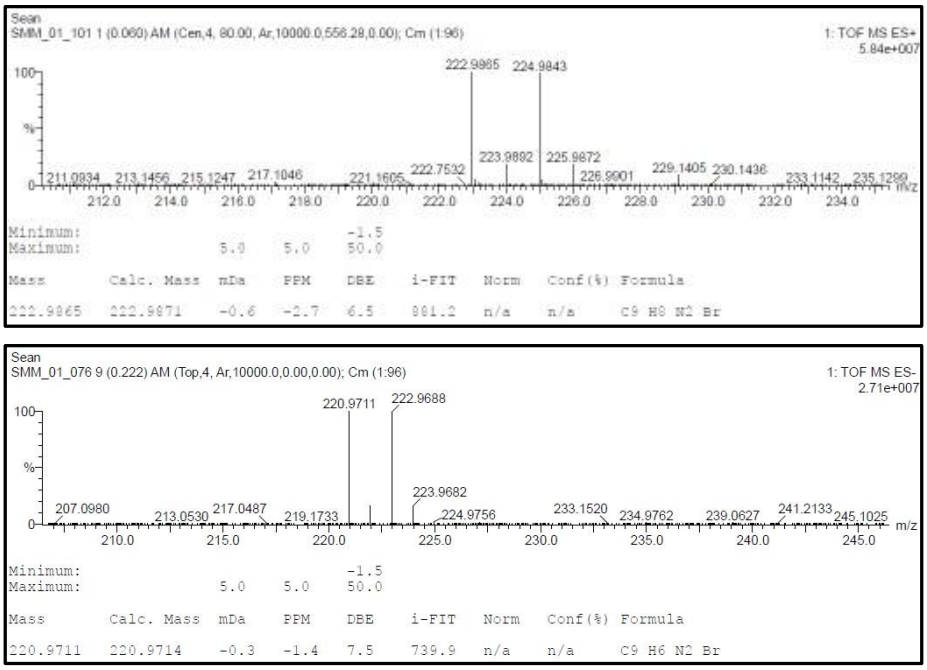

Figure 3.28: HRMS spectra of compound **3.3** (+/- mode).

The trityl group was identified as a potential protecting group for our study. The only thing left to explore is its potential as a fluorination-directing group. However, a method for removing the ethoxymethyl group was discovered before we could explore this.

3.6 Removal of ethoxymethyl protecting group

From a study done by Basarab *et al*.[133], a reaction involving the deprotection of an alkyloxymethyl ether very similar to the one used in our study was found. The reaction conditions were harsh, but we had to explore them since this protecting group was our best candidate for the fluorination reaction. This procedure involved heating compound **3.4** in a microwave reactor at 120 °C for two hours with acetic acid/water (8:1) as the solvent. The residue was then partitioned between a solution of sodium bicarbonate and ethyl acetate. The organic layer was washed with brine and concentrated.

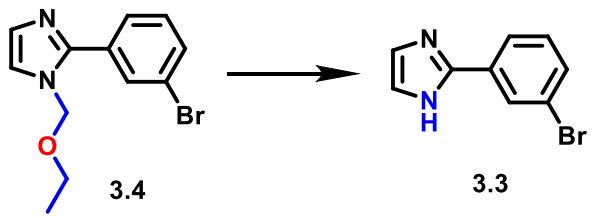

Scheme 3.20: Deprotection of compound **3.4**.

Reaction conditions: **3.4**, acetic acid/water (8:1), MW, 120°C, 2 h.

The ^{1}H NMR spectrum of the crude product clearly shows the emergence of the expected N-H signal at 12.6 ppm while also showing traces of the ethoxymethyl chain protons upfield (**Figure 3.29**). The biggest challenge at this stage was the fluorination reaction, which was not working on our amine-coupled compounds. Due to time and resource limitations, we were unsuccessful at fluorinating our compounds **3.9**, **3.10** and **3.11**, and therefore we did not reach this deprotection step.

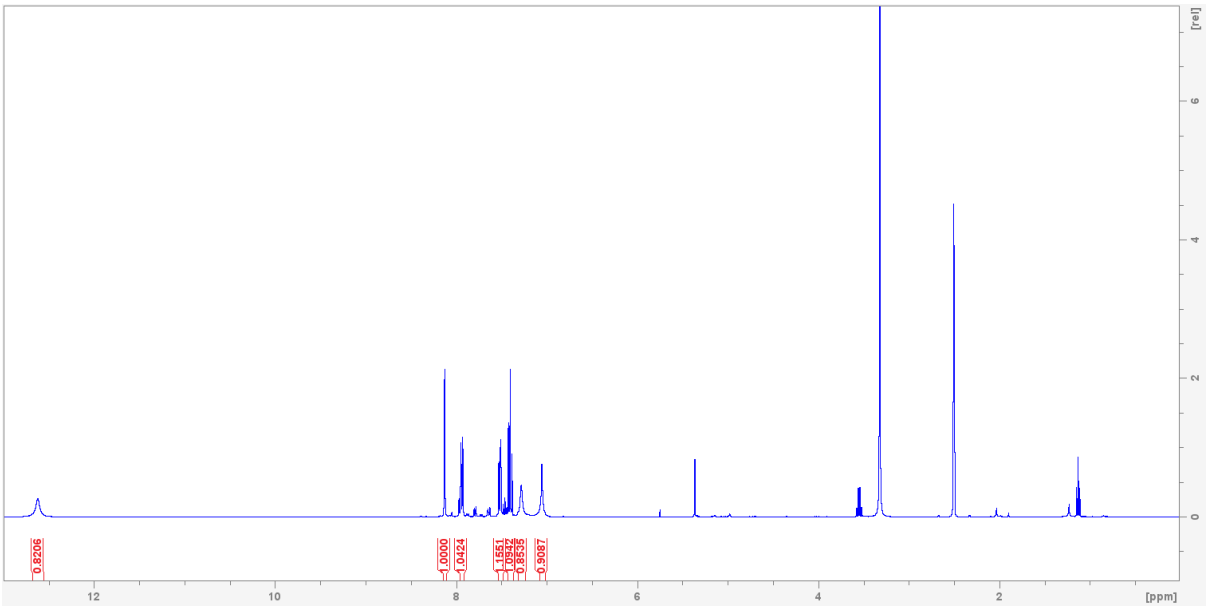

Figure 3.29: ^{1}H NMR spectrum of crude deprotection reaction (DMSO-d_6, 400MHz).

3.7 Conclusion

The methods adopted from the Eseola and Hedström groups for synthesising the imidazole compounds **3.1**, **3.2** and **3.3** were carried out successfully despite poor yields (33 – 42 %). Further exploration of methods that can produce these compounds in good yields is imperative, considering the fact that this is the first step of this synthesis. Starting a five-step synthesis with poor yields is concerning. Nonetheless, the compounds were successfully obtained and characterised.

The ethoxymethyl protection of compounds **3.2** and **3.3** through a method adopted from Albertshofer and Mani resulted in the successful production of compounds **3.4**, **3.5** and **3.6**. The subsequent cross-coupling reaction also successfully produced compounds **3.9**, **3.10** and **3.11**, though in very poor yields (7 – 41 %). The greatest challenge we faced was the fluorination of the three compounds (**3.9**, **3.10** and **3.11**). An establishment made by Albertshofer and Mani was that the success of the fluorination reaction in each case is substrate-specific, suggesting that the substituents present in the substrate and the positioning thereof, all affect the success of the reaction.

Since the fluorination reactions were unsuccessful, it was unfortunate that we could not proceed onto the biological assays to determine the antiplasmodial activity of the compounds. The study aimed to functionalise hit compound MMV023227, create analogues of it through fluorine functionalisation, and assess the antiplasmodial activity of the synthesised analogues. Since we were unsuccessful, this hindered us from exploring the structure-activity relationship of MMV023227 and its analogues, hampering our efforts towards developing new antiplasmodial agents.

3.8 Future work extending from this study

- Exploring better yielding reactions for the imidazole-forming and cross-coupling reactions.
- The fluorination reaction performed in this study reflected a hint of hope. However, another method should be considered to explore its potential for success to lead us to our anticipated analogues.
- Upon the success of the fluorination reactions, the antiplasmodial activity of the compounds can be assessed against Plasmodium parasites.

4. CHAPTER FOUR: EXPERIMENTAL DATA

4.1 General Experimental Information

4.1.1 Materials

All solvents and reagents used were purchased from Honeywell or Sigma-Aldrich and were used as bought. All reactions incorporating the use of moisture-sensitive reagents were performed under inert conditions under nitrogen using oven-dried glassware and anhydrous solvents.

4.1.2 Chromatography

Thin layer chromatography (TLC) analysis was carried out aluminium-backed silica gel 60 F_{254} plates visualized under ultraviolet light. All compounds were purified by column chromatography packing silica gel 60, 0.063-0.0200 mm, 70-230 Mesh ASTM. Radial chromatography was performed on the Chromatotron™ with a circular glass plate coated with 2 mm thick preparative silica gel 60 PF_{254} containing gypsum, particle size ≤ 45 µm.

4.1.3 Analysis

All nuclear magnetic resonance (**NMR**) data were obtained using standard pulse sequences on the Bruker Avance III 500 (500 MHz for ^{1}H, 125 MHz for ^{13}C, and 470 MHz for ^{19}F) and 400 (400 MHz for ^{1}H, 100 MHz for ^{13}C, and 376 MHz for ^{19}F). Proton chemical shifts are expressed in parts per million (ppm) and are compared to the NMR solvent, which serves as the internal standard ($CDCl_3$: δ 7.26; CD3OD: δ 3.31; (CD3)2SO: δ 2.50; (CD3)2CO: δ 2.05). Carbon chemical shifts are expressed in parts per million (ppm) and are compared to the NMR solvent peak ($CDCl_3$: δ 77.16; CD3OD: δ 49.00; (CD3)2SO: δ 39.52; (CD3)2CO: δ 29.84). NMR spectral data is reported as: chemical shift, multiplicity (b = broad, s = singlet, d = doublet, t = triplet, q = quartet, m = multiplet), coupling constants (J) in Hertz (Hz) and integration.

Infrared (**IR**) spectra were recorded on an Alpha ll FTIR spectrometer. Absorption maxima are expressed in wavenumbers (cm^{-1}).

High-Resolution Mass Spectrometric (**HRMS**) analysis was performed on a Waters Synapt XS TOF spectrometer with an ESI source.

Melting points were obtained using Kofler hot stage melting point apparatus and are expressed in °C.

4.1.4 X-ray crystallography

An Incoatec microsource with 30 W power and an Oxford Instruments Cryojet operating at 100(2) K were used to record the X-ray data on a Bruker Apex Duo. Tabulated in **Table 4.1** are the results of crystal and structural refinement. At a distance of 50 mm between the crystal and detector, the data were acquired using CuKα radiation (λ = 1.54178 Å). To gather this data, we employed the following conditions: APEX2[134] was used to take exposures of omega and phi scans with X-ray power of 30 W and frame widths of 0.50°. The SAINT[134] program was used to compress the data by applying typical Lorentz and polarization correction factors, scaling the scan speed, and outlier rejection. The information was subjected to a SADABS semi-empirical multi-scan absorption correction.[134] To solve both structures, direct approaches SHELX-2014[135] and WinGX[136] were utilized. The difference density map was used to locate all non-hydrogen atoms, which were then refined anisotropically with SHELX-2014.[135] The least squares method idealized the contribution of all hydrogen atoms. They were located according to a conventional riding model that took into account $C\text{-}H_{aromatic}$ distances of 0.93 Å and U_{iso} = 1.2 Ueq, $C\text{-}H_{methylene}$ distances of 0.99 Å and U_{iso} = 1.2 Ueq, and $C\text{-}H_{methyl}$ distances of 0.98 Å and U_{iso} = 1.5 Ueq.

Table 4.1: Crystal data and structure refinement summary for compounds **3.2** and **3.18**.

Crystal Data	**3.2**	**3.18**
Chemical Formula	$C_{10}H_9BrN_2$	$C_{28}H_{21}BrN_2$
Molar Mass g mol^{-1}	237.10	465.38
Crystal system, space group	Monoclinic, $P2_1/n$	Monoclinic, $P2_1/n$
a, b, c/Å	5.0339(4), 20.3252(15), 9.2226(7)	8.7664(16), 10.3419(19), 23.552(4)
α, β, γ °	α = 90 β = 98.178(3) γ = 90	α = 90 β = 93.841(3) γ = 90
Temperature/K	100(2)	100(2)
Z	4	4
V/Å^3	934.01(12)	2130.5(7)
T_{min}, T_{max}		
S	1.121	1.065
μ/mm^{-1}	5.589	1.948
Crystal Dim./mm^3	0.375 × 0.295 × 0.175	0.26 × 0.25 × 0.135
Data Collection		
Total, unique data	36203, 1798	76498, 4586
R_{int}	0.0473	0.1371
Refinement		
Final R indices, [I>2σ(I)]	R_1 = 0.0326, wR_2 = 0.0823	R_1 = 0.0411, wR_2 = 0.1001

4.2 Experimental Procedures and Characterizations

4.2.1 Synthesis of 2-(3-bromophenyl)-4,5-disubstituted imidazole derivatives

2-(3-bromophenyl)-4,5-dimethyl-1*H*-imidazole (3.1)

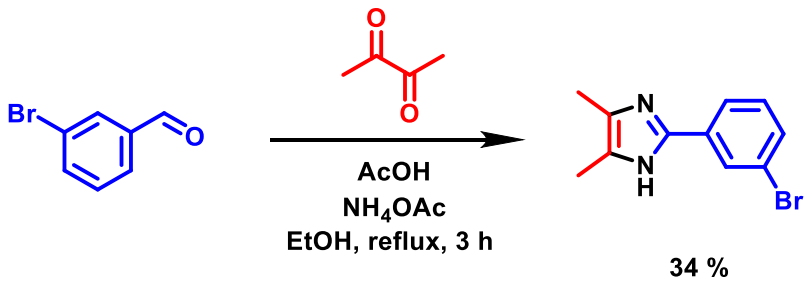

A solution of 2,3-butanedione (87 µL, 1.00 mmol, 1.00 eq.), 3-bromobenzaldehyde (116.6 µL, 1.00 mmol, 1.00 eq.), and ammonium acetate (1.00 g, 12.97 mmol, 12.97 eq.) in ethanol (1.00 mL) was refluxed with acetic acid (50 µL) as a catalyst. After stirring for 3 hours, the reaction mixture was cooled. The mixture was then diluted with distilled water (10 mL) and then concentrated ammonia solution was added dropwise to neutralize the solution. The crude product was filtered and purified by column chromatography using ethyl acetate/*n*-hexane (1:1, v/v) isocratic system as eluent, yielding a pale yellow solid (85.4 mg, 0.34 mmol, 34% yield).

2-(3-bromophenyl)-4,5-dimethyl-1*H*-imidazole: yellow solid (34% yield); **Mp:** 201 – 202 °C; **IR** (vmax cm^{-1}) 3148, 2626, 1684, 1253, 713; **^{1}H NMR** (DMSO-d_6, 400MHz): δ_H 12.12 (bs, 1H), 8.04 – 8.01 (m, 1H), 7.86 – 7.82 (m, 1H), 7.45 – 7.41 (m, 1H), 7.37 – 7.32 (m, 1H), 2.11 (bs, 6H); **^{13}C NMR** (DMSO-d_6, 400MHz): δ_C 141.0, 133.2, 130.8, 129.6, 126.5, 122.9, 122.1 ppm; **HRMS** (ESI) m/z 249.0026 (calculated for $C_{11}H_{10}N_2Br$ $[M-H]^-$ 249.0027).

2-(3-bromophenyl)-4-methyl-1*H*-imidazole (3.2)

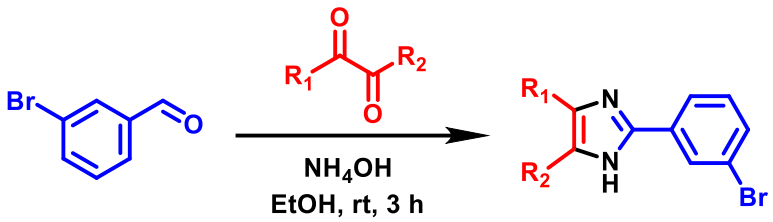

(3.2) R_1 = CH_3, R_2 = H, **33 %**
(3.3) R_1 = R_2 = H, **42 %**

To a solution of 3-bromobenzaldehyde (5.82 mL, 50.00 mmol, 1 eq.) in ethanol (100 mL) at 0 °C, methylglyoxal solution (15.4 mL, 100.00 mmol, 2 eq.) and ammonia solution (70 mL) were added. The reaction mixture was stirred at room temperature for 3 hours and then the solvent was removed by rotary evaporation until a precipitate formed in the water layer. The precipitate was filtered off by vacuum filtration and washed with distilled water and dried. A white filtrant was obtained (2.39 g, 10.07 mmol, 20 % yield). The filtrate was collected and extracted with dichloromethane/methanol (10:1, v/v). Following extraction, the organic phase was washed with brine and concentrated by rotary evaporation, resulting in a brown oil. The brown oil was purified by silica gel chromatography using ethyl acetate/*n*-hexane (1:1, v/v) isocratic system as eluent, yielding a yellow precipitate (1.55 g, 6.55 mmol, 13 % yield). The column extract was mixed with the white filtrant after they showed identical proton NMR spectra. The two, combined, yielded a yellow solid (3.94 g, 16.61 mmol, 33% yield).

2-(3-bromophenyl)-4-methyl-1*H*-imidazole: yellow solid (33% yield); **Mp:** 215 – 216 °C; **IR** (vmax cm^{-1}) 3063, 2668, 1576, 1088, 671; **^{1}H NMR** (DMSO-d_6, 500MHz): δ_H 12.40 (bs, 1H), 8.10 – 8.06 (m, 1H), 7.90 – 7.86 (m, 1H), 7.49 – 7.44 (m, 1H), 7.39 – 7.34 (m, 1H), 6.84 (s, 1H), 2.19 (bs, 3H); **^{13}C NMR** (DMSO-d_6, 500MHz): δ_C 143.1, 133.1, 130.8, 130.0, 126.8, 123.3, 122.1, 13.7 ppm; **HRMS** (ESI) m/z 237.0030 (calculated for $C_{10}H_{10}N_2Br$ $[M+H]^+$ 237.0027).

2-(3-bromophenyl)-1*H*-imidazole (3.3)

A solution of glyoxal solution (1.17 µL, 10.00 mmol, 1 eq.) and ammonia solution (14 mL) was added into a solution of 3-bromobenzaldehyde (2.33 µL, 20.00 mmol, 2 eq.) in ethanol (20 mL) at 0 °C. The reaction mixture was stirred for 3 hours at room temperature, thereafter, diluted with distilled water and extracted with dichloromethane. The organic phase was washed with brine and concentrated by rotary evaporation to give a brown oil, which was then dry-loaded into a silica gel column and purified using ethyl-acetate/*n*-hexane (1:1, v/v) isocratic system as eluent. A yellow solid was obtained (932 mg, 0.418 mmol, 42% yield).

2-(3-bromophenyl)-1*H*-imidazole: yellow solid (42% yield); **Mp:** 154 – 155 °C; **IR** (vmax cm^{-1}) 3121, 2733, 1678, 1170, 676; **^{1}H NMR** (DMSO-d_6, 500MHz): δ_H 12.63 (bs, 1H), 8.18 – 8.09 (m, 1H), 7.98 – 7.92 (m, 1H), 7.55 – 7.47 (m, 1H), 7.44 – 7.35 (m, 1H), 7.17 (bs, 2H); **^{13}C NMR** (DMSO-d_6, 500MHz): δ_C 144.0, 133.0, 130.9, 130.4, 127.2, 123.6, 122.1 ppm; **HRMS** (ESI) m/z 220.9711 (calculated for $C_9H_6N_2Br$ $[M-H]^-$ 220.9714).

4.2.2 Synthesis of ether-protected imidazole derivatives

General procedure for the imidazole protection (A): The imidazole (1 eq.) was dissolved in tetrahydrofuran, followed by sodium hydride (60% dispersion in oil) (4 eq.) and chloromethyl ethyl ether (1.2 eq.) to give a brown suspension. After stirring for 3 hours at room temperature, the solvent was removed by rotary evaporation. The remaining contents of the flask were dissolved in chloroform and washed with ammonium chloride. The resulting organic layer was dried and concentrated, giving a brown oil. The crude product was purified by silica gel chromatography using chloroform/methanol (9.5:0.5, v/v) as eluent.

2-(3-bromophenyl)-1-(ethoxymethyl)-1*H*-imidazole (3.4)

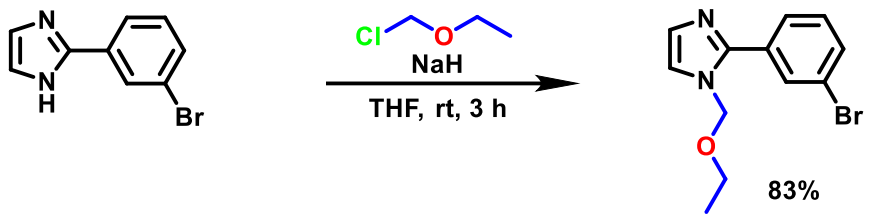

Synthesized according to General Procedure A, starting with sodium hydride (667.05 mg, 16.68 mmol, 4 eq.), chloromethyl ethyl ether (464 µL, 5.00 mmol, 1.2 eq.) and 2-(3-bromophenyl)-1*H*-imidazole (920 mg, 4.12 mmol, 1 eq.) in tetrahydrofuran (8 mL). A reddish-brown oil was obtained (959 mg, 3.42 mmol, 83% yield).

2-(3-bromophenyl)-1-(ethoxymethyl)-1*H*-imidazole: reddish-brown oil (83% yield); **IR** (vmax cm^{-1}) 2894, 1597, 1253, 1083, 687; **^{1}H NMR** ($CDCl_3$-*d*, 400MHz): δ_H 7.93 – 7.91 (m, 1H), 7.68 – 7.64 (m, 1H), 7.46 – 7.42 (m, 1H), 7.25 – 7.20 (m, 1H), 7.06 – 7.02 (m, 2H), 5.16 (s, 2H), 3.47 (q, *J* = 7.0 Hz, 2H), 1.14 (t, *J* = 7.07 Hz, 3H); **^{13}C NMR** ($CDCl_3$-*d*, 400MHz): δ_C 146.9, 132.3, 131.9, 131.8, 130.2, 128.8, 127.3, 122.8, 122.3, 75.8, 64.5, 15.0 ppm; **HRMS** (ESI) m/z 281.0300 (calculated for $C_{12}H_{14}N_2OBr$ $[M+H]^+$ 281.0290).

2-(3-bromophenyl)-1-(ethoxymethyl)-4-methyl-1*H*-imidazole (3.5) and 2-(3-bromophenyl)-1-(ethoxymethyl)-5-methyl-1*H*-imidazole (3.6)

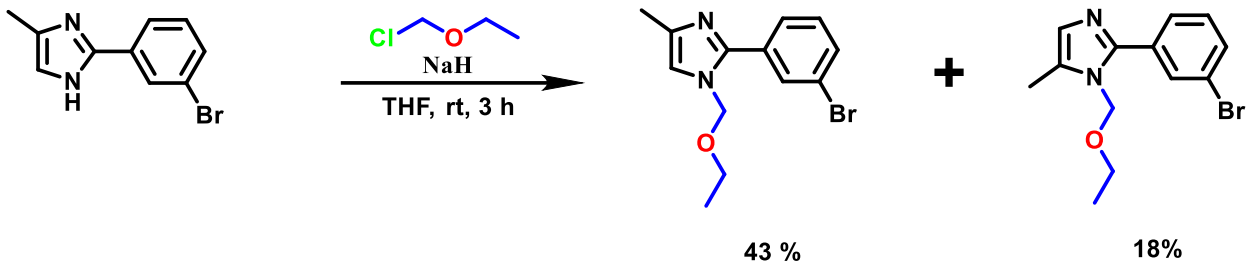

Also synthesized according to General Procedure A, this time starting with sodium hydride (1.79 g, 43.02 mmol, 4 eq.), chloromethyl ethyl ether (1.25 mL, 12.91 mmol, 1.2 eq.) and 2-(3-bromophenyl)-4-methyl-1*H*-imidazole (2.55 g, 10.76 mmol, 1 eq.) in tetrahydrofuran (20 mL). Two isomers (both yellow oils) were obtained (1.31 g, 4.63 mmol, 43% yield and 556 mg, 1.94 mmol, 18% yield).

2-(3-bromophenyl)-1-(ethoxymethyl)-4-methyl-1*H*-imidazole: yellow oil (43% yield); **IR** (vmax cm^{-1}) 2888, 1677, 1165, 1089, 630; **^{1}H NMR** (DMSO-d_6, 400MHz): δ_H 7.95 – 7.93 (m, 1H), 7.78 – 7.74 (m, 1H), 7.62 – 7.58 (m, 1H), 7.46 – 7.40 (m, 1H), 7.18 – 7.16 (m, 1H), 5.27 (s, 2H), 3.54 (q, *J* = 7.02 Hz, 2H), 2.15 (s, 3H), 1.13 (t, *J* = 7.0 Hz, 3H); **^{13}C NMR** (DMSO-d_6, 400MHz): δ_C 144.6, 136.3, 132.5, 131.1, 130.7, 130.4, 126.8, 121.8, 120.0, 74.9, 63.5, 14.7, 13.3 ppm; **HRMS** (ESI) m/z 295.0443 (calculated for $C_{13}H_{16}N_2OBr$ $[M+H]^+$ 295.0446).

2-(3-bromophenyl)-1-(ethoxymethyl)-5-methyl-1*H*-imidazole: yellow oil (18% yield); **IR** (vmax cm^{-1}) 2889, 1676, 1163, 1085, 685; **^{1}H NMR** (DMSO-d_6, 400MHz): δ_H 7.90 – 7.87 (m, 1H), 7.72 – 7.68 (m, 1H), 7.64 – 7.60 (m, 1H), 7.47 – 7.42 (m, 1H), 6.81 (bs, 1H), 5.22 (s, 2H), 3.50 (q, *J* = 7.0 Hz, 2H), 2.28 (s, 3H), 1.14 (t, *J* = 7.0 Hz, 3H); **^{13}C NMR** (DMSO-d_6, 400MHz): δ_C 145.9, 133.0,

131.3, 130.9, 130.7, 130.1, 127.1, 126.4, 121.9, 72.6, 63.2, 14.8, 9.4 ppm; **HRMS** (ESI) m/z 295.0437 (calculated for $C_{13}H_{16}N_2OBr$ $[M+H]^+$ 295.0446).

4.2.3 Buchwald-Hartwig Amination of Brominated Imidazoles

General procedure for the Palladium-Catalyzed Coupling reactions (B): The imidazole (1 eq.) and sodium *tert*-butoxide (2 eq.) were dissolved in anhydrous THF. Thereafter, $(DPPF)PdCl_2$ (5 mol%) and DPPF (10 mol%) were added to the mixture, with 2-chlorobenzylamine (4 eq.) being added lastly. After refluxing for 24 hours, the reaction mixture was concentrated and passed through a silica gel column eluted with ethyl acetate/*n*-hexane (1:1, v/v) for purification. The collected organic material was loaded into a chromatotron plate for further isolation by radial chromatography, using ethyl acetate/*n*-hexane (1:9, v/v) as eluent.

_N_-(2-chlorobenzyl)-3-(1-(ethoxymethyl)-1_H_-imidazol-2-yl)aniline (3.9)

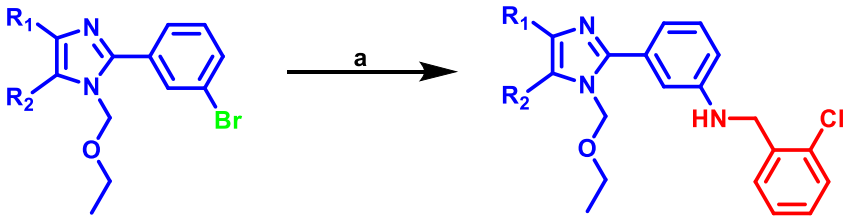

	R_1	R_2	
3.4	H	H	
3.5	Me	H	
3.6	H	Me	
3.9	H	H	41 %
3.10	Me	H	13 %
3.11	H	Me	7 %

Reaction conditions: (a) 2-chlorobenzylamine, **3.8**, DPPF, NaO-*t*-Bu, THF, reflux, 24 h

Following General Procedure B, starting with sodium *tert*-butoxide (695 mg, 7.24 mmol, 2 eq.), 2-(3-bromophenyl)-1-(ethoxymethyl)-1*H*-imidazole (1.02 g, 3.62 mmol, 1 eq.), $(DPPF)PdCl_2$ (133 mg, 0.181 mmol, 5 mol %), DPPF (200 mg, 0.362 mmol, 10 mol %), and 2-chlorobenzylamine (1.75

mL, 14.48 mmol, 4 eq.) in anhydrous THF. A brown oil was obtained (511 mg, 1.48 mmol, 41% yield).

***N*-(2-chlorobenzyl)-3-(1-(ethoxymethyl)-1*H*-imidazol-2-yl)aniline:** brown oil (41% yield); **IR** (vmax cm^{-1}) 2889, 1673, 1091, 1037, 641, 537; **^{1}H NMR** ($CDCl_3$-*d*, 400MHz): δ_H 7.36 – 7.30 (m, 2H), 7.20 – 7.01 (m, 8H), 6.63 – 6.59 (m, 1H), 5.18 (bs, 2H), 4.40 (s, 2H), 3.42 (q, *J* = 7.02 Hz, 2H), 1.13 (t, *J* = 7.02 Hz, 3H); **^{13}C NMR** ($CDCl_3$-*d*, 400MHz): δ_C 149.0, 148.1, 136.6, 133.2, 131.0, 129.4, 128.8, 128.3, 128.3, 126.9, 121.2, 118.1, 113.6, 113.1, 75.7, 64.3, 45.5, 14.8 ppm; **HRMS** (ESI) m/z 342.1370 (calculated for $C_{19}H_{21}N_3OCl$ $[M+H]^+$ 342.1373).

***N*-(2-chlorobenzyl)-3-(1-(ethoxymethyl)-4-methyl-1*H*-imidazol-2-yl)aniline (3.10)**

Synthesized according to General Procedure B, now starting with sodium *tert*-butoxide (651 mg, 6.78 mmol, 2 eq.), 2-(3-bromophenyl)-1-(ethoxymethyl)-4-methyl-1*H*-imidazole (1.0 g, 3.39 mmol, 1 eq.), (DPPF)$PdCl_2$ (124 mg, 0.170 mmol, 5 mol %), DPPF (188 mg, 0.339 mmol, 10 mol %), and 2-chlorobenzylamine (1.64 mL, 13.55 mmol, 4 eq.) in anhydrous THF. An orange-brown oil was obtained (161 mg, 0.441 mmol, 13% yield).

***N*-(2-chlorobenzyl)-3-(1-(ethoxymethyl)-4-methyl-1*H*-imidazol-2-yl)aniline:** orange-brown oil (13% yield); **IR** (vmax cm^{-1}) 2922, 1671, 1163, 1093, 625, 527; **^{1}H NMR** ($CDCl_3$-*d*, 400MHz): δ_H 7.35 – 7.09 (m, 6H), 7.03 – 6.97 (m, 2H), 6.76 (s, 1H), 6.58 (bd, *J* = 7.64 Hz, 1H), 5.10 (s, 2H), 4.40 (s, 2H), 3.44 – 3.36 (m, 2H), 2.22 (s, 3H), 1.14 – 1.08 (m, 3H); **^{13}C NMR** ($CDCl_3$-*d*, 400MHz): δ_C 148.4, 148.2, 137.4, 136.8, 133.3, 131.2, 129.6, 129.6, 129.0, 128.5, 127.1, 118.2, 117.8, 113.6, 113.3, 75.6, 64.3, 45.7, 15.0, 13.7 ppm; **HRMS** (ESI) m/z 356.1526 (calculated for $C_{20}H_{23}N_3OCl$ $[M+H]^+$ 356.1530).

***N*-(2-chlorobenzyl)-3-(1-(ethoxymethyl)-5-methyl-1*H*-imidazol-2-yl)aniline (3.11)**

Still following General Procedure B, sodium tert-butoxide (260 mg, 2.71 mmol, 2 eq.), 2-(3-bromophenyl)-1-(ethoxymethyl)-5-methyl-1*H*-imidazole (400 mg, 1.36 mmol, 1 eq.), (DPPF)$PdCl_2$ (50 mg, 0.068 mmol, 5 mol %), DPPF (75 mg, 0.136 mmol, 10 mol %), and 2-chlorobenzylamine (700 µL, 5.42 mmol, 4 eq.) were the amounts mixed in anhydrous THF. A brown oil was obtained (33 mg, 0.0952 mmol, 7% yield).

***N*-(2-chlorobenzyl)-3-(1-(ethoxymethyl)-5-methyl-1*H*-imidazol-2-yl)aniline:** brown oil (7% yield); **IR** (vmax cm^{-1}) 2915, 1671, 1159, 1088, 637, 535; **^{1}H NMR** ($CDCl_3$-*d*, 400MHz): δ_H 7.42 – 7.30 (m, 3H), 7.22 – 7.15 (m, 3H), 6.98 – 6.92 (m, 2H), 6.82 (s, 1H), 6.65 – 6.60 (m, 1H), 5.16 (s, 2H), 4.44 (s, 2H), 3.35 (q, *J* = 7.02 Hz, 2H), 2.29 (s, 3H), 1.12 (t, *J* = 7.02 Hz, 3H); **^{13}C NMR** ($CDCl_3$-*d*, 400MHz): δ_C 149.4, 148.4, 136.9, 133.7, 132.0, 129.9, 129.8, 129.3, 128.8, 127.3, 126.6, 118.7, 113.9, 113.7, 73.6, 63.9, 46.1, 15.3, 10.1 ppm; **HRMS** (ESI) m/z 356.1523 (calculated for $C_{20}H_{23}N_3OCl$ $[M+H]^+$ 356.1530).

4.2.4 Synthesis of derivatives of other explored potential protecting groups

***tert*-butyl 2-(3-bromophenyl)-1*H*-imidazole-1-carboxylate (3.19)**

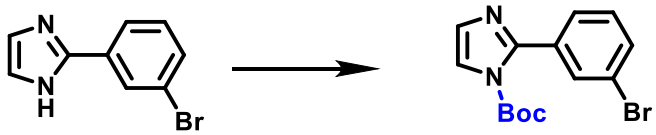

3.3 **3.19**

14 %

Reaction conditions: (a) **3.3**, $NaHCO_3$, BOC_2O, acetone/water (1:1), rt, overnight

Sodium bicarbonate (84 mg, 1.00 mmol, 1 eq.) and di-*tert*-butyl dicarbonate (436.5 mg, 2.00 mmol, 2 eq.) were added to a solution of 2-(3-bromophenyl)-1*H*-imidazole (223 mg, 1.00 mmol, 1 eq.) in acetone/water (1:1, v/v) and stirred at room temperature overnight. After the reaction

was stopped, acetone was evaporated and the remaining fraction of water was acidified to a pH of approximately 7 with 32 % hydrochloric acid. The organic contents were extracted with ethyl acetate and the organic layer was washed with brine. The product was isolated from the mixture by column chromatography, eluting ethyl acetate/*n*-hexane (1:1, v/v). The product was obtained as a brown oil (45 mg, 0.140 mmol, 14% yield).

***tert*-butyl 2-(3-bromophenyl)-1*H*-imidazole-1-carboxylate:** brown oil (14% yield); **IR** (ν_{max} cm^{-1}) 3158, 2931, 1752, 1602, 1142, 1080, 704; **^{1}H NMR** (DMSO-d_6, 400MHz): δ_H 7.78 – 7.75 (m, 1H), 7.67 (d, *J* = 1.63 Hz, 1H), 7.66 – 7.63 (m, 1H), 7.58 – 7.54 (m, 1H), 7.43 – 7.38 (m, 1H), 7.10 (d, *J* = 1.63 Hz, 1H), 1.37 (s, 9H); **^{13}C NMR** (DMSO-d_6, 400MHz): δ_C 147.5, 146.6, 134.5, 132.5, 132.0, 130.3, 129.1, 128.9, 121.2, 121.1, 85.9, 27.5 ppm; **HRMS** (ESI) m/z 323.0394 (calculated for $C_{14}H_{16}N_2O_2Br$ $[M+H]^+$ 323.0395).

2-(3-bromophenyl)-1-trityl-1*H*-imidazole (3.20)

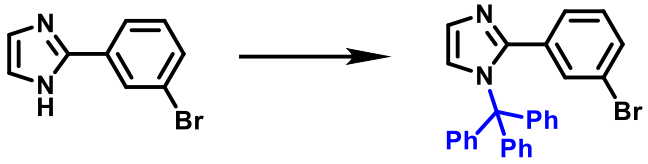

3.3 **3.20**

53 %

Reaction conditions: **3.3**, TEA, trityl chloride, DCM, rt, 3 h.

To a solution of 2-(3-bromophenyl)-1*H*-imidazole (669 mg, 3.00 mmol, 1 eq.) in dichloromethane (10 mL) at 0 °C, triethylamine (1.26 mL, 9.00 mmol, 3 eq.) was added dropwise followed by trityl chloride (2.52 g, 9.00 mmol, 3 eq.). The mixture was stirred at room temperature for 3 hours, thereafter, concentrated and purified by ethyl acetate/*n*-hexane (3:7, v/v) through column

chromatography. Yellow clouded crystals were obtained, further recrystallized in dichloromethane to give glacial crystals (741 mg, 1.59 mmol, 53% yield).

2-(3-bromophenyl)-1-trityl-1*H*-imidazole: glacial crystal solid (53% yield); **Mp:** 181 – 182 °C; **IR** (ν_{max} cm^{-1}) 3046, 2878, 1578, 1232, 639; **^{1}H NMR** (DMSO-d_6, 400MHz): δ_H 7.30 – 7.23 (m, 9H), 7.20 – 7.14 (m, 7H), 7.11 – 7.07 (m, 2H), 6.92 – 6.88 (m, 1H), 6.84 – 6.82 (m, 1H), 6.75 – 6.69 (m, 1H); **^{13}C NMR** (DMSO-d_6, 400MHz): δ_C 147.8, 147.6, 142.4, 135.4, 133.7, 130.8, 130.7, 129.1, 128.5, 128.4, 128.3, 128.1, 127.3, 126.9, 123.5, 121.2, 82.2, 76.4 ppm; **HRMS** (ESI) m/z 465.0973 (calculated for $C_{28}H_{22}N_2Br$ $[M+H]^+$ 465.0966).

2-(3-bromophenyl)-1*H*-imidazole (3.3)

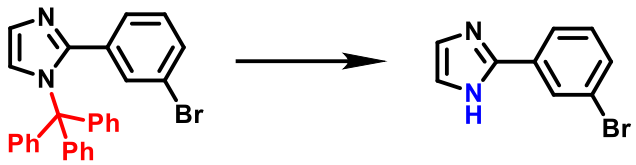

3.20 **3.3**

13 %

Reaction conditions: **3.20**, 1.0 M NaOH, MeOH, reflux, overnight.

Sodium hydroxide (1.0 M) (10 mL) was added dropwise to a solution of 2-(3-bromophenyl)-1-trityl-1*H*-imidazole (613 mg, 1.32 mmol) in methanol (75 mL) and stirred overnight at reflux. Methanol was then evaporated and the reaction mixture was diluted with distilled water. It was then acidified to a pH of approximately 4 with 3.0 M hydrochloric acid and extracted with dichloromethane. The organic layer was dried with magnesium sulphate, concentrated *in vacuo,* and loaded into a silica gel column eluting ethyl acetate/*n*-hexane (5.5:4.5, v/v) to yield a light brown precipitate (38.9 mg, 0.172 mmol, 13% yield).

2-(3-bromophenyl)-1*H*-imidazole: light brown solid (13% yield); **Mp:** 154 – 155 °C; **IR** (vmax cm^{-1}); **^{1}H NMR** (DMSO-d_6, 400MHz): δ_H 12.63 (s, 1H), 8.18 – 8.12 (m, 1H), 7.98 – 7.92 (m, 1H), 7.54 – 7.48 (m, 1H), 7.44 – 7.36 (m, 1H), 7.17 (s, 2H); **^{13}C NMR** (DMSO-d_6, 400MHz): δ_C 144.5, 133.5, 131.4, 130.9, 127.7, 124.1, 122.6 ppm; **HRMS** (ESI) m/z 222.9865 (calculated for $C_9H_8N_2Br$ $[M+H]^+$ 222.9871).

1-benzyl-2-(3-bromophenyl)-1*H*-imidazole (3.17)

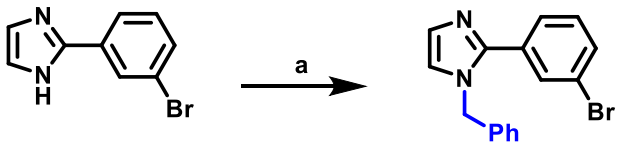

75 %

3.4 **3.17**

Reaction conditions: (a) **3.4**, sodium tert-butoxide, benzyl bromide, DMF, 60°C, 1 h

Sodium *tert*-butoxide (345 mg, 3.59 mmol, 4 eq.) and benzyl bromide (213 µL, 1.79 mmol, 2 eq.) were added into a solution of 2-(3-bromophenyl)-1*H*-imidazole (200 mg, 0.897 mmol, 1 eq.) in dimethylformamide (5 mL) and stirred for an hour at 60 °C. The reaction mixture was then extracted with dichloromethane. The organic layer was washed with brine, dried with magnesium sulphate and concentrated *in vacuo* to give a brown oil which was purified by dichloromethane/methanol (9.5:0.5, v/v) in a silica gel column. A yellow-orange oil was obtained (210 mg, 0.672 mmol, 75% yield).

1-benzyl-2-(3-bromophenyl)-1*H*-imidazole: yellow-orange oil (75% yield); **IR** (vmax cm^{-1}) 2769, 1596, 1174, 650; **^{1}H NMR** (DMSO-d_6, 400MHz): δ_H 7.73 – 7.69 (m, 1H), 7.61 – 7.53 (m, 2H), 7.40 – 7.30 (m, 4H), 7.30 – 7.23 (m, 1H), 7.09 (bd, J = 1.13 Hz, 1H), 7.05 – 7.00 (m, 2H), 5.36 (s, 2H); **^{13}C**

NMR (DMSO-d_6, 400MHz): δ_C 145.5, 137.9, 133.4, 131.7, 131.2, 131.1, 129.2, 128.9, 128.1, 127.4, 126.9, 123.9, 122.2, 50.3 ppm; **HRMS** (ESI) m/z 313.0350 (calculated for $C_{16}H_{14}N_2Br$ $[M+H]^+$ 313.0340).

4.2.5 Synthesis of Palladium Catalyst $(DPPF)PdCl_2$

$(DPPF)PdCl_2$ (3.8)

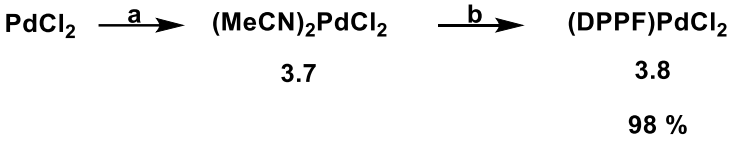

Reaction conditions: (a) MeCN, reflux, 4 h, $N_{2(g)}$; (b) DPPF, reflux, 1 h

$PdCl_2$ (120 mg, 0.678 mmol, 1 eq.) was dissolved in refluxing acetonitrile, with a nitrogen balloon to maintain dry-reaction conditions. After 4 hours of reflux, DPPF was added in a 1:1 ratio with the formed metal ion. The mixture was further stirred. After an hour, the product was concentrated *in vacuo*, recrystallized from DMF, and filtered off to give a red solid (486 mg, 0.664 mmol, 98% yield).

dppf-$PdCl_2$: red solid (98% yield); **Mp:** 261 – 262 °C; **IR** (ν_{max} cm^{-1}) 3044, 1426, 1087, 744, 687, 487; **^{1}H NMR** (CD_2Cl_2-*d*2, 400MHz): δ_H 7.95 – 7.84 (m, 8H), 7.57 – 7.52 (m, 4H), 7.48 – 7.41 (m, 8H), 4.43 (s, 4H), 4.26 – 4.20 (m, 4H); **^{31}P NMR** (CD_2Cl_2-*d*2, 400MHz): δ_P 34.01.

REFERENCES

1. WHO. *World Health Organization: Malaria*. **2023**. https://www.who.int/news-room/fact-sheets/detail/malaria (accessed 2023 August 4).

2. Tizifa, T. A.; Kabaghe, A. N.; McCann, R. S.; van den Berg, H.; Van Vugt, M.; Phiri, K. S. Prevention efforts for malaria. *Current tropical medicine reports* **2018**, *5*, 41-50.

3. Obasohan, P. E.; Walters, S. J.; Jacques, R.; Khatab, K. A Scoping Review of Selected Studies on Predictor Variables Associated with the Malaria Status among Children under Five Years in Sub-Saharan Africa. *International Journal of Environmental Research and Public Health* **2021**, *18* (4), 2119.

4. Lunga, M. J.; Chisango, R. L.; Weyers, C.; Isaacs, M.; Taylor, D.; Edkins, A. L.; Khanye, S. D.; Hoppe, H. C.; Veale, C. G. Expanding the SAR of nontoxic antiplasmodial indolyl-3-ethanone ethers and thioethers. *ChemMedChem* **2018**, *13* (13), 1353-1362.

5. Tuteja, R. Malaria − an overview. *The FEBS Journal* **2007**, *274* (18), 4670-4679.

6. Sato, S. Plasmodium—a brief introduction to the parasites causing human malaria and their basic biology. *Journal of Physiological Anthropology* **2021**, *40* (1), 1.

7. WHO. *World malaria report 2022*; **2022**. (accessed August 7, 2023).

8. Bedair, N. H.; Zeki, I. N. Prevalence of Some Parasitic Infections in Iraq from 2019 to 2020. *Iraqi Journal of Science* **2023**, *64* (7), 4181-4191. (acccessed 2023/08/03).

9. Aitken, E. H.; Mahanty, S.; Rogerson, S. J. Antibody effector functions in malaria and other parasitic diseases: a few needles and many haystacks. *Immunology & Cell Biology* **2020**, *98* (4), 264-275.

10. Molina-Franky, J.; Cuy-Chaparro, L.; Camargo, A.; Reyes, C.; Gómez, M.; Salamanca, D. R.; Patarroyo, M. A.; Patarroyo, M. E. Plasmodium falciparum pre-erythrocytic stage vaccine development. *Malaria Journal* **2020**, *19* (1), 56.

11. Nureye, D.; Assefa, S. Old and Recent Advances in Life Cycle, Pathogenesis, Diagnosis, Prevention, and Treatment of Malaria Including Perspectives in Ethiopia. *The Scientific World Journal* **2020**, *2020*, 1295381.

12. Bell, D.; Wongsrichanalai, C.; Barnwell, J. W. Ensuring quality and access for malaria diagnosis: how can it be achieved? *Nature Reviews Microbiology* **2006**, *4* (9), 682-695.

13. Melato, S.; Coghi, P.; Basilico, N.; Prosperi, D.; Monti, D. Novel 4-aminoquinolines through microwave-assisted snar reactions: a practical route to antimalarial agents. Wiley Online Library: 2007.

14. (CDC), C. f. D. C. a. P. *Malaria Diagnosis (United States)*. **2023**. https://www.cdc.gov/malaria/diagnosis_treatment/diagnosis.html (accessed 2024 31 January).

15. Zimmerman, P. A.; Howes, R. E. Malaria diagnosis for malaria elimination. *Current Opinion in Infectious Diseases* **2015**, *28* (5), 446-454.

16. Gillet, P.; Mumba Ngoyi, D.; Lukuka, A.; Kande, V.; Atua, B.; van Griensven, J.; Muyembe, J.-J.; Jacobs, J.; Lejon, V. False Positivity of Non-Targeted Infections in Malaria Rapid Diagnostic Tests: The Case of Human African Trypanosomiasis. *PLOS Neglected Tropical Diseases* **2013**, *7* (4), e2180.

17. Leshem, E.; Keller, N.; Guthman, D.; Grossman, T.; Solomon, M.; Marva, E.; Schwartz, E. False-positive Plasmodium falciparum histidine-rich protein 2 immunocapture assay results for acute schistosomiasis caused by Schistosoma mekongi. *J Clin Microbiol* **2011**, *49* (6), 2331-2332. From NLM.

18. Gilbert, I. H. Drug Discovery for Neglected Diseases: Molecular Target-Based and Phenotypic Approaches. *Journal of Medicinal Chemistry* **2013**, *56* (20), 7719-7726.

19. Hovlid, M. L.; Winzeler, E. A. Phenotypic screens in antimalarial drug discovery. *Trends in parasitology* **2016**, *32* (9), 697-707.

20. Francklyn, C. S.; Mullen, P. Progress and challenges in aminoacyl-tRNA synthetase-based therapeutics. *Journal of Biological Chemistry* **2019**, *294* (14), 5365-5385.

21. White, L. J.; Flegg, J. A.; Phyo, A. P.; Wiladpai-ngern, J. H.; Bethell, D.; Plowe, C.; Anderson, T.; Nkhoma, S.; Nair, S.; Tripura, R.; et al. Defining the In Vivo Phenotype of Artemisinin-Resistant Falciparum Malaria: A Modelling Approach. *PLOS Medicine* **2015**, *12* (4), e1001823.

22. Ranford-Cartwright, L. C.; Mwangi, J. M. Analysis of malaria parasite phenotypes using experimental genetic crosses of Plasmodium falciparum. *International journal for parasitology* **2012**, *42* (6), 529-534.

23. Paquet, T.; Le Manach, C.; Cabrera, D. G.; Younis, Y.; Henrich, P. P.; Abraham, T. S.; Lee, M. C. S.; Basak, R.; Ghidelli-Disse, S.; Lafuente-Monasterio, M. J.; et al. Antimalarial efficacy of MMV390048, an inhibitor of Plasmodium phosphatidylinositol 4-kinase. *Science Translational Medicine* **2017**, *9* (387), eaad9735.

24. Nwaka, S.; Riopel, L.; Ubben, D.; Craft, J. C. Medicines for Malaria Venture new developments in antimalarials. *Travel Medicine and Infectious Disease* **2004**, *2* (3), 161-170.

25. Hotez, P.; Aksoy, S. PLOS Neglected Tropical Diseases: Ten years of progress in neglected tropical disease control and elimination … More or less. *PLOS Neglected Tropical Diseases* **2017**, *11* (4), e0005355.

26. Veale, C. G. Unpacking the Pathogen Box—an open source tool for fighting neglected tropical disease. *ChemMedChem* **2019**, *14* (4), 386-453.

27. Simon, G. G. Impacts of neglected tropical disease on incidence and progression of HIV/AIDS, tuberculosis, and malaria: scientific links. *Int J Infect Dis* **2016**, *42*, 54-57. From NLM.

28. Veale, C. G. L.; Hoppe, H. C. Screening of the Pathogen Box reveals new starting points for anti-trypanosomal drug discovery. *MedChemComm* **2018**, *9* (12), 2037-2044, 10.1039/C8MD00319J.

29. Kipandula, W.; Young, S. A.; MacNeill, S. A.; Smith, T. K. Screening of the MMV and GSK open access chemical boxes using a viability assay developed against the kinetoplastid Crithidia fasciculata. *Molecular and biochemical parasitology* **2018**, *222*, 61-69.

30. Hennessey, K. M.; Rogiers, I. C.; Shih, H.-W.; Hulverson, M. A.; Choi, R.; McCloskey, M. C.; Whitman, G. R.; Barrett, L. K.; Merritt, E. A.; Paredez, A. R. Screening of the Pathogen Box for inhibitors with dual efficacy against Giardia lamblia and Cryptosporidium parvum. *PLoS neglected tropical diseases* **2018**, *12* (8), e0006673.

31. Mayer, F.; Kronstad, J. Discovery of a novel antifungal agent in the Pathogen Box. mSphere 2: e00120-17. 2017.

32. Preston, S.; Jiao, Y.; Jabbar, A.; McGee, S. L.; Laleu, B.; Willis, P.; Wells, T. N. C.; Gasser, R. B. Screening of the 'Pathogen Box' identifies an approved pesticide with major anthelmintic activity against the barber's pole worm. *International Journal for Parasitology: Drugs and Drug Resistance* **2016**, *6* (3), 329-334.

33. Dize, D.; Tata, R. B.; Keumoe, R.; Kouipou Toghueo, R. M.; Tchatat, M. B.; Njanpa, C. N.; Tchuenguia, V. C.; Yamthe, L. T.; Fokou, P. V. T.; Laleu, B. Preliminary Structure–Activity Relationship Study of the MMV Pathogen Box Compound MMV675968 (2, 4-Diaminoquinazoline) Unveils Novel Inhibitors of Trypanosoma brucei brucei. *Molecules* **2022**, *27* (19), 6574.

34. Asif, M. A mini review: biological significances of nitrogen hetero atom containing heterocyclic compounds. *Int. J. Bioorg. Chem* **2017**, *2* (3), 146-152.

35. Zhao, C.; Qiao, X.; Yi, Z.; Guan, Q.; Li, W. Active centre and reactivity descriptor of a green single component imidazole catalyst for acetylene hydrochlorination. *Physical Chemistry Chemical Physics* **2020**, *22* (5), 2849-2857.

36. Wan, Y.; Hur, W.; Cho, C. Y.; Liu, Y.; Adrian, F. J.; Lozach, O.; Bach, S.; Mayer, T.; Fabbro, D.; Meijer, L. Synthesis and target identification of hymenialdisine analogs. *Chemistry & biology* **2004**, *11* (2), 247-259.

37. Gaba, M.; Mohan, C. Development of drugs based on imidazole and benzimidazole bioactive heterocycles: recent advances and future directions. *Medicinal Chemistry Research* **2016**, *25* (2), 173-210.

38. DeSimone, R.; Currie, K.; Mitchell, S.; Darrow, J.; Pippin, D. Privileged structures: applications in drug discovery. *Combinatorial chemistry & high throughput screening* **2004**, *7* (5), 473-493.

39. Kudelko, A.; Zieliński, W.; Jasiak, K. Synthesis of novel 1-[(1-ethoxymethylene)amino]imidazol-5(4H)-ones and 1,2,4-triazin-6(5H)-ones from optically active α-aminocarboxylic acid hydrazides. *Tetrahedron Letters* **2013**, *54* (35), 4637-4640.

40. Debus, H. Ueber die einwirkung des ammoniaks auf glyoxal. *Justus Liebigs Annalen der Chemie* **1858**, *107* (2), 199-208.

41. Radziszewski, B. Ber. dtsch. chem. *Ges. 15* **1882**, *1493*.

42. Weidenhagen, R.; Herrmann, R. Eine neue Synthese von Imidazol-Derivaten. *Berichte der deutschen chemischen Gesellschaft (A and B Series)* **1935**, *68* (10), 1953-1961.

43. Fei, F.; Zhou, Z. New substituted benzimidazole derivatives: a patent review (2010–2012). *Expert opinion on therapeutic patents* **2013**, *23* (9), 1157-1179.

44. Gupta, P.; Gupta, J. K. Synthesis of bioactive imidazoles: a review. *Chem. Sci. J* **2015**, *6* (2), 1-12.

45. Verma, A.; Joshi, S.; Singh, D. Imidazole: having versatile biological activities. *Journal of Chemistry* **2013**, *2013*.

46. Alghamdi, S. S.; Suliman, R. S.; Almutairi, K.; Kahtani, K.; Aljatli, D. Imidazole as a Promising Medicinal Scaffold: Current Status and Future Direction. *Drug Des Devel Ther* **2021**, *15*, 3289-3312. From NLM.

47. Bhatnagar, A.; Sharma, P.; Kumar, N. A review on "Imidazoles": Their chemistry and pharmacological potentials. *Int J PharmTech Res* **2011**, *3* (1), 268-282.

48. Cai, J.; Lu, Y.; Gan, L.; Zhang, Y.; Zhou, C. Recent advance in the research of piperazine-containing compounds as antimicrobial agents. *Chin. J. Antibiot* **2009**, *34*, 454-462.

49. Zhou, C.; Mi, J.; Wu, J.; Luo, Y.; Bai, X.; Gan, L.; Geng, R. Triazole onium compound with antimicrobial activity, preparation method and medical use. *CN Patent* **2009**, *101391985*.

50. Wang, X.-L.; Wan, K.; Zhou, C.-H. Synthesis of novel sulfanilamide-derived 1, 2, 3-triazoles and their evaluation for antibacterial and antifungal activities. *European journal of medicinal chemistry* **2010**, *45* (10), 4631-4639.

51. Peng, X.-M.; Cai, G.-X.; Zhou, C.-H. Recent developments in azole compounds as antibacterial and antifungal agents. *Current topics in medicinal chemistry* **2013**, *13* (16), 1963-2010.

52. Zhang, S.-L.; Chang, J.-J.; Damu, G. L.; Fang, B.; Zhou, X.-D.; Geng, R.-X.; Zhou, C.-H. Novel berberine triazoles: synthesis, antimicrobial evaluation and competitive interactions with metal ions to human serum albumin. *Bioorganic & medicinal chemistry letters* **2013**, *23* (4), 1008-1012.

53. Vijesh, a. A.; Isloor, A. M.; Telkar, S.; Peethambar, S.; Rai, S.; Isloor, N. Synthesis, characterization and antimicrobial studies of some new pyrazole incorporated imidazole derivatives. *European journal of medicinal chemistry* **2011**, *46* (8), 3531-3536.

54. Jain, A. K.; Ravichandran, V.; Sisodiya, M.; Agrawal, R. Synthesis and antibacterial evaluation of 2–substituted–4, 5–diphenyl–N–alkyl imidazole derivatives. *Asian Pacific Journal of Tropical Medicine* **2010**, *3* (6), 471-474.

55. Padmavathi, V.; Venkatesh, B.; Padmaja, A. Synthesis and antimicrobial activity of amido linked pyrrolyl and pyrazolyl-oxazoles, thiazoles and imidazoles. *European journal of medicinal chemistry* **2011**, *46* (11), 5317-5326.

56. Sharma, D.; Narasimhan, B.; Kumar, P.; Judge, V.; Narang, R.; De Clercq, E.; Balzarini, J. Synthesis, antimicrobial and antiviral evaluation of substituted imidazole derivatives. *European Journal of Medicinal Chemistry* **2009**, *44* (6), 2347-2353.

57. Brahmbhatt, H.; Molnar, M.; Pavić, V. Pyrazole nucleus fused tri-substituted imidazole derivatives as antioxidant and antibacterial agents. *Karbala International Journal of Modern Science* **2018**, *4* (2), 200-206.

58. Chen, L.; Deng, H.; Cui, H.; Fang, J.; Zuo, Z.; Deng, J.; Li, Y.; Wang, X.; Zhao, L. Inflammatory responses and inflammation-associated diseases in organs. *Oncotarget* **2018**, *9* (6), 7204.

59. Youssef, J.; Novosad, S. A.; Winthrop, K. L. Infection risk and safety of corticosteroid use. *Rheumatic Disease Clinics* **2016**, *42* (1), 157-176.

60. Sostres, C.; Gargallo, C. J.; Arroyo, M. T.; Lanas, A. Adverse effects of non-steroidal anti-inflammatory drugs (NSAIDs, aspirin and coxibs) on upper gastrointestinal tract. *Best practice & research Clinical gastroenterology* **2010**, *24* (2), 121-132.

61. Husain, A.; Drabu, S.; Kumar, N.; Alam, M. M.; Bawa, S. Synthesis and biological evaluation of di- and tri-substituted imidazoles as safer anti-inflammatory-antifungal agents. *J Pharm Bioallied Sci* **2013**, *5* (2), 154-161. From NLM.

62. Raghavendra, P.; Veena, G.; Kumar, G. A.; Kumar, E. R.; Sangeetha, N.; Sirivennela, B.; Smarani, S.; Kumar, H. P.; Suthakaran, R. Microwave synthesis and anti-inflammatory evaluation of some new imidazolo quinoline analogs. *RASAYAN Journal of Chemistry* **2011**, *4* (1), 91-102.

63. Achar, K. C.; Hosamani, K. M.; Seetharamareddy, H. R. In-vivo analgesic and anti-inflammatory activities of newly synthesized benzimidazole derivatives. *European journal of medicinal chemistry* **2010**, *45* (5), 2048-2054.

64. Shankar, B.; Jalapathi, P.; Valeru, A.; Kishor Kumar, A.; Saikrishna, B.; Kudle, K. r. Synthesis and biological evaluation of new 2-(6-alkyl-pyrazin-2-yl)-1H-benz[d]imidazoles as potent anti-inflammatory and antioxidant agents. *Medicinal Chemistry Research* **2017**, *26* (9), 1835-1846.

65. Katikireddy, R.; Kakkerla, R.; Krishna, M. P. S. M.; Durgaiah, G.; Reddy, Y. N.; Satyanarayana, M. Synthesis and Biological Evaluation of (E)-N'-Benzylidene-7-methyl-2-propyl-1H-benzo[d] imidazole-5-

carbohydrazides as Antioxidant, Anti-inflammatory and Analgesic agents. *Heterocyclic Communications* **2019**, *25* (1), 27-38. (acccessed 2023-10-05).

66. Nascimento, M. V. P. S.; Munhoz, A. C. M.; Theindl, L. C.; Mohr, E. T. B.; Saleh, N.; Parisotto, E. B.; Rossa, T. A.; Zamoner, A.; Creczynski-Pasa, T. B.; Filippin-Monteiro, F. B.; et al. A Novel Tetrasubstituted Imidazole as a Prototype for the Development of Anti-inflammatory Drugs. *Inflammation* **2018**, *41* (4), 1334-1348.

67. Shantharam, C.; Swaroopa, M.; Darshini, N.; Mallesha, N.; Rakesh, K. Synthesis and SAR studies of potent antioxidant and anti-inflammatory activities of imidazole Derived Schiff base analogues. *Biochem Anal Biochem* **2017**, *6*, 314.

68. Virgin, H. W.; Wherry, E. J.; Ahmed, R. Redefining chronic viral infection. *Cell* **2009**, *138* (1), 30-50.

69. Zhan, P.; Liu, X.; Zhu, J.; Fang, Z.; Li, Z.; Pannecouque, C.; Clercq, E. D. Synthesis and biological evaluation of imidazole thioacetanilides as novel non-nucleoside HIV-1 reverse transcriptase inhibitors. *Bioorganic & Medicinal Chemistry* **2009**, *17* (16), 5775-5781.

70. Zhang, L.; Peng, X.-M.; Damu, G. L. V.; Geng, R.-X.; Zhou, C.-H. Comprehensive Review in Current Developments of Imidazole-Based Medicinal Chemistry. *Medicinal Research Reviews* **2014**, *34* (2), 340-437.

71. Le, G.; Vandegraaff, N.; Rhodes, D. I.; Jones, E. D.; Coates, J. A. V.; Thienthong, N.; Winfield, L. J.; Lu, L.; Li, X.; Yu, C.; et al. Design of a series of bicyclic HIV-1 integrase inhibitors. Part 2: Azoles: Effective metal chelators. *Bioorganic & Medicinal Chemistry Letters* **2010**, *20* (19), 5909-5912.

72. Jia, W.; Zhao, Y.; Li, R.; Wu, Y.; Li, Z.; Gong, P. Synthesis and In-Vitro Anti-Hepatitis-B Virus Activity of 6H-[1]Benzothiopyrano[4,3-b] quinolin-10-ols. *Archiv der Pharmazie* **2009**, *342* (9), 507-512.

73. Liu, Y.; Zhao, Y.; Zhai, X.; Liu, X.; Sun, L.; Ren, Y.; Gong, P. Synthesis and Anti-HBV Activities Evaluation of New Ethyl 8-Imidazolylmethyl-7-hydroxyquinoline-3-carboxylate Derivatives in vitro. *Archiv der Pharmazie* **2008**, *341* (7), 446-452.

74. De Martino, G.; La Regina, G.; Di Pasquali, A.; Ragno, R.; Bergamini, A.; Ciaprini, C.; Sinistro, A.; Maga, G.; Crespan, E.; Artico, M.; Silvestri, R. Novel 1-[2-(Diarylmethoxy)ethyl]-2-methyl-5-nitroimidazoles as HIV-1 Non-Nucleoside Reverse Transcriptase Inhibitors. A Structure−Activity Relationship Investigation. *Journal of Medicinal Chemistry* **2005**, *48* (13), 4378-4388.

75. Zhou, C.; Hassner, A. Synthesis and anticancer activity of novel chiral D-glucose derived bis-imidazoles and their analogs. *Carbohydrate Research* **2001**, *333* (4), 313-326.

76. Baroniya, S.; Anwer, Z.; Sharma, P. K.; Dudhe, R.; Kumar, N. Recent advancement in imidazole as anti cancer agents: A review. *Der Chemica Sinica* **2010**.

77. Cai, J.; Li, S.; Zhou, C.; Wu, J. Advance in research of imidazoles as anti-tumor agents. *Chin. J. New Drugs* **2009**, *18*, 598-608.

78. Yurttaş, L.; Ertaş, M.; Çiftçi, G. A.; Temel, H. E.; Demirayak, Ş. Novel benzothiazole based imidazole derivatives as new cytotoxic agents against glioma (C6) and liver (HepG2) cancer cell lines. **2017**.

79. Romagnoli, R.; Baraldi, P. G.; Prencipe, F.; Oliva, P.; Baraldi, S.; Tabrizi, M. A.; Lopez-Cara, L. C.; Ferla, S.; Brancale, A.; Hamel, E.; et al. Design and Synthesis of Potent in Vitro and in Vivo Anticancer Agents Based on 1-(3′,4′,5′-Trimethoxyphenyl)-2-Aryl-1H-Imidazole. *Scientific Reports* **2016**, *6* (1), 26602.

80. Hsieh, C.-Y.; Ko, P.-W.; Chang, Y.-J.; Kapoor, M.; Liang, Y.-C.; Chu, H.-L.; Lin, H.-H.; Horng, J.-C.; Hsu, M.-H. Design and Synthesis of Benzimidazole-Chalcone Derivatives as Potential Anticancer Agents. *Molecules* **2019**, *24* (18), 3259.

81. Roopashree, R.; Mohan, C. D.; Swaroop, T. R.; Jagadish, S.; Rangappa, K. S. Synthesis, characterization, and in vivo biological evaluation of novel benzimidazoles as potential anticancer agents. *Asian Journal of Pharmaceutical and Clinical Research* **2014**, *7* (5), 309-313.

82. Rajendran, S.; Geetha, G.; Venkatanarayanan, R.; Santhi, N. Synthesis, characterization and in-vitro anticancer evaluation of novel benzo [D] imidazole derivatives. *International Journal of Pharmaceutical Sciences and Research* **2017**, *8* (7), 3014-3024.

83. Meenakshisundaram, S.; Manickam, M.; Pillaiyar, T. Exploration of imidazole and imidazopyridine dimers as anticancer agents: Design, synthesis, and structure–activity relationship study. *Archiv der Pharmazie* **2019**, *352* (12), 1900011.

84. Schuh, E.; Pflüger, C.; Citta, A.; Folda, A.; Rigobello, M. P.; Bindoli, A.; Casini, A.; Mohr, F. Gold (I) carbene complexes causing thioredoxin 1 and thioredoxin 2 oxidation as potential anticancer agents. *Journal of medicinal chemistry* **2012**, *55* (11), 5518-5528.

85. Showalter, H. D. Recent progress in the discovery and development of 2-nitroimidazooxazines and 6-nitroimidazooxazoles to treat tuberculosis and neglected tropical diseases. *Molecules* **2020**, *25* (18), 4137.

86. Siwach, A.; Verma, P. K. Synthesis and therapeutic potential of imidazole containing compounds. *BMC chemistry* **2021**, *15*, 1-69.

87. Nandha, B.; Nargund, L. G.; Nargund, S. L.; Bhat, K. Design and Synthesis of Some Novel Fluorobenzimidazoles Substituted with Structural Motifs Present in Physiologically Active Natural Products for Antitubercular Activity. *Iran J Pharm Res* **2017**, *16* (3), 929-942. From NLM.

88. Gising, J.; Nilsson, M. T.; Odell, L. R.; Yahiaoui, S.; Lindh, M.; Iyer, H.; Sinha, A. M.; Srinivasa, B. R.; Larhed, M.; Mowbray, S. L.; Karlén, A. Trisubstituted Imidazoles as Mycobacterium tuberculosis Glutamine Synthetase Inhibitors. *Journal of Medicinal Chemistry* **2012**, *55* (6), 2894-2898.

89. Pieroni, M.; Wan, B.; Zuliani, V.; Franzblau, S. G.; Costantino, G.; Rivara, M. Discovery of antitubercular 2,4-diphenyl-1H-imidazoles from chemical library repositioning and rational design. *European Journal of Medicinal Chemistry* **2015**, *100*, 44-49.

90. Kishk, S. M.; McLean, K. J.; Sood, S.; Smith, D.; Evans, J. W. D.; Helal, M. A.; Gomaa, M. S.; Salama, I.; Mostafa, S. M.; de Carvalho, L. P. S.; et al. Design and Synthesis of Imidazole and Triazole Pyrazoles as Mycobacterium Tuberculosis CYP121A1 Inhibitors. *ChemistryOpen* **2019**, *8* (7), 995-1011.

91. Raghu, M. S.; Pradeep Kumar, C. B.; Prasad, K. N. N.; Prashanth, M. K.; Kumarswamy, Y. K.; Chandrasekhar, S.; Veeresh, B. MoS2–Calix[4]arene Catalyzed Synthesis and Molecular Docking Study of 2,4,5-Trisubstituted Imidazoles As Potent Inhibitors of Mycobacterium tuberculosis. *ACS Combinatorial Science* **2020**, *22* (10), 509-518.

92. Gemma, S.; Camodeca, C.; Brindisi, M.; Brogi, S.; Kukreja, G.; Kunjir, S.; Gabellieri, E.; Lucantoni, L.; Habluetzel, A.; Taramelli, D. Mimicking the intramolecular hydrogen bond: synthesis, biological evaluation, and molecular modeling of benzoxazines and quinazolines as potential antimalarial agents. *Journal of medicinal chemistry* **2012**, *55* (23), 10387-10404.

93. Cornut, D.; Lemoine, H.; Kanishchev, O.; Okada, E.; Albrieux, F.; Beavogui, A. H.; Bienvenu, A.-L.; Picot, S. p.; Bouillon, J.-P.; Médebielle, M. Incorporation of a 3-(2, 2, 2-trifluoroethyl)-γ-hydroxy-γ-lactam motif

in the side chain of 4-aminoquinolines. Syntheses and antimalarial activities. *Journal of medicinal chemistry* **2013**, *56* (1), 73-83.

94. Roy, D.; Anas, M.; Manhas, A.; Saha, S.; Kumar, N.; Panda, G. Synthesis, biological evaluation, Structure − Activity relationship studies of quinoline-imidazole derivatives as potent antimalarial agents. *Bioorganic Chemistry* **2022**, *121*, 105671.

95. Kondaparla, S.; Manhas, A.; Dola, V. R.; Srivastava, K.; Puri, S. K.; Katti, S. B. Design, synthesis and antiplasmodial activity of novel imidazole derivatives based on 7-chloro-4-aminoquinoline. *Bioorganic Chemistry* **2018**, *80*, 204-211.

96. Casagrande, M.; Barteselli, A.; Basilico, N.; Parapini, S.; Taramelli, D.; Sparatore, A. Synthesis and antiplasmodial activity of new heteroaryl derivatives of 7-chloro-4-aminoquinoline. *Bioorganic & Medicinal Chemistry* **2012**, *20* (19), 5965-5979.

97. Roman, G.; Crandall, I. E.; Szarek, W. A. Synthesis and Anti-Plasmodium Activity of Benzimidazole Analogues Structurally Related to Astemizole. *ChemMedChem* **2013**, *8* (11), 1795-1804.

98. Sharma, K.; Shrivastava, A.; Mehra, R.; Deora, G.; Alam, M.; Zaman, S.; Akhter, M. Synthesis of novel benzimidazole acrylonitriles for inhibition of Plasmodium falciparum growth by dual target inhibition. *Archiv der Pharmazie* **2017**, *351*, e1700251.

99. Le Manach, C.; Gonzàlez Cabrera, D.; Douelle, F.; Nchinda, A. T.; Younis, Y.; Taylor, D.; Wiesner, L.; White, K. L.; Ryan, E.; March, C. Medicinal chemistry optimization of antiplasmodial imidazopyridazine hits from high throughput screening of a SoftFocus kinase library: part 1. *Journal of medicinal chemistry* **2014**, *57* (6), 2789-2798.

100. Purwono, B.; Nurohmah, B.; Fathurrohman, P.; Syahri, J. Some 2-arylbenzimidazole derivatives as an antimalarial agent: Synthesis, activity assay, molecular docking and pharmacological evaluation. *Rasayan J. Chem* **2021**, *14* (1), 94-100.

101. Patel, K.; Karthikeyan, C.; Hari Narayana Moorthy, N.; Deora, G. S.; Solomon, V. R.; Lee, H.; Trivedi, P. Design, synthesis and biological evaluation of some novel 3-cinnamoyl-4-hydroxy-2H-chromen-2-ones as antimalarial agents. *Medicinal Chemistry Research* **2012**, *21*, 1780-1784.

102. Syahri, J.; Nasution, H.; Achromi, B.; Bambang, P.; Yuanita, E. Novel aminoalkylated chalcone: Synthesis, biological evaluation, and docking simulation as potent antimalarial agents. *Novel aminoalkylated chalcone: Synthesis, biological evaluation, and docking simulation as potent antimalarial agents* **2020**, *10* (6), 1-5.

103. Septiana, I.; Purwono, B.; Anwar, C.; Nurohmah, B. A.; Syahri, J. Synthesis and Docking Study of 2–Aryl-4, 5-diphenyl-1 H-imidazole Derivatives as Lead Compounds for Antimalarial Agent. *Indonesian Journal of Chemistry* **2022**, *22* (1), 105-113.

104. Bheemanaboina, R. R. Y.; de Souza, M. L.; Gonzalez, M. L.; Mahmood, S. U.; Eck, T.; Kreiss, T.; Aylor, S. O.; Roth, A.; Lee, P.; Pybus, B. S.; et al. Discovery of Imidazole-Based Inhibitors of Plasmodium falciparum cGMP-Dependent Protein Kinase. *ACS Med Chem Lett* **2021**, *12* (12), 1962-1967. From NLM.

105. Eseola, A. O.; Görls, H.; Woods, J. A.; Plass, W. Cyclometallation, steric and electronic tendencies in a series of Pd (II) complex pre-catalysts bearing imidazole–phenol ligands and effects on Suzuki–Miyaura catalytic efficiencies. *Journal of Molecular Catalysis A: Chemical* **2015**, *406*, 224-237.

106. Patil, R. D.; Adimurthy, S. Catalytic Methods for Imine Synthesis. *Asian Journal of Organic Chemistry* **2013**, *2* (9), 726-744.

107. Hedström, U.; Norberg, M.; Evertsson, E.; Lever, S. R.; Munck af Rosenschöld, M.; Lönn, H.; Bold, P.; Käck, H.; Berntsson, P.; Vinblad, J. An Angle on MK2 Inhibition—Optimization and Evaluation of Prevention of Activation Inhibitors. *ChemMedChem* **2019**, *14* (19), 1701-1709.

108. Albertshofer, K.; Mani, N. S. Regioselective electrophilic fluorination of rationally designed imidazole derivatives. *The Journal of Organic Chemistry* **2016**, *81* (3), 1269-1276.

109. Kharaka, Y. K.; Hanor, J. S. 7.14 - Deep Fluids in Sedimentary Basins. In *Treatise on Geochemistry (Second Edition)*, Holland, H. D., Turekian, K. K. Eds.; Elsevier, 2014; pp 471-515.

110. Gelman, F.; Dybala-Defratyka, A. Bromine isotope effects: Predictions and measurements. *Chemosphere* **2020**, *246*, 125746.

111. Tang, C.; Tan, J.; Shi, Z.; Fan, Y.; Yu, Z.; Peng, X. Chlorine and bromine isotope fractionations of halogenated organic compounds in fragmentation by gas chromatography-electron ionization high resolution mass spectrometry. *Journal of Chromatography A* **2019**, *1603*, 278-287.

112. Yang, B. H.; Buchwald, S. L. Palladium-catalyzed amination of aryl halides and sulfonates. *Journal of Organometallic Chemistry* **1999**, *576* (1-2), 125-146.

113. Driver, M. S.; Hartwig, J. F. A Second-Generation Catalyst for Aryl Halide Amination: Mixed Secondary Amines from Aryl Halides and Primary Amines Catalyzed by (DPPF)PdCl2. *Journal of the American Chemical Society* **1996**, *118* (30), 7217-7218.

114. Schulz, T.; Torborg, C.; Enthaler, S.; Schäffner, B.; Dumrath, A.; Spannenberg, A.; Neumann, H.; Börner, A.; Beller, M. A General Palladium-Catalyzed Amination of Aryl Halides with Ammonia. *Chemistry – A European Journal* **2009**, *15* (18), 4528-4533.

115. Davies, J. A.; Hartley, F. R.; Murray, S. G. Hard ligands as donors to soft metals. Part 1. Formation of oxygen-bonded dimethyl sulphoxide complexes of palladium(II) and platinum(II) promoted by steric crowding. *Journal of the Chemical Society, Dalton Transactions* **1979**, (11), 1705-1708.

116. Guilbaud, J.; Labonde, M.; Selmi, A.; Kammoun, M.; Cattey, H.; Pirio, N.; Roger, J.; Hierso, J.-C. Palladium-catalyzed heteroaryl thioethers synthesis overcoming palladium dithiolate resting states inertness: Practical road to sulfones and NH-sulfoximines. *Catalysis Communications* **2018**, *111*, 52-58.

117. Kaufmann, R.; Long, A.; Bentley, H.; Davis, S. Natural chlorine isotope variations. *Nature* **1984**, *309* (5966), 338-340.

118. Van Warmerdam, E.; Frape, S.; Aravena, R.; Drimmie, R.; Flatt, H.; Cherry, J. Stable chlorine and carbon isotope measurements of selected chlorinated organic solvents. *Applied Geochemistry* **1995**, *10* (5), 547-552.

119. Torrentó, C.; Palau, J.; Rodríguez-Fernández, D.; Heckel, B.; Meyer, A.; Domènech, C.; Rosell, M. n.; Soler, A.; Elsner, M.; Hunkeler, D. Carbon and chlorine isotope fractionation patterns associated with different engineered chloroform transformation reactions. *Environmental science & technology* **2017**, *51* (11), 6174-6184.

120. Purser, S.; Moore, P. R.; Swallow, S.; Gouverneur, V. Fluorine in medicinal chemistry. *Chemical Society Reviews* **2008**, *37* (2), 320-330.

121. Hagmann, W. K. The many roles for fluorine in medicinal chemistry. *Journal of medicinal chemistry* **2008**, *51* (15), 4359-4369.

122. Wang, J.; Sánchez-Roselló, M.; Aceña, J. L.; Del Pozo, C.; Sorochinsky, A. E.; Fustero, S.; Soloshonok, V. A.; Liu, H. Fluorine in pharmaceutical industry: fluorine-containing drugs introduced to the market in the last decade (2001–2011). *Chemical reviews* **2014**, *114* (4), 2432-2506.

123. Fan, J.; Dolensky, B.; Kim, I. H.; Kirk, K. L. Syntheses of E-and Z-2-and 4-fluorourocanic acids. *Journal of fluorine chemistry* **2002**, *115* (2), 137-142.

124. Hu, L.; Joshi, S. B.; Andra, K. K.; Thakkar, S. V.; Volkin, D. B.; Bann, J. G.; Middaugh, C. R. Comparison of the structural stability and dynamic properties of recombinant anthrax protective antigen and its 2-fluorohistidine-labeled analogue. *Journal of pharmaceutical sciences* **2012**, *101* (11), 4118-4128.

125. Chadwick, D. J.; Ngochindo, R. I. 2,5-Dilithiation of N-protected imidazoles. Syntheses of 2,5-disubstituted derivatives of 1-methoxymethyl-, 1-triphenylmethyl-, and 1-(N,N-dimethylsulphonamido)-imidazole. *Journal of the Chemical Society, Perkin Transactions 1* **1984**, (0), 481-486, 10.1039/P19840000481.

126. Coppi, D. I.; Salomone, A.; Perna, F. M.; Capriati, V. Exploiting the Lithiation-Directing Ability of Oxetane for the Regioselective Preparation of Functionalized 2-Aryloxetane Scaffolds under Mild Conditions. *Angewandte Chemie* **2012**, *124* (30), 7650-7654.

127. Sedano, C.; Velasco, R.; Feberero, C.; Suárez-Pantiga, S.; Sanz, R. α-Lithiobenzyloxy as a Directed Metalation Group in ortho-Lithiation Reactions. *Organic Letters* **2020**, *22* (16), 6365-6369.

128. Taylor, S. D.; Kotoris, C. C.; Hum, G. Recent advances in electrophilic fluorination. *Tetrahedron* **1999**, *55* (43), 12431-12477.

129. Cerezo, V.; Afonso, A.; Planas, M.; Feliu, L. Synthesis of 5-arylhistidines via a Suzuki–Miyaura cross-coupling. *Tetrahedron* **2007**, *63* (42), 10445-10453.

130. Park, E.; Lee, S. J.; Moon, H.; Park, J.; Jeon, H.; Hwang, J. S.; Hwang, H.; Hong, K. B.; Han, S.-H.; Choi, S.; Kang, S. Discovery and Biological Evaluation of N-Methyl-pyrrolo[2,3-b]pyridine-5-carboxamide Derivatives as JAK1-Selective Inhibitors. *Journal of Medicinal Chemistry* **2021**, *64* (2), 958-979.

131. Okano, A.; Isley, N. A.; Boger, D. L. Total Syntheses of Vancomycin-Related Glycopeptide Antibiotics and Key Analogues. *Chem Rev* **2017**, *117* (18), 11952-11993. From NLM.

132. Zhang, C. X.; Zheng, G. J.; Bi, F. Q.; Li, Y. L. A simple and efficient synthesis of the valsartan. *Chinese Chemical Letters* **2008**, *19* (7), 759-761.

133. Basarab, G. S.; Hill, P. J.; Garner, C. E.; Hull, K.; Green, O.; Sherer, B. A.; Dangel, P. B.; Manchester, J. I.; Bist, S.; Hauck, S. Optimization of pyrrolamide topoisomerase II inhibitors toward identification of an antibacterial clinical candidate (AZD5099). *Journal of Medicinal Chemistry* **2014**, *57* (14), 6060-6082.

134. Bruker, S.; SAINT, S. Bruker AXS Inc. *Madison, Wisconsin, USA* **2002**.

135. Sheldrick, G. M. Crystal structure refinement with SHELXL. *Acta Crystallographica Section C: Structural Chemistry* **2015**, *71* (1), 3-8.

136. Farrugia, L. J. WinGX and ORTEP for Windows: an update. *Journal of Applied Crystallography* **2012**, *45* (4), 849-854.

APPENDIX A

2-(3-bromophenyl)-4,5-dimethyl-1H-imidazole (3.1)

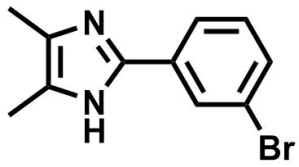

^{1}H NMR

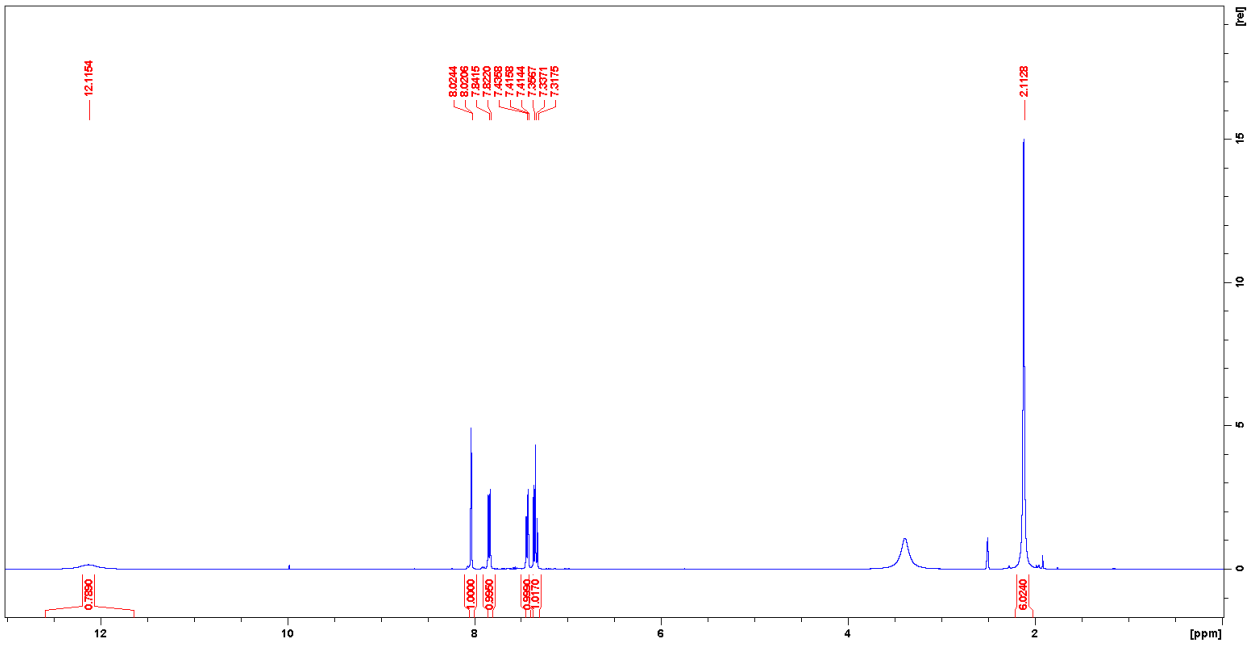

^{13}C NMR

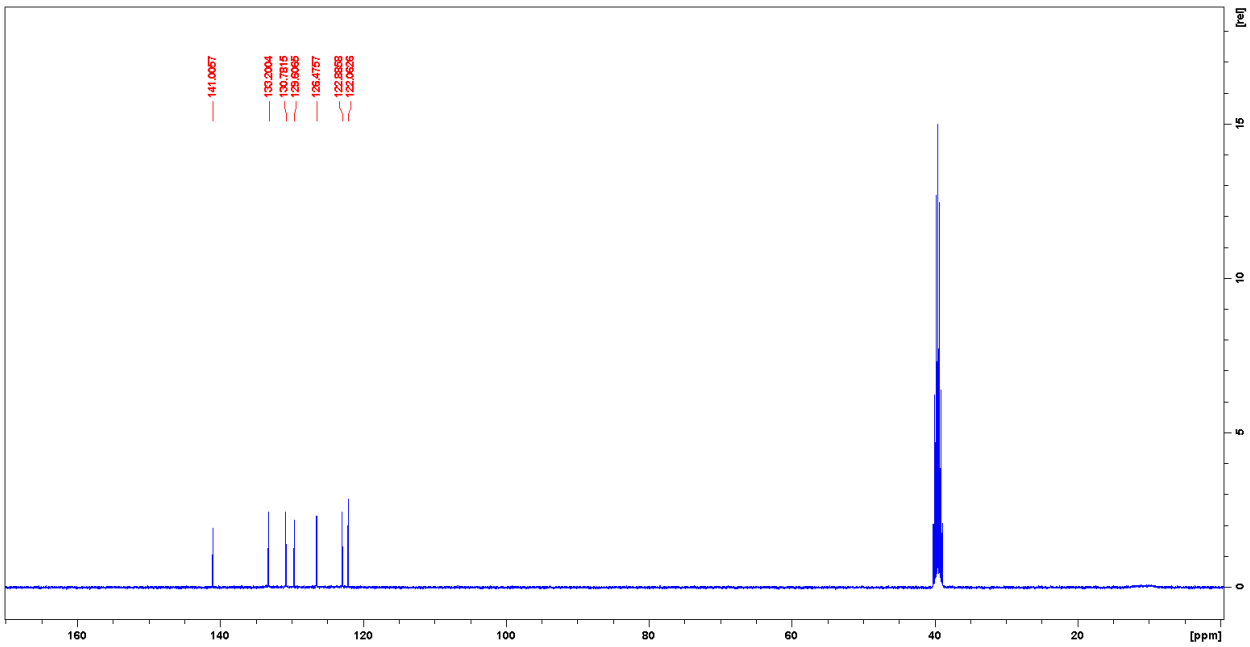

HRMS (ESI)

Elemental Composition Report **Page 1**

Single Mass Analysis
Tolerance = 5.0 PPM / DBE: min = -1.5, max = 50.0
Element prediction: Off

Monoisotopic Mass, Even Electron Ions
8 formula(e) evaluated with 1 results within limits (up to 50 closest results for each mass)
Elements Used:
C: 10-15 H: 10-15 N: 0-5 Br: 0-1

Sean
SMM_01_032 89 (1.842) Cm (1:96)

1: TOF MS ES-
1.18e+007

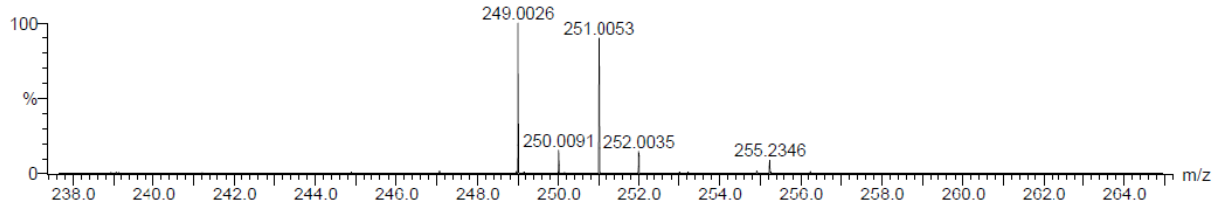

Minimum:				-1.5	
Maximum:		5.0	5.0	50.0	
Mass	Calc. Mass	mDa	PPM	DBE	Formula
249.0026	249.0027	-0.1	-0.4	7.5	C11 H10 N2 Br

FTIR

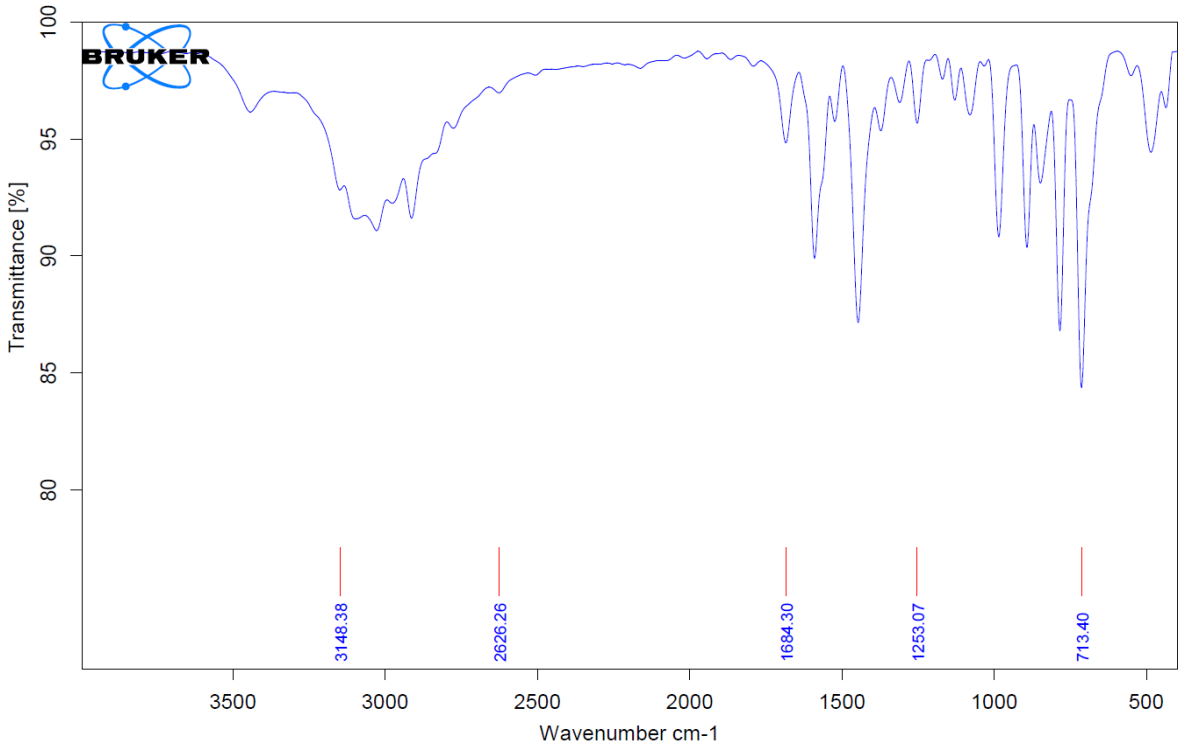
BRUKER
Transmittance [%]
100
95
90
85
80
3148.38
2626.26
1684.30
1253.07
713.40
3500
3000
2500
2000
1500
1000
500
Wavenumber cm-1

2-(3-bromophenyl)-4-methyl-1H-imidazole (3.2)

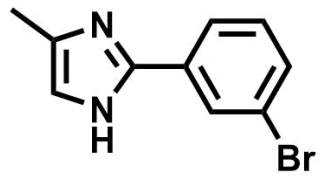

^{1}H NMR

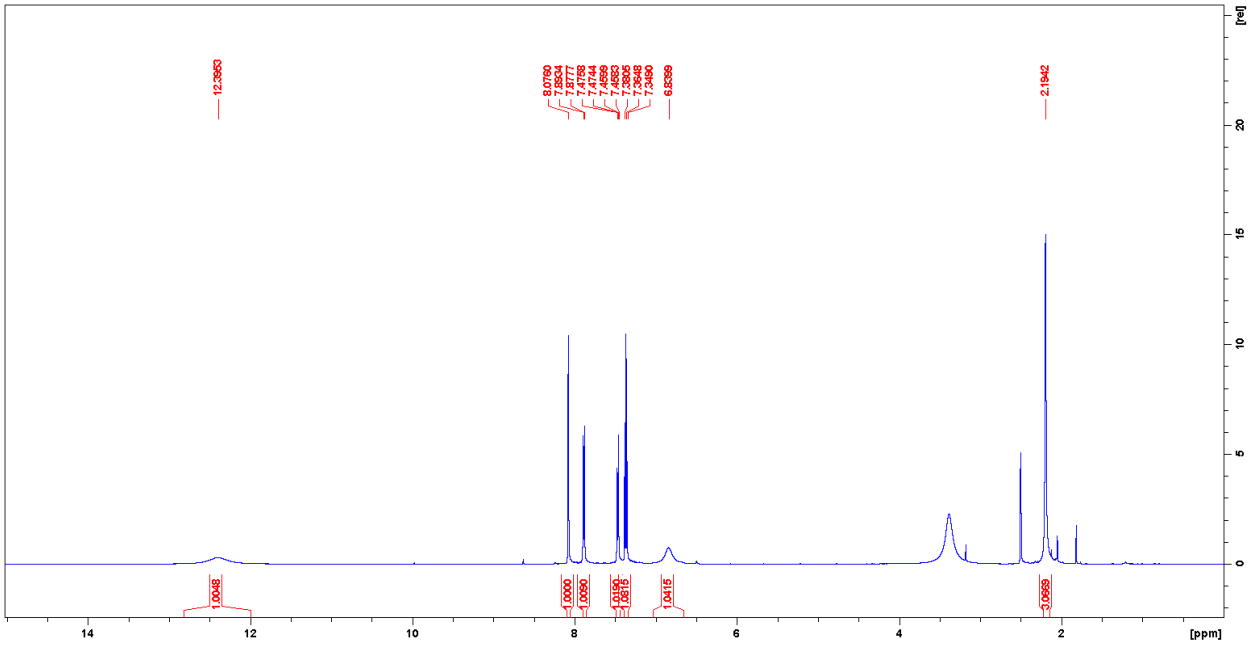

^{13}C NMR

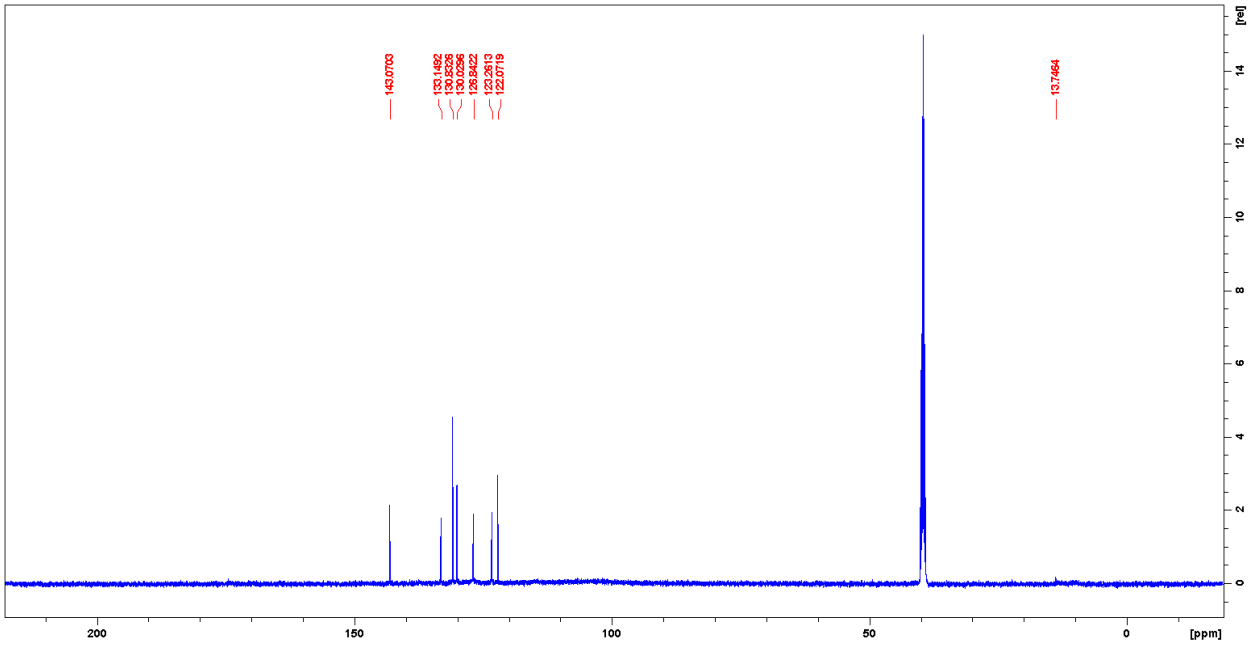

HRMS (ESI)

Elemental Composition Report **Page 1**

Single Mass Analysis
Tolerance = 500.0 PPM / DBE: min = -1.5, max = 50.0
Element prediction: Off
Number of isotope peaks used for i-FIT = 3

Monoisotopic Mass, Even Electron Ions
4 formula(e) evaluated with 1 results within limits (up to 50 closest results for each mass)
Elements Used:
C: 10-15 H: 5-10 N: 0-5 Br: 0-1

Sean
SMM_01_095 65 (1.356) AM (Top,4, Ar,10000.0,0.00,0.00); Cm (1:96)

1: TOF MS ES+
2.05e+007

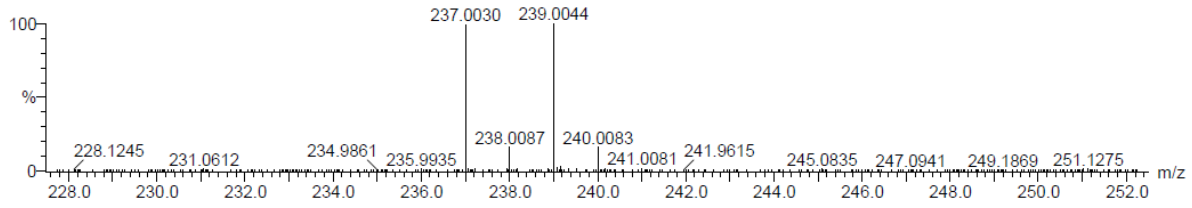

Minimum:				-1.5				
Maximum:		5.0	500.0	50.0				
Mass	Calc. Mass	mDa	PPM	DBE	i-FIT	Norm	Conf(%)	Formula
237.0030	237.0027	0.3	1.3	6.5	726.4	n/a	n/a	C10 H10 N2 Br

FTIR

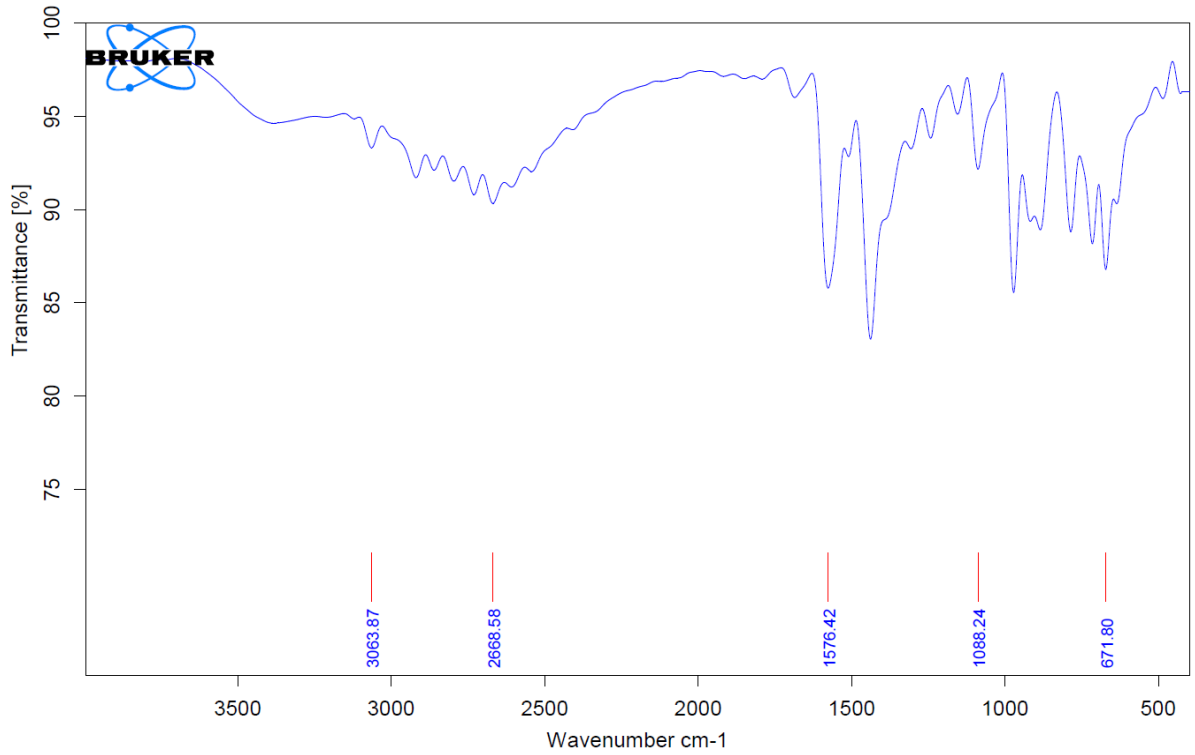
BRUKER
Transmittance [%]
100
95
90
85
80
75
3063.87
2668.58
1576.42
1088.24
671.80
3500
3000
2500
2000
1500
1000
500
Wavenumber cm-1

2-(3-bromophenyl)-1H-imidazole (3.3)

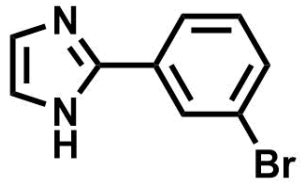

^{1}H NMR

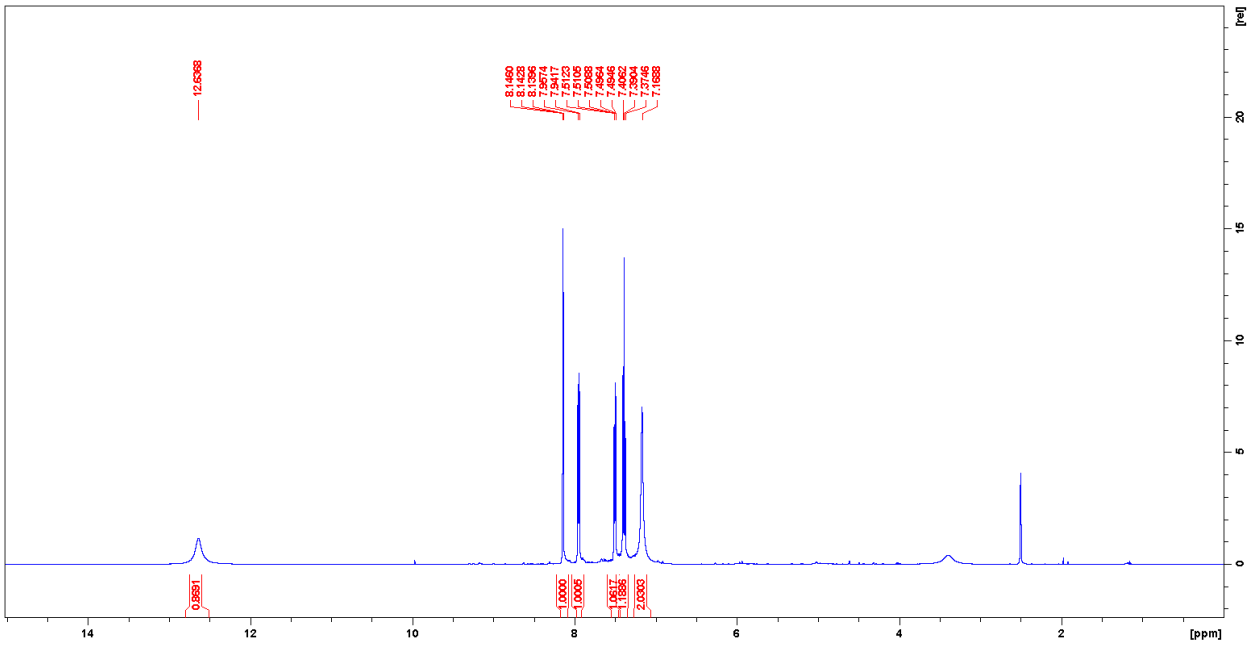

^{13}C NMR

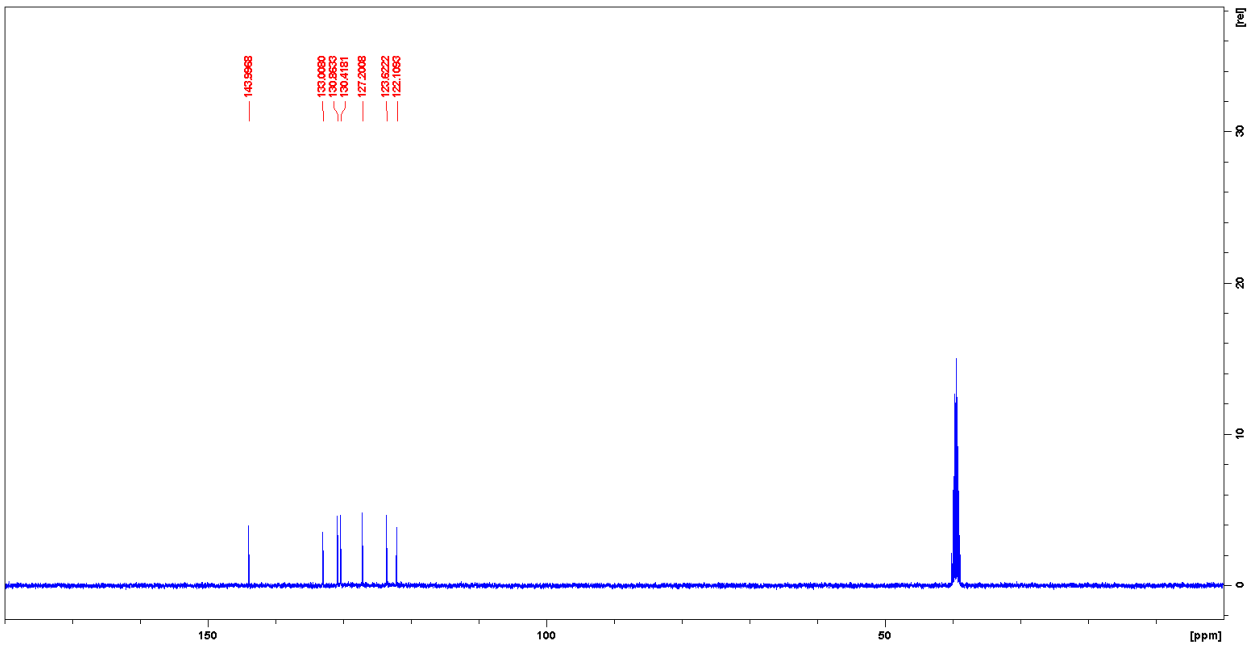

HRMS (ESI)

Elemental Composition Report **Page 1**

Single Mass Analysis
Tolerance = 5.0 PPM / DBE: min = -1.5, max = 50.0
Element prediction: Off
Number of isotope peaks used for i-FIT = 3

Monoisotopic Mass, Even Electron Ions
7 formula(e) evaluated with 1 results within limits (up to 50 closest results for each mass)
Elements Used:
C: 5-10 H: 5-10 N: 0-5 Br: 0-1

Sean
SMM_01_076 9 (0.222) AM (Top,4, Ar,10000.0,0.00,0.00); Cm (1:96) 1: TOF MS ES-
2.71e+007

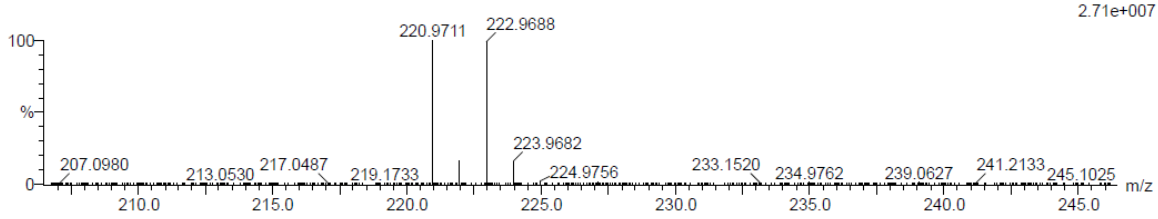

Minimum:				-1.5				
Maximum:		5.0	5.0	50.0				
Mass	Calc. Mass	mDa	PPM	DBE	i-FIT	Norm	Conf(%)	Formula
220.9711	220.9714	-0.3	-1.4	7.5	739.9	n/a	n/a	C9 H6 N2 Br

FTIR

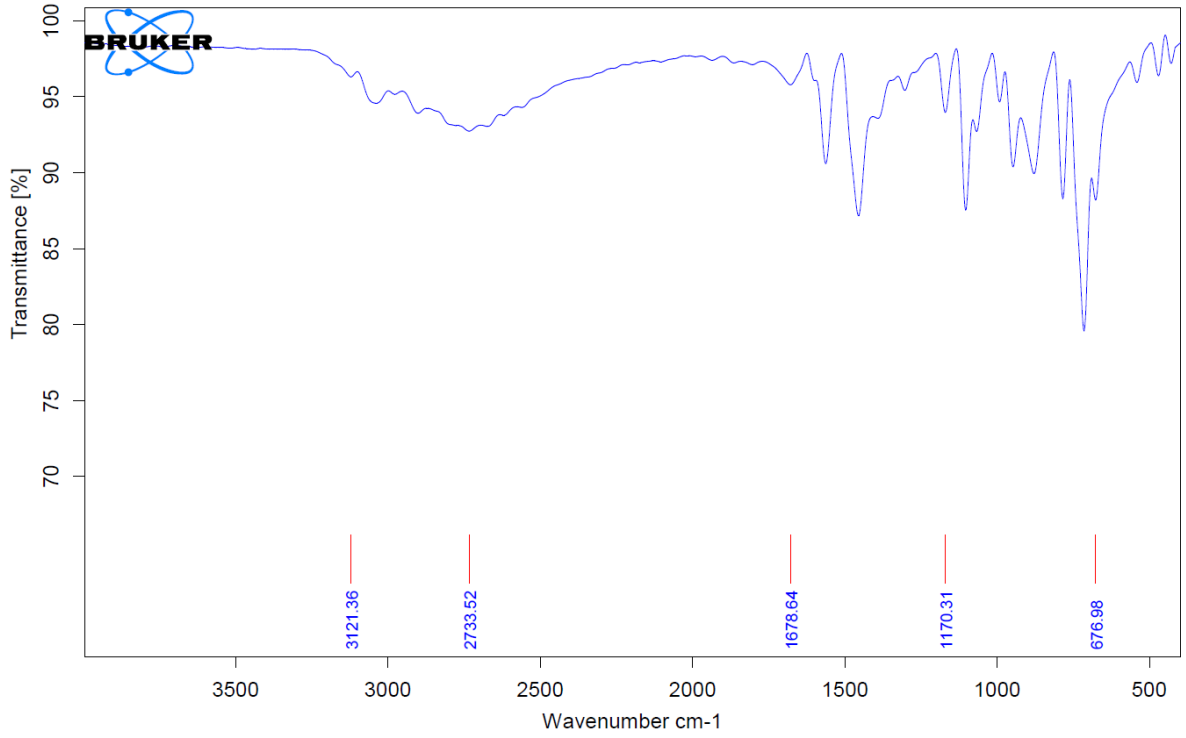
BRUKER
Transmittance [%]
100
95
90
85
80
75
70
3121.36
2733.52
1678.64
1170.31
676.98
3500
3000
2500
2000
1500
1000
500
Wavenumber cm-1

2-(3-bromophenyl)-1-(ethoxymethyl)-1H-imidazole (3.4)

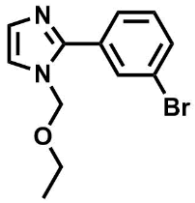

^{1}H NMR

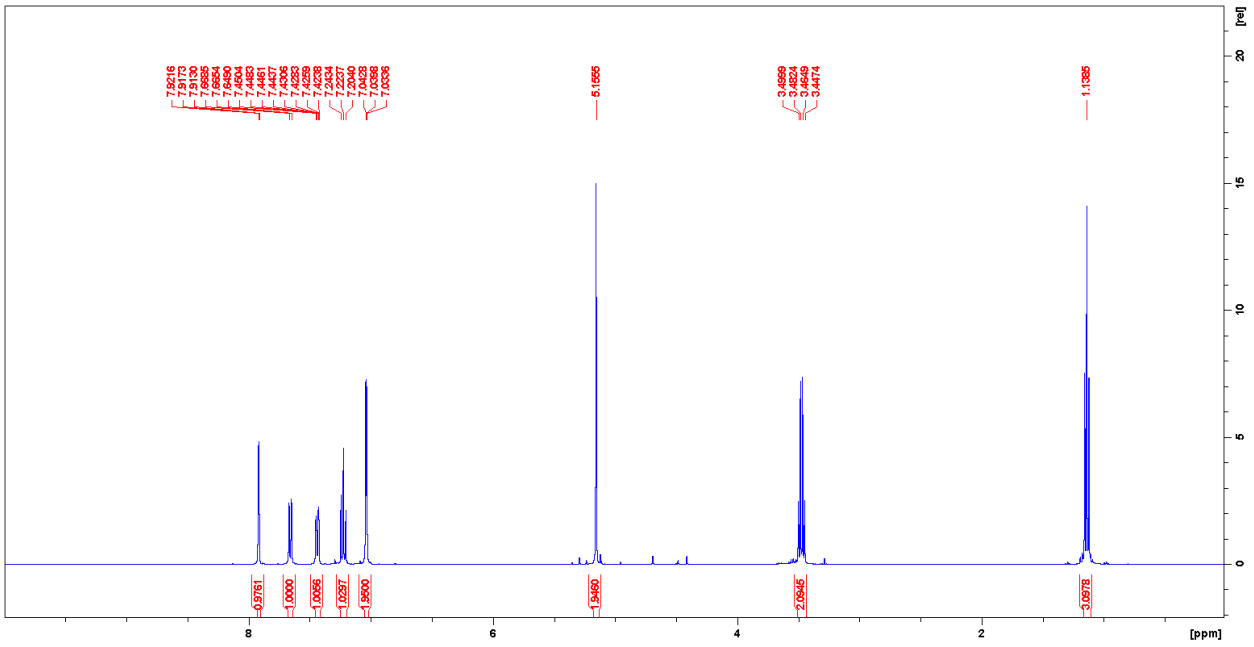

^{13}C NMR

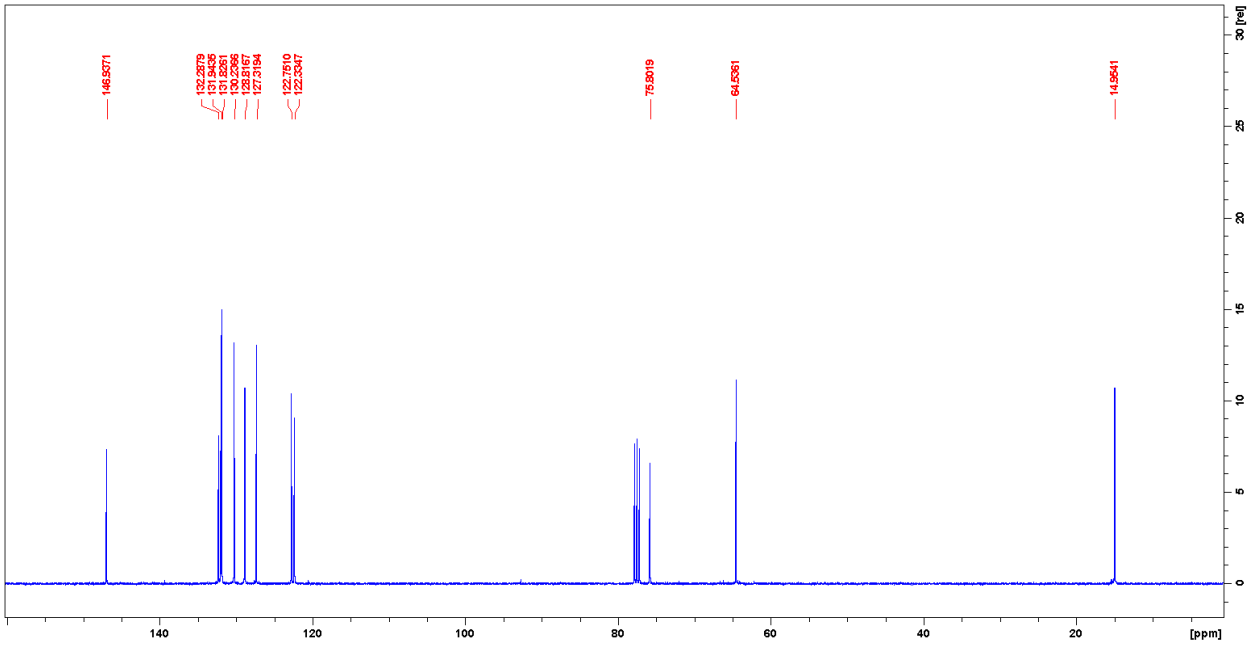

HRMS (ESI)

Elemental Composition Report **Page 1**

Single Mass Analysis
Tolerance = 5.0 PPM / DBE: min = -1.5, max = 50.0
Element prediction: Off
Number of isotope peaks used for i-FIT = 3

Monoisotopic Mass, Even Electron Ions
40 formula(e) evaluated with 1 results within limits (up to 50 closest results for each mass)
Elements Used:
C: 10-15 H: 10-15 N: 0-5 O: 0-5 Br: 0-1

Sean
SMM_01_093 9 (0.222) AM (Top,4, Ar,10000.0,0.00,0.00); Cm (1:96)

1: TOF MS ES+
4.44e+007

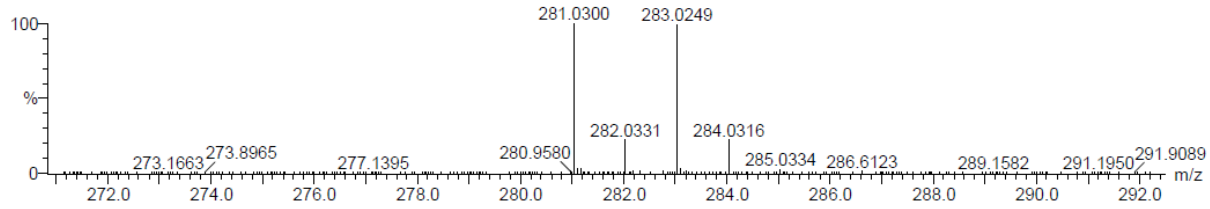

Minimum:				-1.5				
Maximum:		5.0	5.0	50.0				
Mass	Calc. Mass	mDa	PPM	DBE	i-FIT	Norm	Conf(%)	Formula
281.0300	281.0290	1.0	3.6	6.5	857.9	n/a	n/a	C12 H14 N2 O Br

FTIR

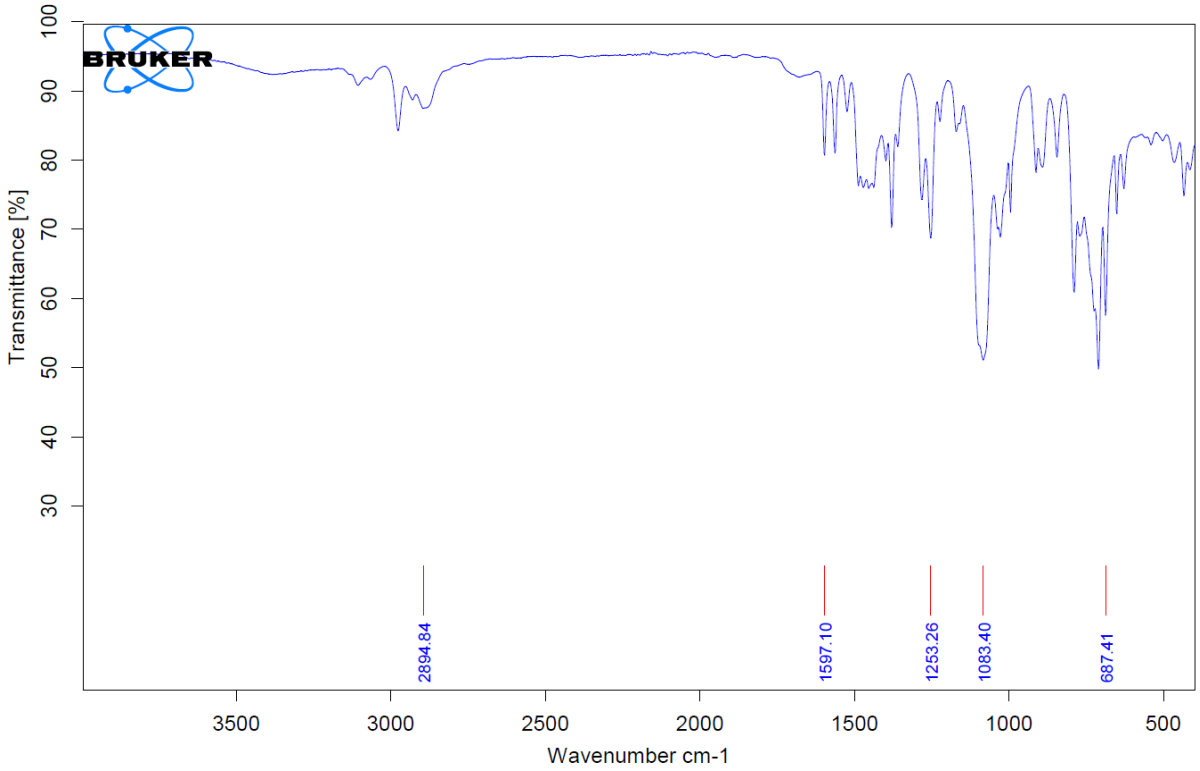
BRUKER
Transmittance [%]
100
90
80
70
60
50
40
30
2894.84
1597.10
1253.26
1083.40
687.41
3500
3000
2500
2000
1500
1000
500
Wavenumber cm-1

2-(3-bromophenyl)-1-(ethoxymethyl)-4-methyl-1H-imidazole (3.5)

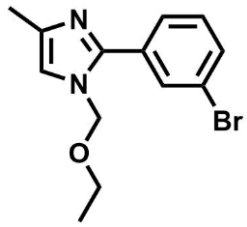

^{1}H NMR

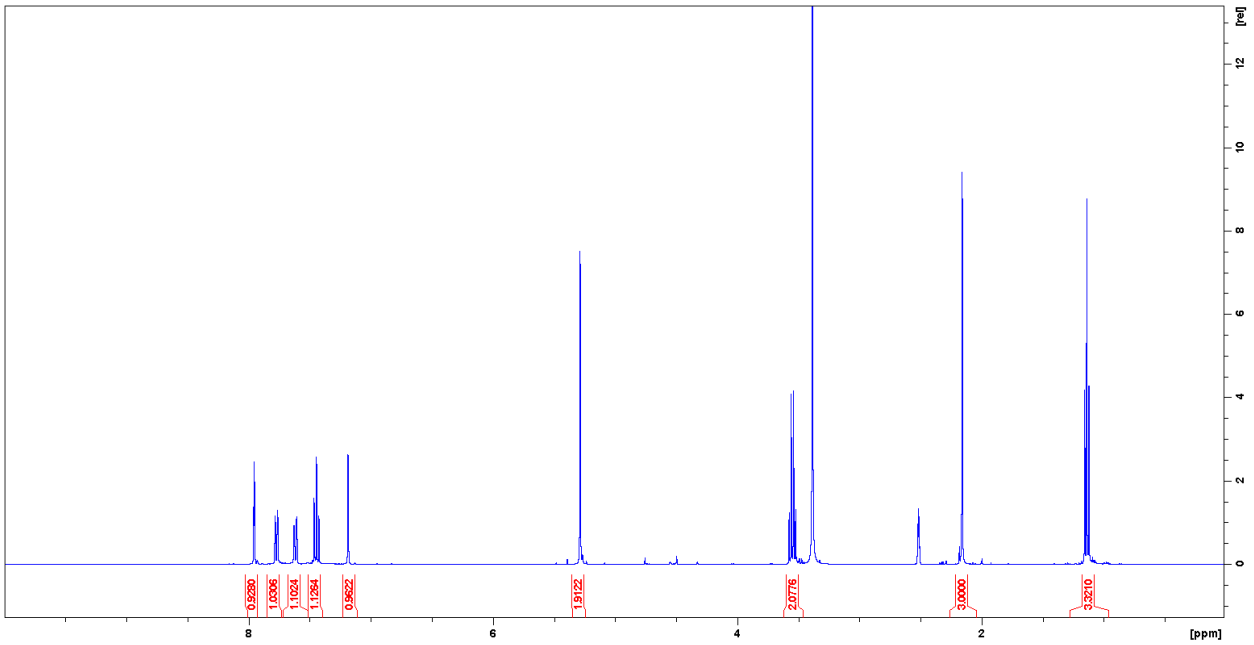

^{13}C NMR

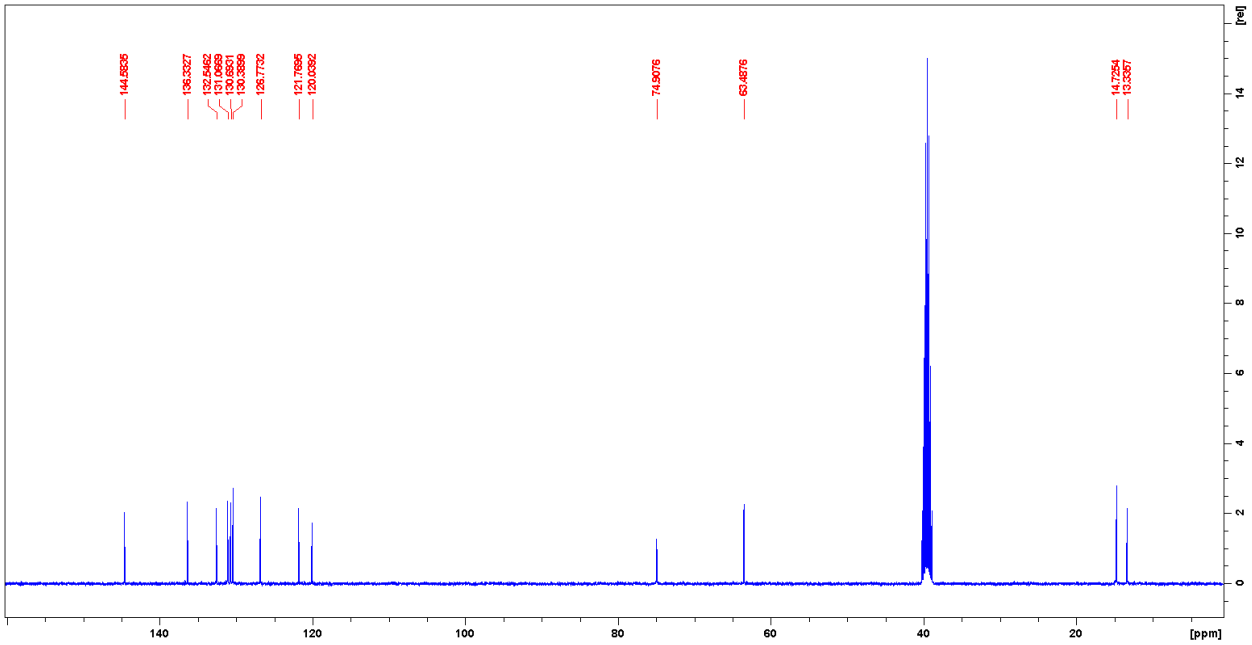

HRMS (ESI)

Elemental Composition Report **Page 1**

Single Mass Analysis
Tolerance = 5.0 PPM / DBE: min = -1.5, max = 50.0
Element prediction: Off
Number of isotope peaks used for i-FIT = 3

Monoisotopic Mass, Even Electron Ions
52 formula(e) evaluated with 1 results within limits (up to 50 closest results for each mass)
Elements Used:
C: 10-15 H: 10-20 N: 0-5 O: 0-5 Br: 0-1

Sean
SMM_01_096A 1 (0.060) AM (Top,4, Ar,10000.0,0.00,0.00); Cm (1:96)

1: TOF MS ES+
4.37e+007

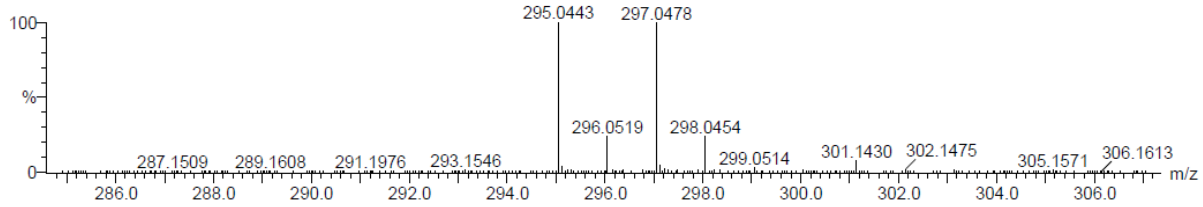

Minimum:				-1.5				
Maximum:		5.0	5.0	50.0				
Mass	Calc. Mass	mDa	PPM	DBE	i-FIT	Norm	Conf(%)	Formula
295.0443	295.0446	-0.3	-1.0	6.5	892.6	n/a	n/a	C13 H16 N2 O Br

FTIR

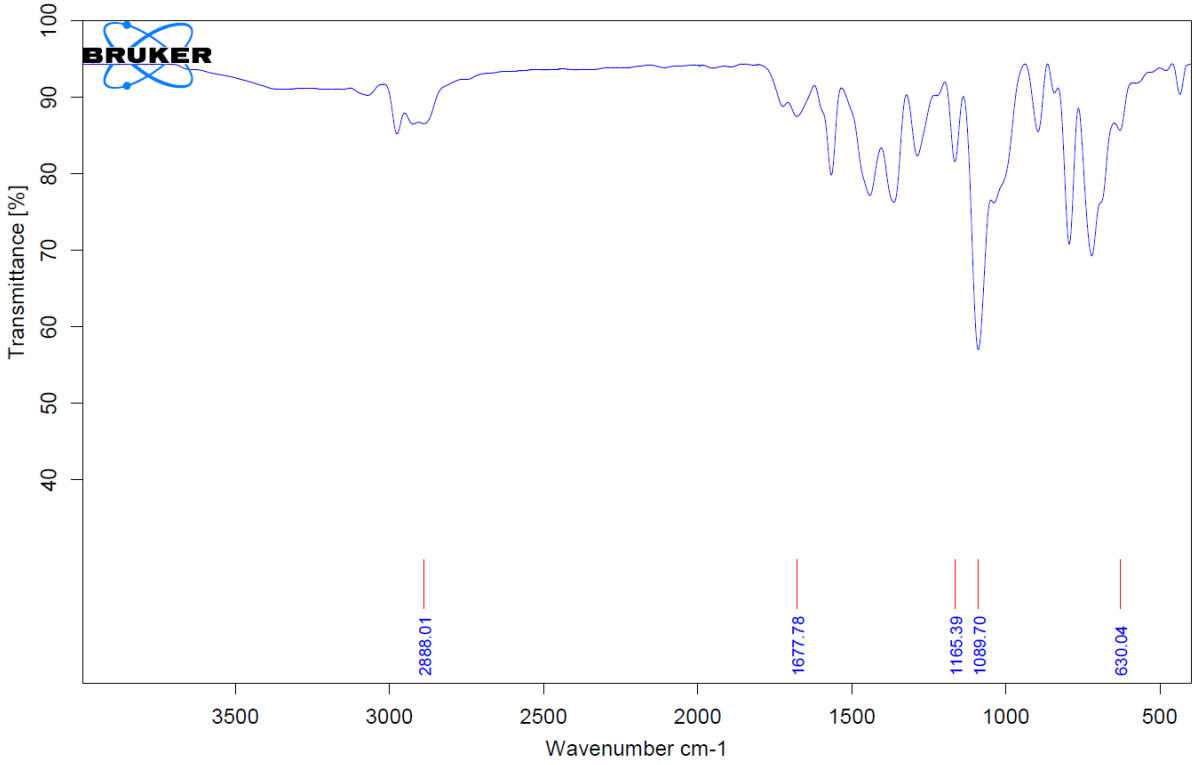
BRUKER
Transmittance [%]
100
90
80
70
60
50
40
2888.01
1677.78
1165.39
1089.70
630.04
3500
3000
2500
2000
1500
1000
500
Wavenumber cm-1

2-(3-bromophenyl)-1-(ethoxymethyl)-5-methyl-1H-imidazole (3.6)

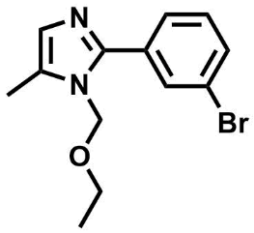

^{1}H NMR

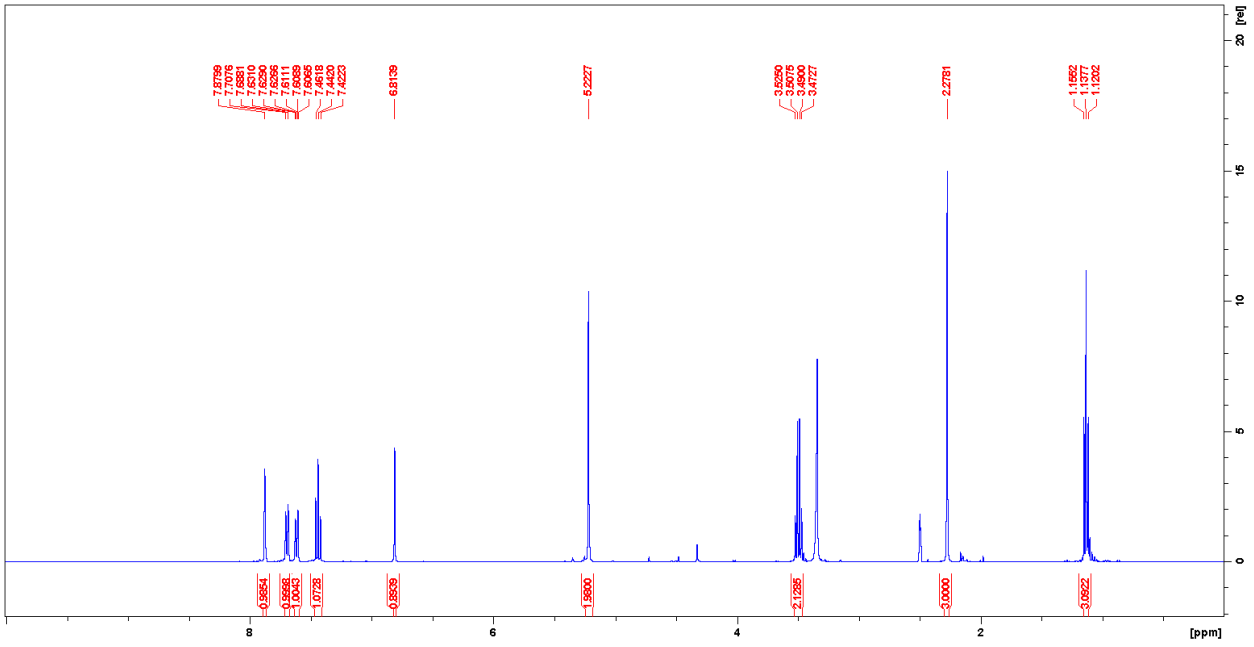

^{13}C NMR

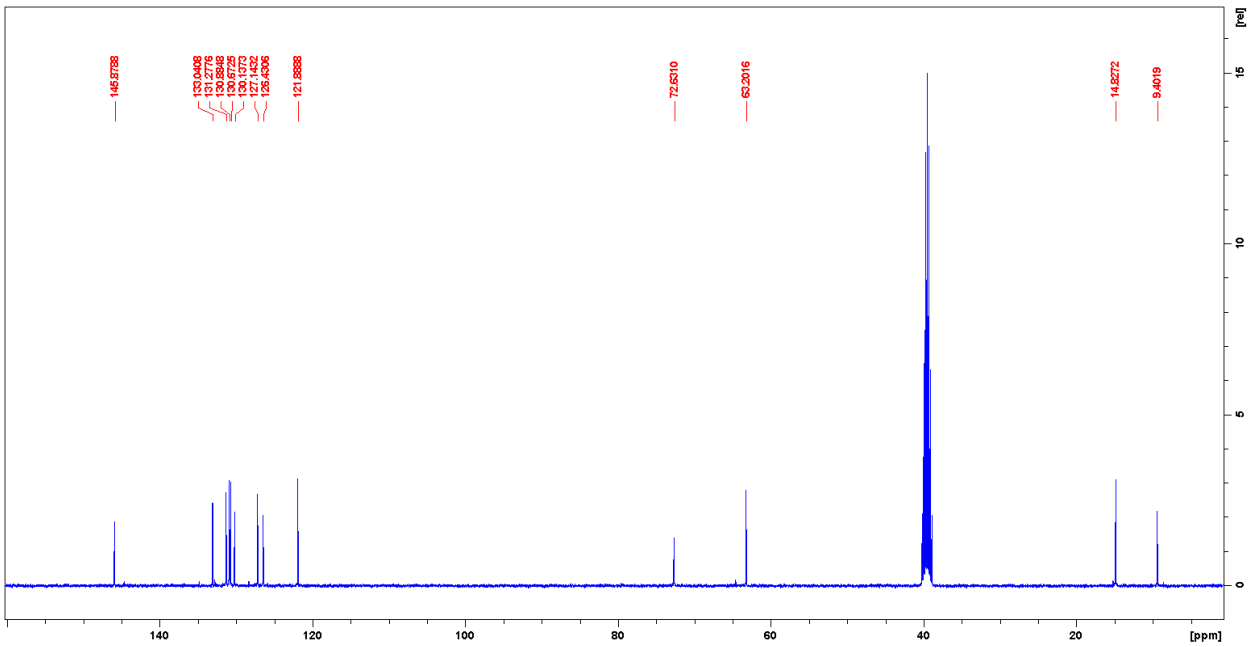

HRMS (ESI)

Elemental Composition Report **Page 1**

Single Mass Analysis
Tolerance = 5.0 PPM / DBE: min = -1.5, max = 50.0
Element prediction: Off
Number of isotope peaks used for i-FIT = 3

Monoisotopic Mass, Even Electron Ions
52 formula(e) evaluated with 1 results within limits (up to 50 closest results for each mass)
Elements Used:
C: 10-15 H: 10-20 N: 0-5 O: 0-5 Br: 0-1

Sean
SMM_01_096B 1 (0.060) AM (Cen,4, 80.00, Ar,10000.0,556.28,0.00); Cm (1:96)

1: TOF MS ES+
5.30e+007

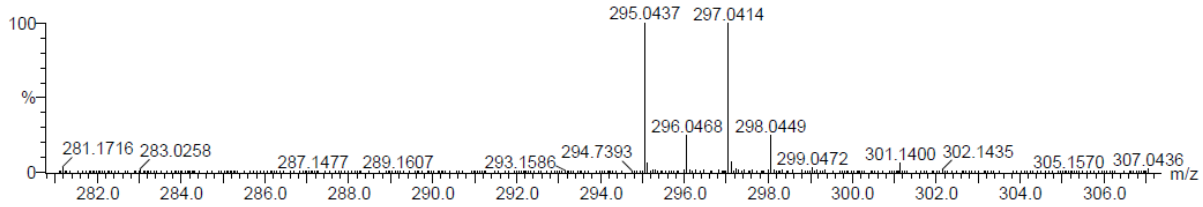

Minimum:				-1.5				
Maximum:		5.0	5.0	50.0				
Mass	Calc. Mass	mDa	PPM	DBE	i-FIT	Norm	Conf(%)	Formula
295.0437	295.0446	-0.9	-3.1	6.5	859.7	n/a	n/a	C13 H16 N2 O Br

FTIR

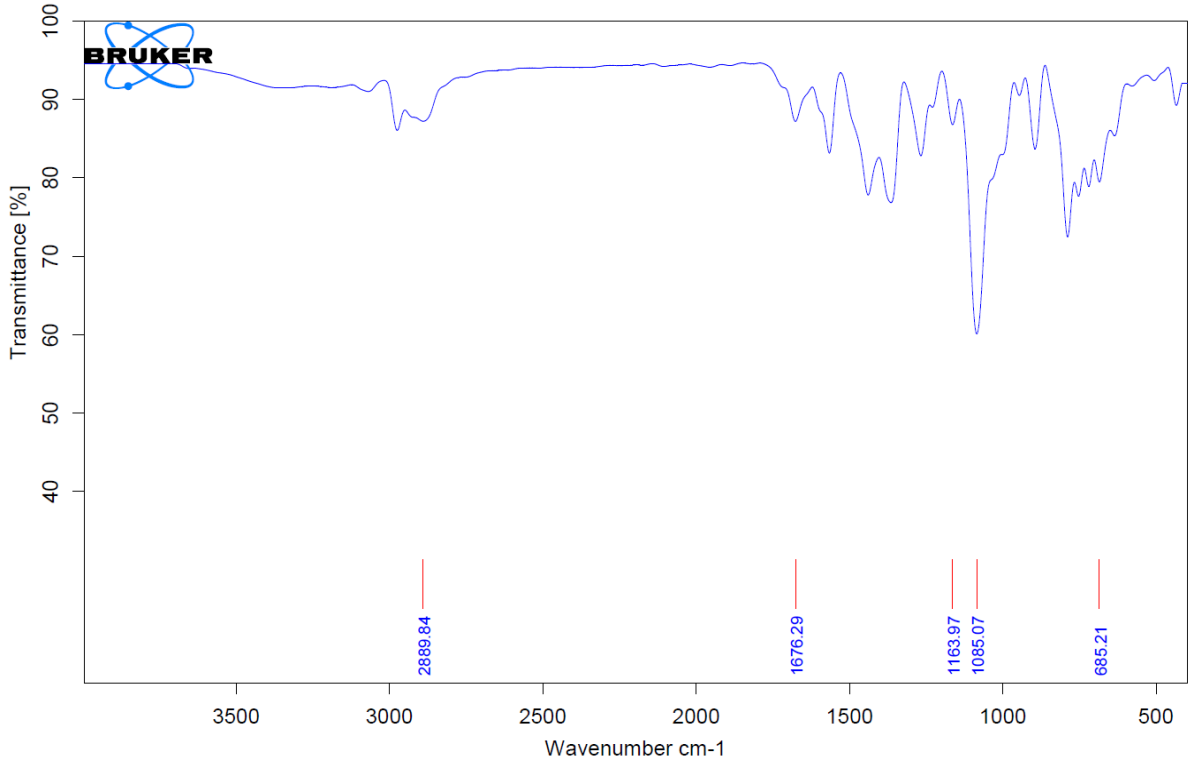
BRUKER
Transmittance [%]
100
90
80
70
60
50
40
2889.84
1676.29
1163.97
1085.07
685.21
3500
3000
2500
2000
1500
1000
500
Wavenumber cm-1

N-(2-chlorobenzyl)-3-(1-(ethoxymethyl)-1H-imidazol-2-yl)aniline (3.9)

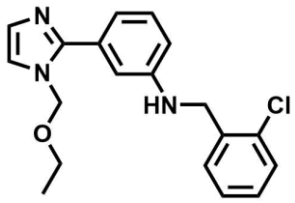

^{1}H NMR

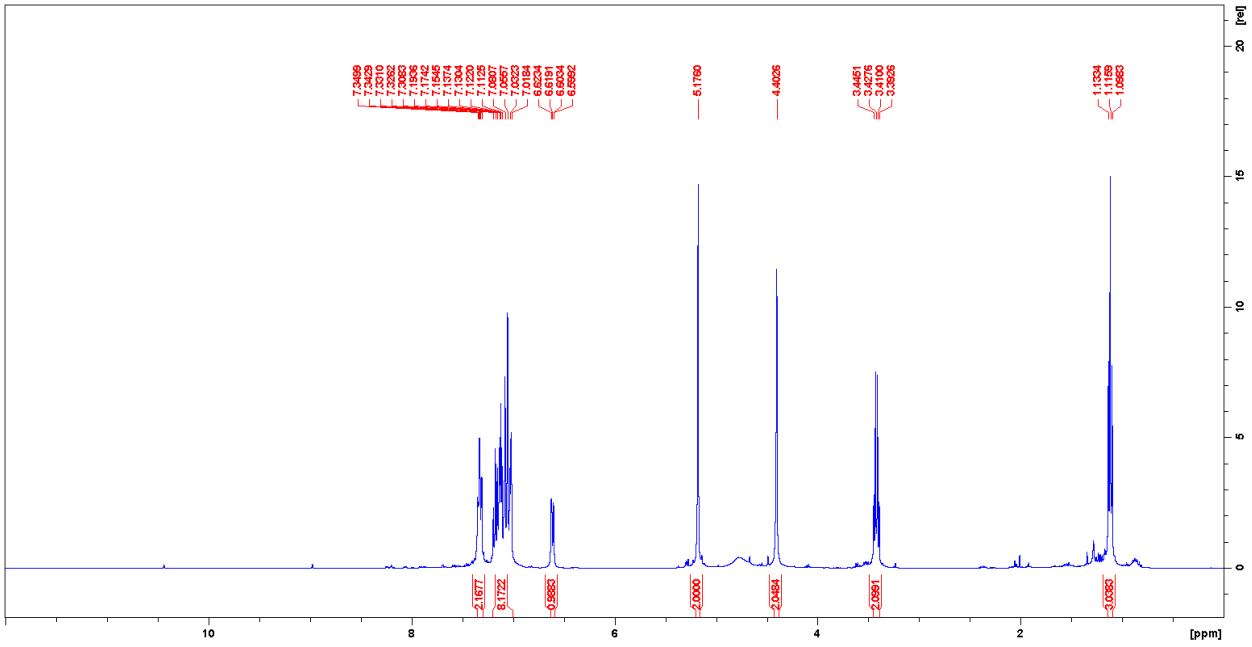

^{13}C NMR

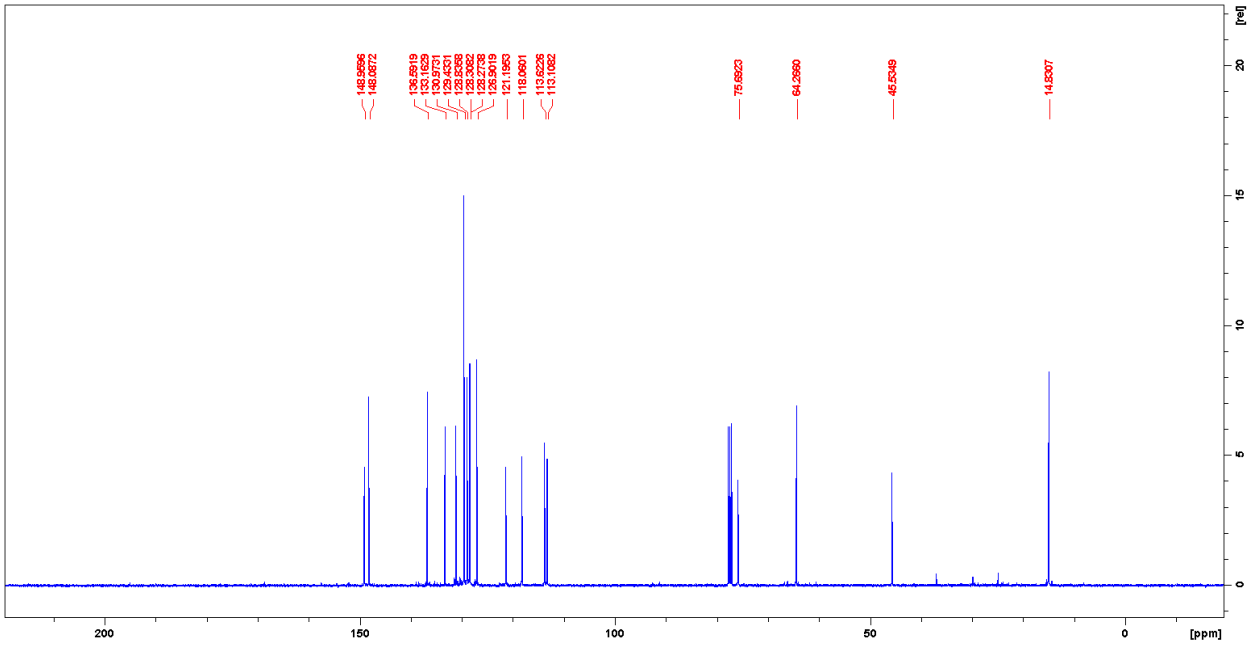

HRMS (ESI)

Elemental Composition Report **Page 1**

Single Mass Analysis
Tolerance = 5.0 PPM / DBE: min = -1.5, max = 50.0
Element prediction: Off
Number of isotope peaks used for i-FIT = 3

Monoisotopic Mass, Even Electron Ions
32 formula(e) evaluated with 1 results within limits (up to 50 closest results for each mass)
Elements Used:
C: 15-20 H: 20-25 N: 0-5 O: 0-5 Cl: 0-1

Sean
SMM_01_097 65 (1.356) AM (Cen,4, 80.00, Ar,10000.0,556.28,0.00); Cm (1:96)

1: TOF MS ES+
5.27e+007

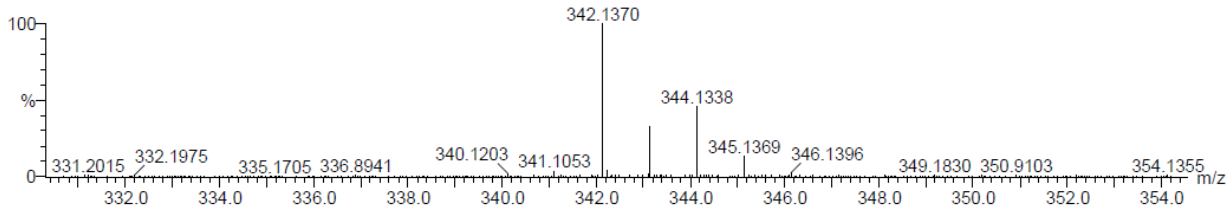

Minimum:				-1.5				
Maximum:		5.0	5.0	50.0				
Mass	Calc. Mass	mDa	PPM	DBE	i-FIT	Norm	Conf(%)	Formula
342.1370	342.1373	-0.3	-0.9	10.5	674.7	n/a	n/a	C19 H21 N3 O Cl

FTIR

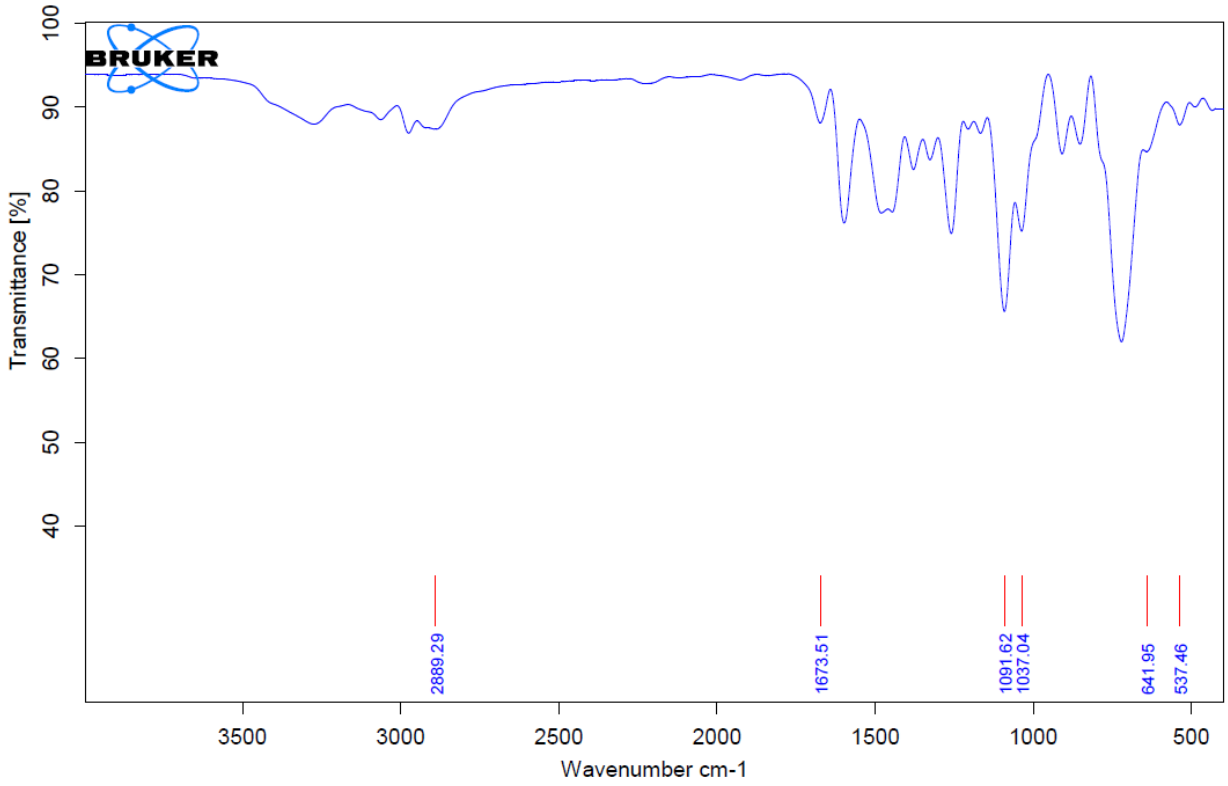
BRUKER
Transmittance [%]
100
90
80
70
60
50
40
2889.29
1673.51
1091.62
1037.04
641.95
537.46
3500
3000
2500
2000
1500
1000
500
Wavenumber cm-1

N-(2-chlorobenzyl)-3-(1-(ethoxymethyl)-4-methyl-1H-imidazol-2-yl)aniline (3.10)

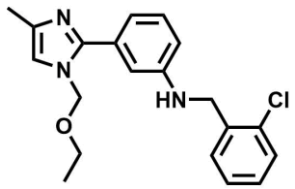

^{1}H NMR

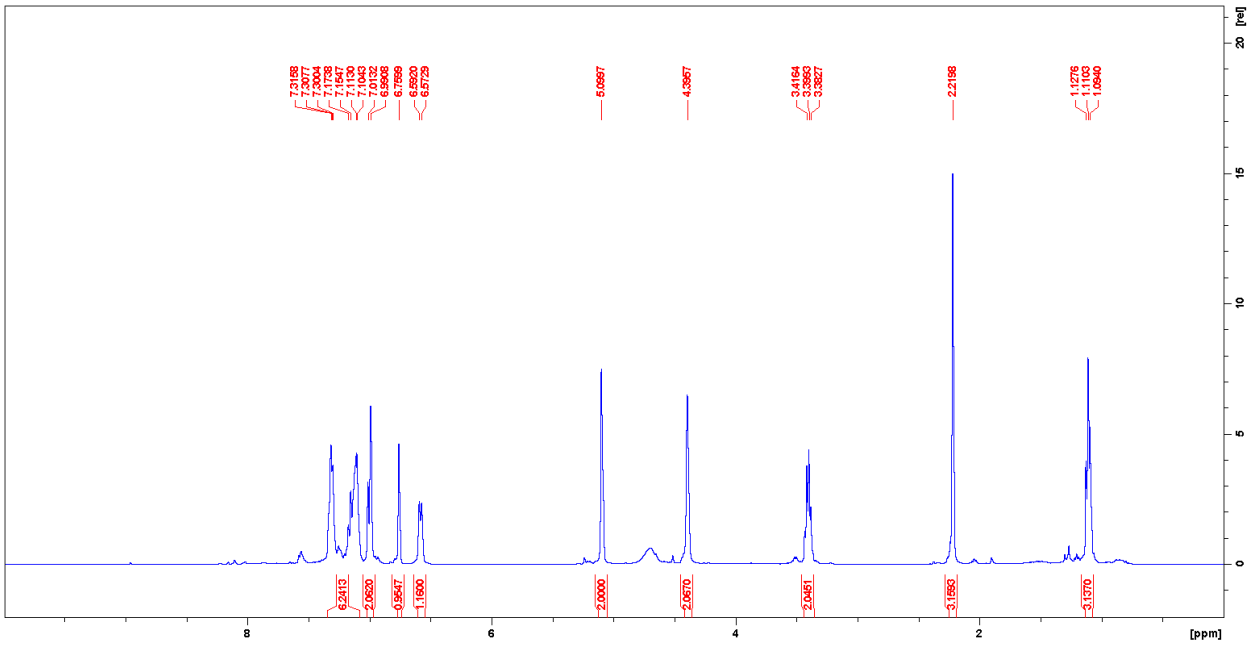

^{13}C NMR

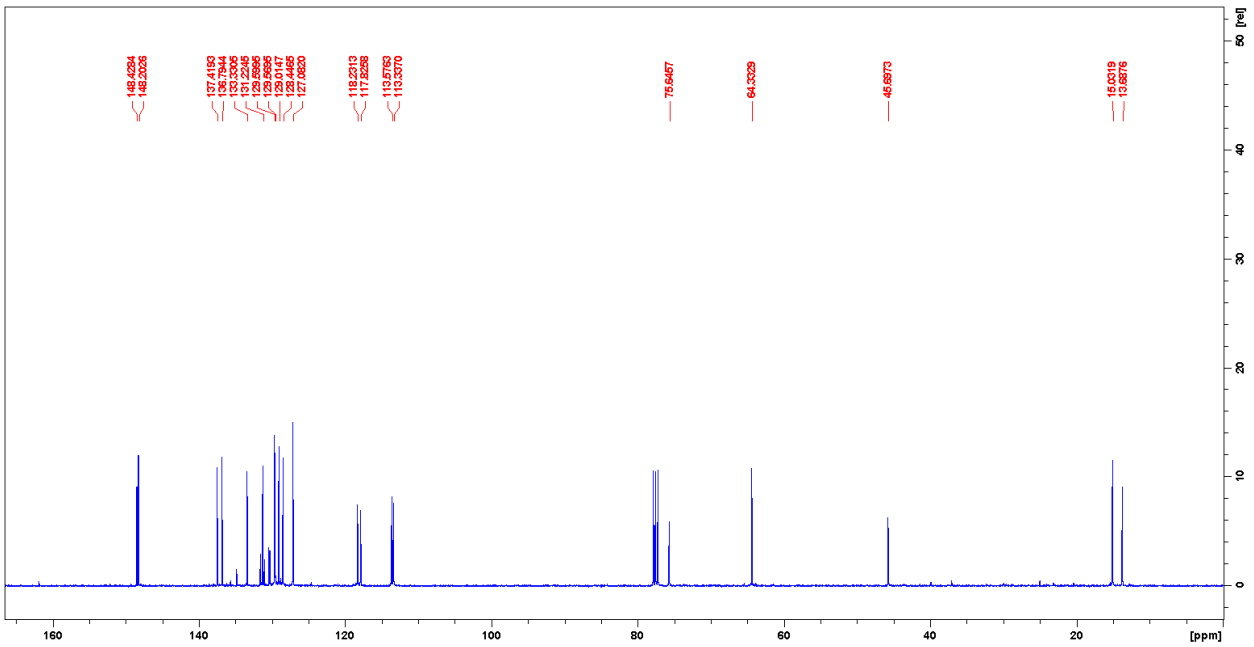

HRMS (ESI)

Elemental Composition Report **Page 1**

Single Mass Analysis
Tolerance = 5.0 PPM / DBE: min = -1.5, max = 50.0
Element prediction: Off
Number of isotope peaks used for i-FIT = 3

Monoisotopic Mass, Even Electron Ions
32 formula(e) evaluated with 1 results within limits (up to 50 closest results for each mass)
Elements Used:
C: 15-20 H: 20-25 N: 0-5 O: 0-5 Cl: 0-1

Sean
SMM_01_098 73 (1.518) AM (Cen,4, 80.00, Ar,10000.0,556.28,0.00); Cm (1:96)

1: TOF MS ES+
5.46e+007

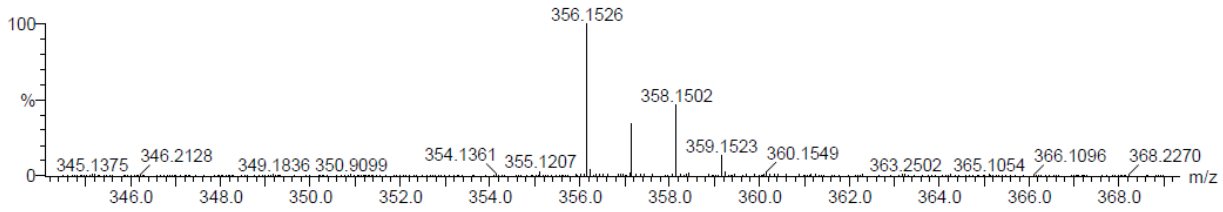

Minimum:				-1.5				
Maximum:		5.0	5.0	50.0				
Mass	Calc. Mass	mDa	PPM	DBE	i-FIT	Norm	Conf(%)	Formula
356.1526	356.1530	-0.4	-1.1	10.5	601.5	n/a	n/a	C20 H23 N3 O Cl

FTIR

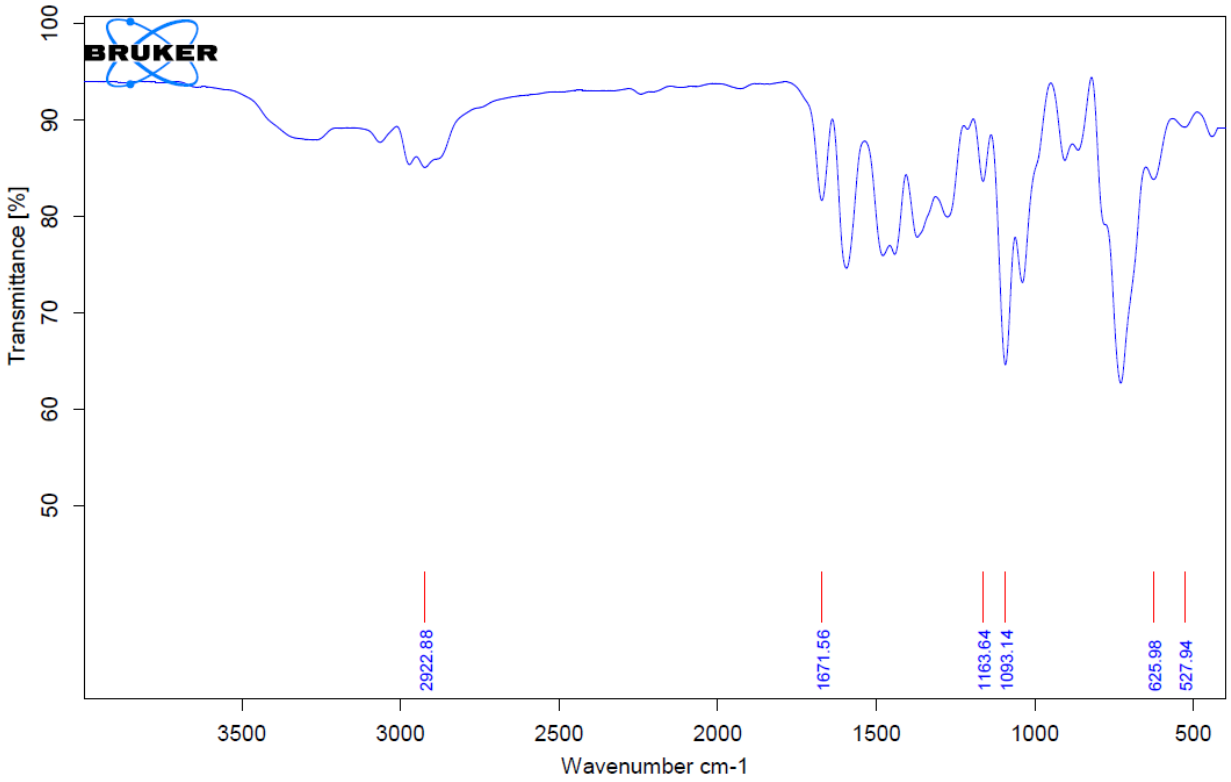
BRUKER
Transmittance [%]
100
90
80
70
60
50
2922.88
1671.56
1163.64
1093.14
625.98
527.94
3500
3000
2500
2000
1500
1000
500
Wavenumber cm-1

N-(2-chlorobenzyl)-3-(1-(ethoxymethyl)-5-methyl-1H-imidazol-2-yl)aniline (3.11)

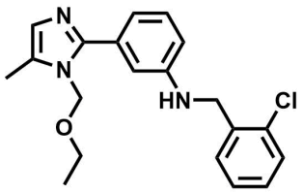

^{1}H NMR

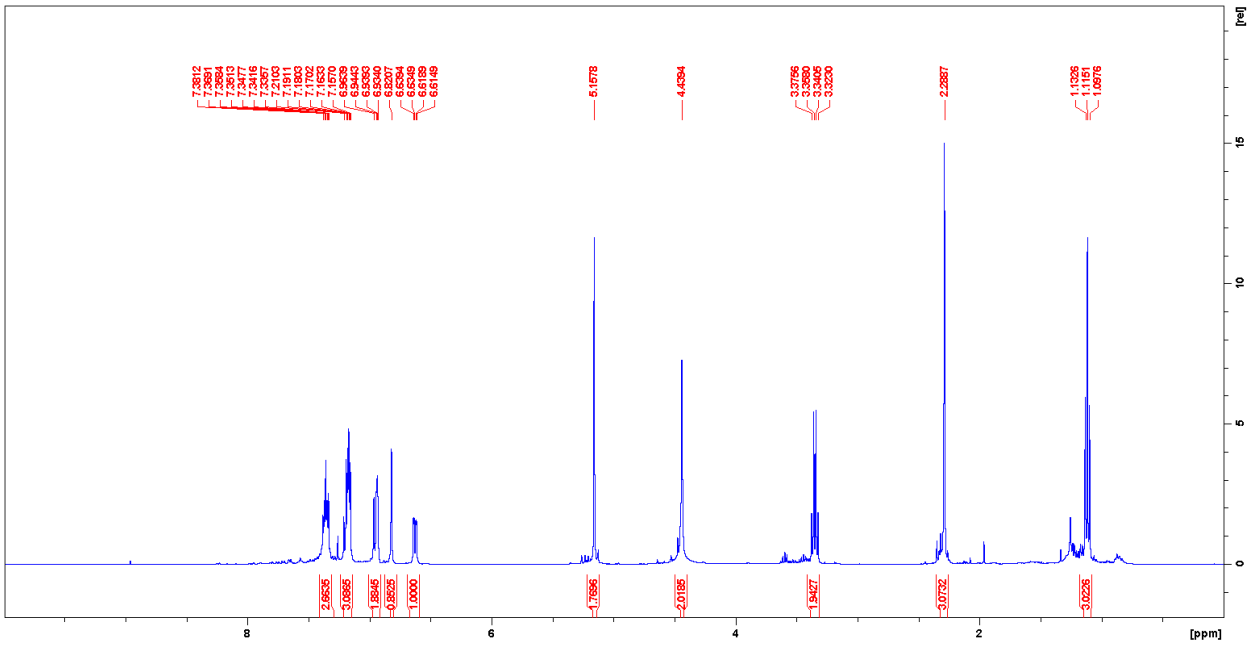

^{13}C NMR

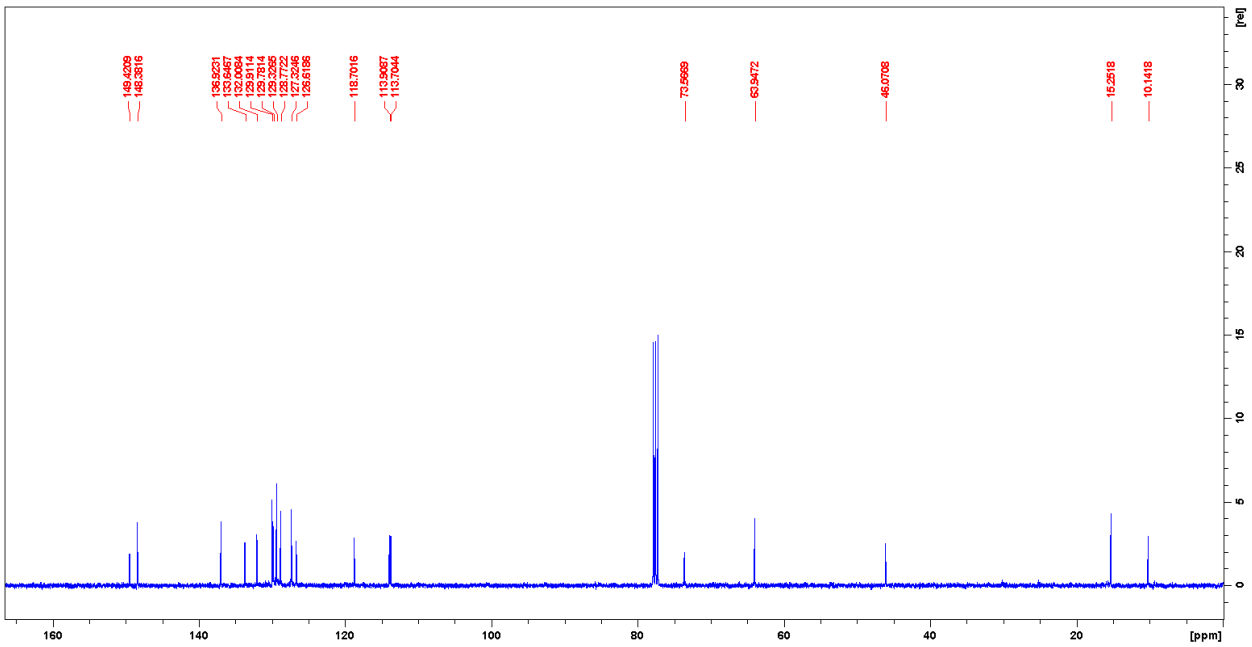

HRMS (ESI)

Elemental Composition Report **Page 1**

Single Mass Analysis
Tolerance = 5.0 PPM / DBE: min = -1.5, max = 50.0
Element prediction: Off
Number of isotope peaks used for i-FIT = 3

Monoisotopic Mass, Even Electron Ions
32 formula(e) evaluated with 1 results within limits (up to 50 closest results for each mass)
Elements Used:
C: 15-20 H: 20-25 N: 0-5 O: 0-5 Cl: 0-1

Sean
SMM_01_099 73 (1.518) AM (Cen,4, 80.00, Ar,10000.0,556.28,0.00); Cm (1:96)

1: TOF MS ES+
4.96e+007

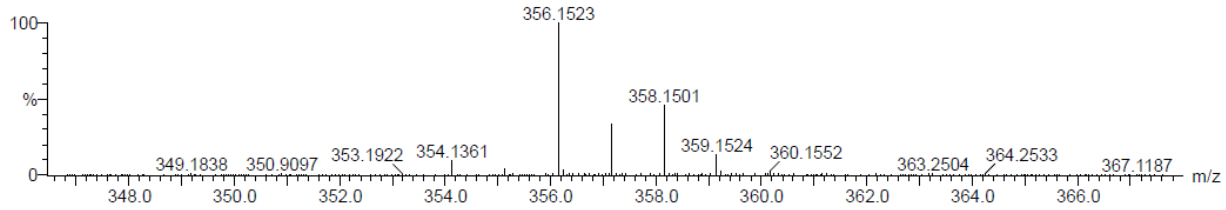

Minimum:				-1.5				
Maximum:		5.0	5.0	50.0				
Mass	Calc. Mass	mDa	PPM	DBE	i-FIT	Norm	Conf(%)	Formula
356.1523	356.1530	-0.7	-2.0	10.5	725.0	n/a	n/a	C20 H23 N3 O Cl

FTIR

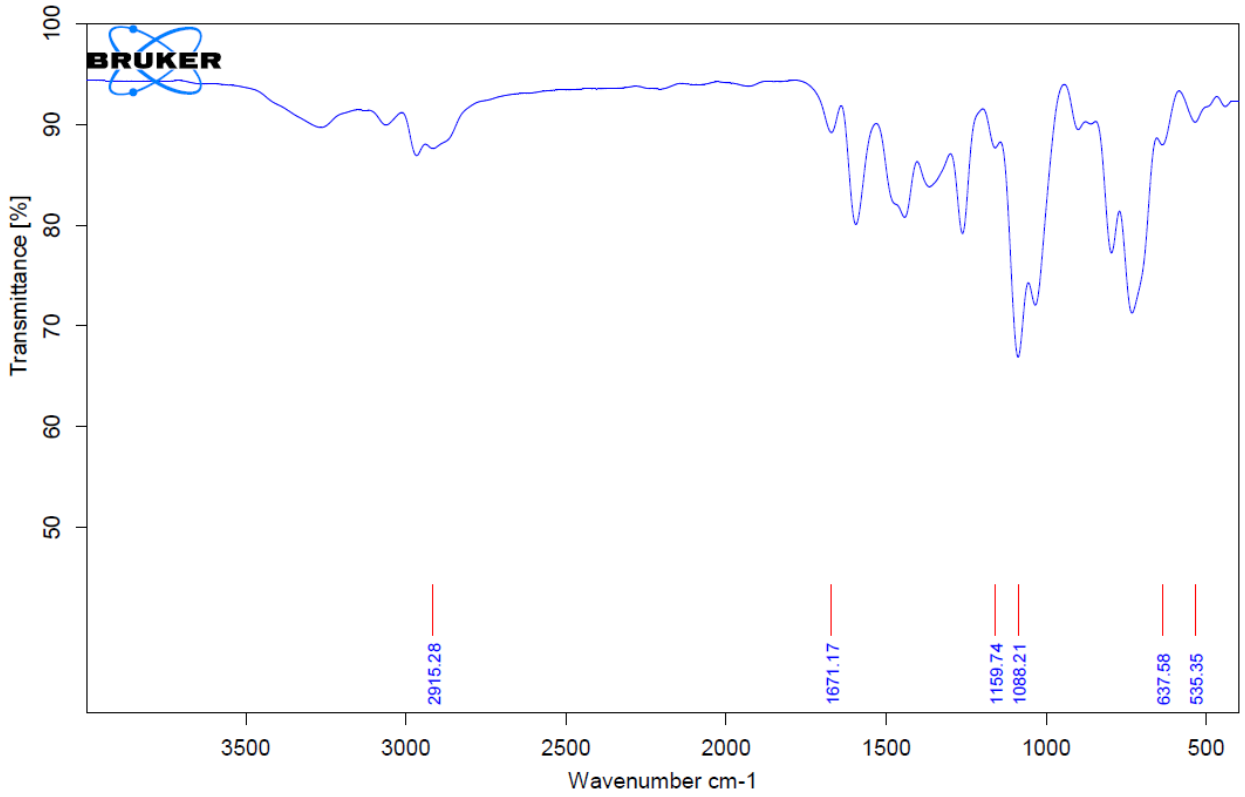
BRUKER
Transmittance [%]
100
90
80
70
60
50
2915.28
1671.17
1159.74
1088.21
637.58
535.35
3500
3000
2500
2000
1500
1000
500
Wavenumber cm-1

tert-butyl 2-(3-bromophenyl)-1H-imidazole-1-carboxylate (3.19)

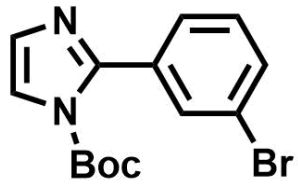

^{1}H NMR

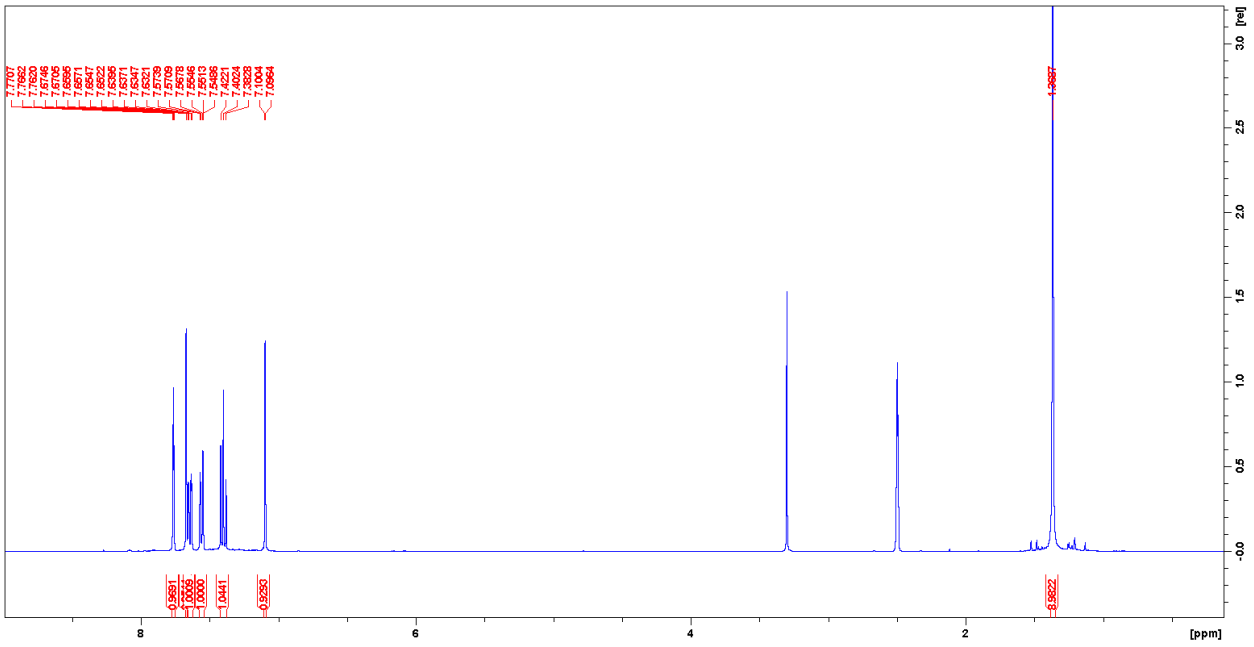

^{13}C NMR

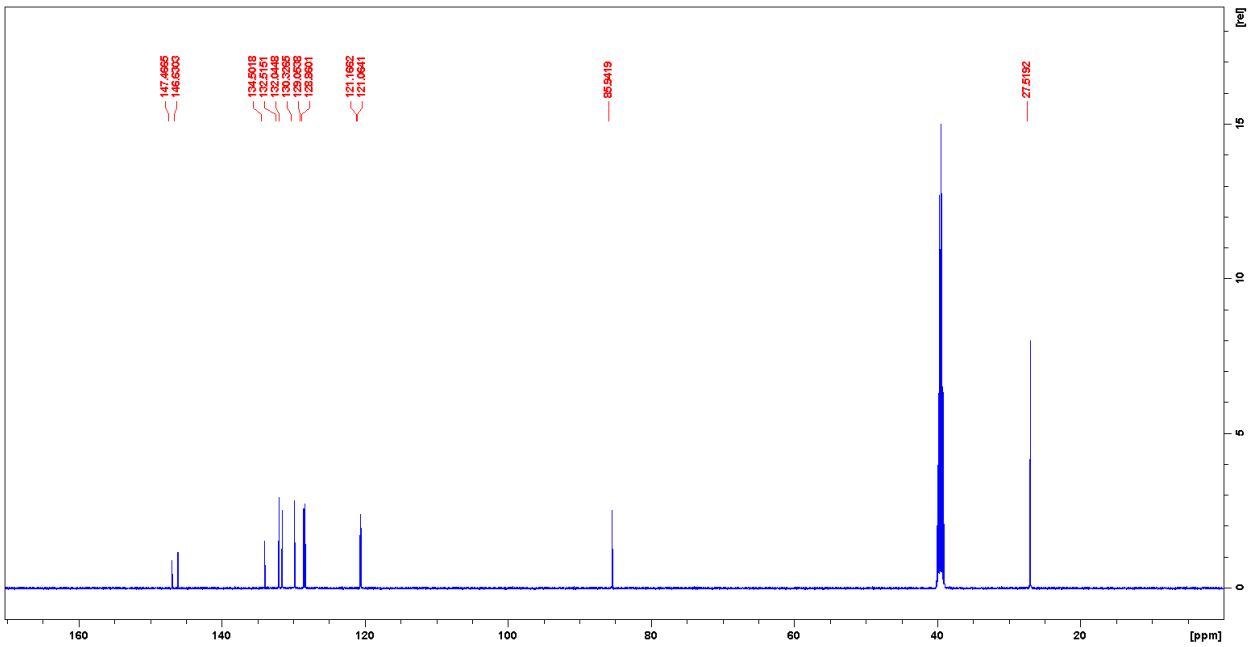

HRMS (ESI)

Elemental Composition Report **Page 1**

Single Mass Analysis
Tolerance = 5.0 PPM / DBE: min = -1.5, max = 50.0
Element prediction: Off
Number of isotope peaks used for i-FIT = 3

Monoisotopic Mass, Even Electron Ions
267 formula(e) evaluated with 1 results within limits (up to 50 closest results for each mass)
Elements Used:
C: 0-50 H: 0-100 N: 0-10 O: 0-10 Br: 1-1

SMM_01_083 100 (1.708)
TOF MS ES+

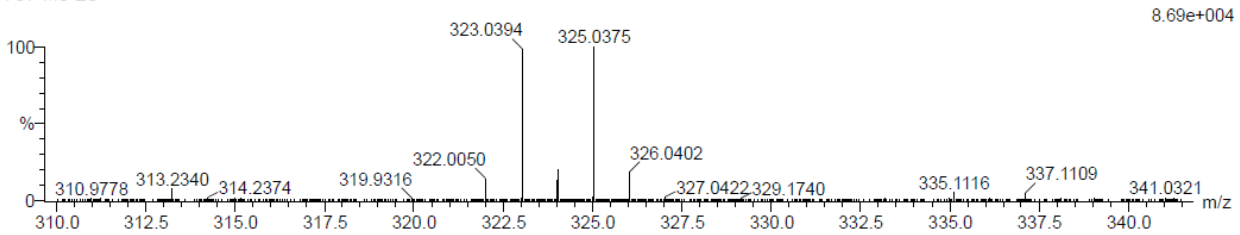

Minimum:				-1.5				
Maximum:		5.0	5.0	50.0				
Mass	Calc. Mass	mDa	PPM	DBE	i-FIT	Norm	Conf(%)	Formula
323.0394	323.0395	-0.1	-0.3	7.5	733.9	n/a	n/a	C14 H16 N2 O2 Br

FTIR

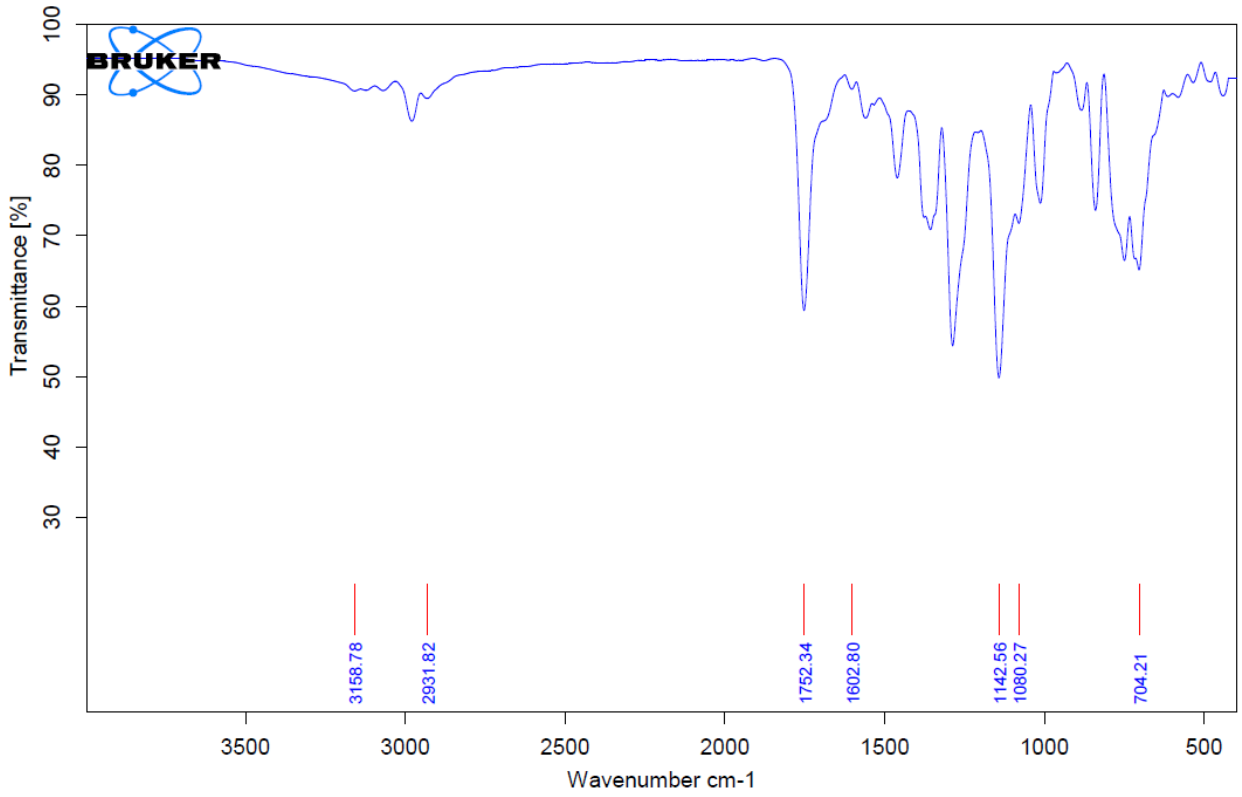
BRUKER
Transmittance [%]
100
90
80
70
60
50
40
30
3158.78
2931.82
1752.34
1602.80
1142.56
1080.27
704.21
3500
3000
2500
2000
1500
1000
500
Wavenumber cm-1

2-(3-bromophenyl)-1-trityl-1H-imidazole (3.20)

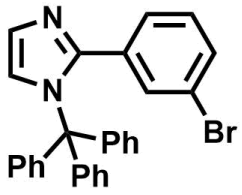

^{1}H NMR

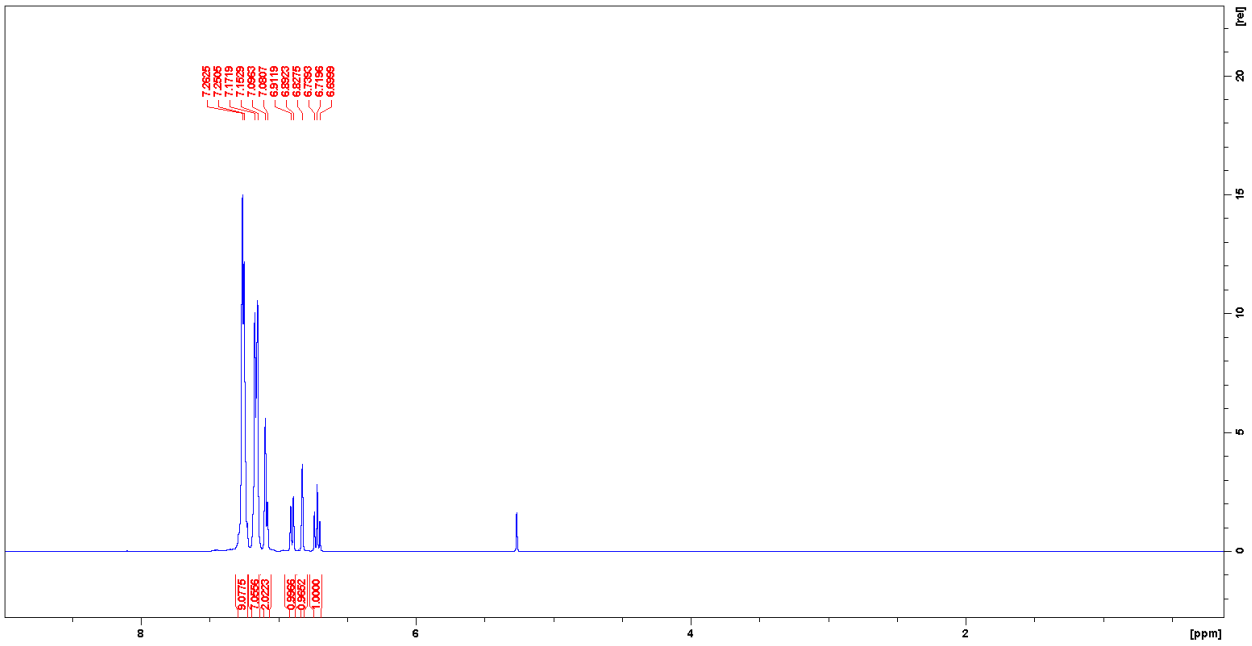

^{13}C NMR

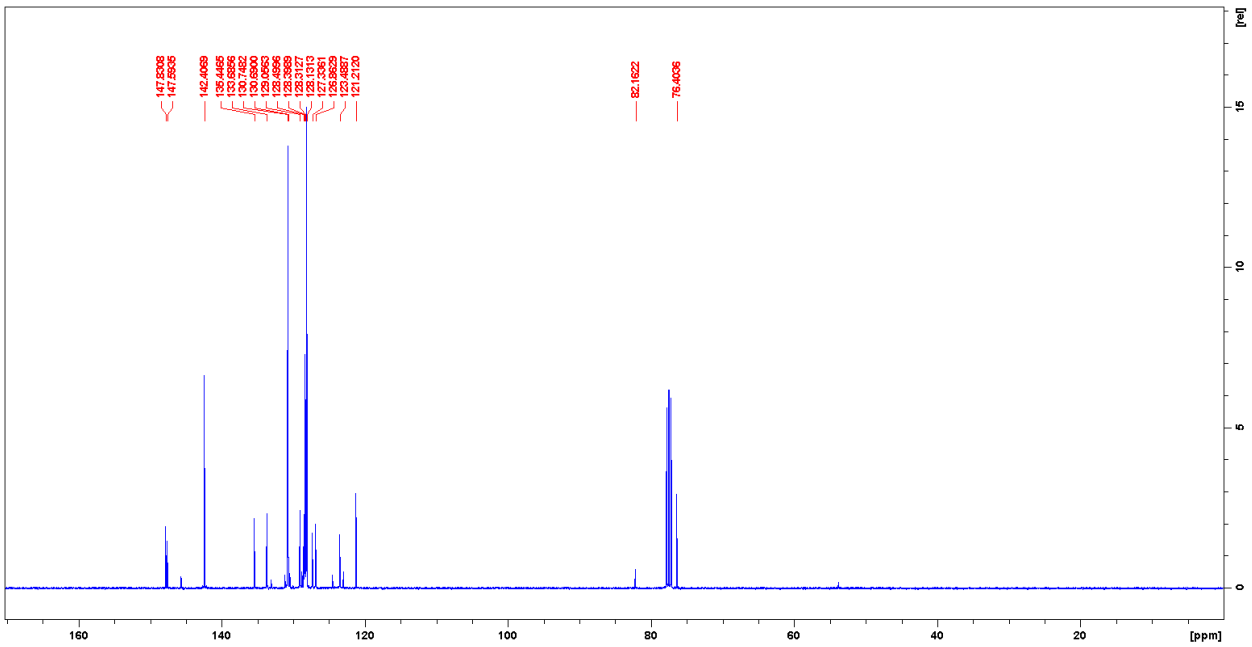

HRMS (ESI)

Elemental Composition Report **Page 1**

Single Mass Analysis
Tolerance = 5.0 PPM / DBE: min = -1.5, max = 50.0
Element prediction: Off
Number of isotope peaks used for i-FIT = 3

Monoisotopic Mass, Even Electron Ions
54 formula(e) evaluated with 1 results within limits (up to 50 closest results for each mass)
Elements Used:
C: 0-50 H: 0-100 N: 0-10 Br: 1-1

SMM_01_100 83 (1.420)
TOF MS ES+

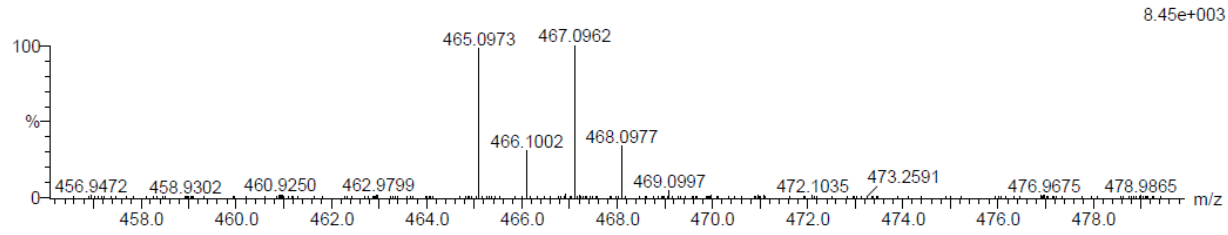

Minimum:				-1.5				
Maximum:		5.0	5.0	50.0				
Mass	Calc. Mass	mDa	PPM	DBE	i-FIT	Norm	Conf(%)	Formula
465.0973	465.0966	0.7	1.5	18.5	193.6	n/a	n/a	C28 H22 N2 Br

FTIR

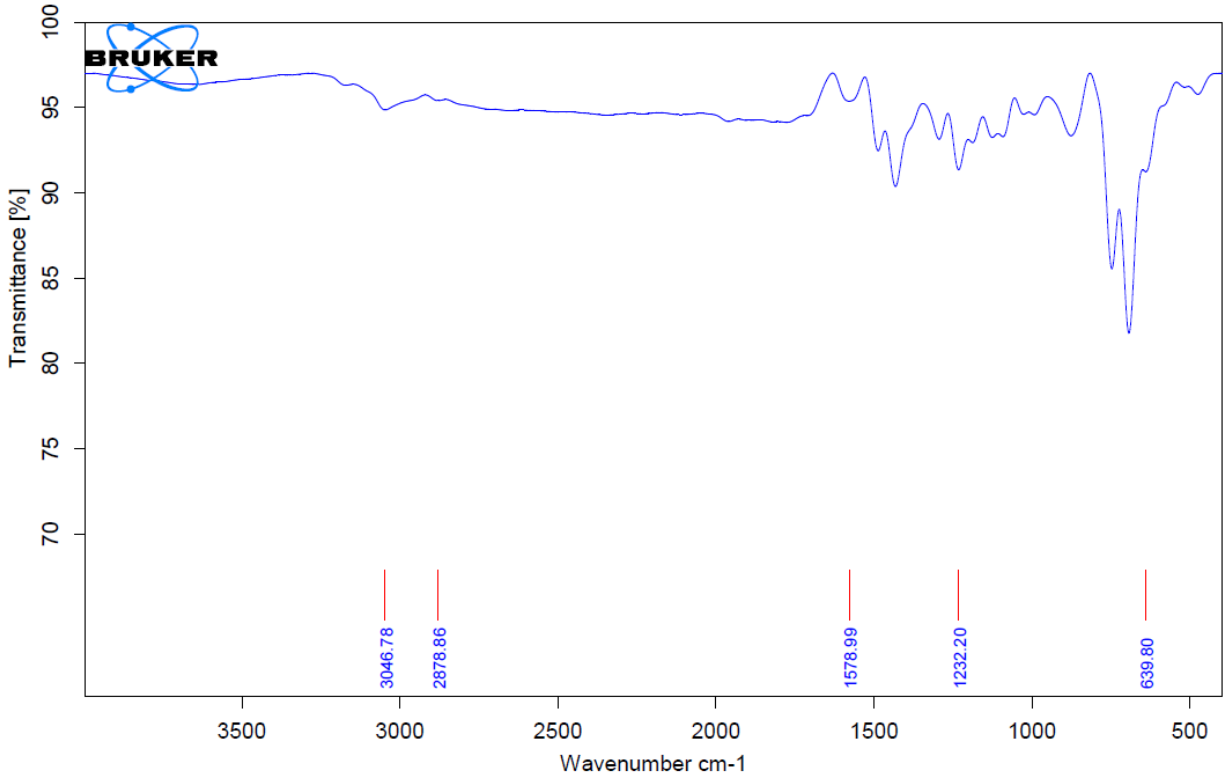
BRUKER
Transmittance [%]
100
95
90
85
80
75
70
3046.78
2878.86
1578.99
1232.20
639.80
3500
3000
2500
2000
1500
1000
500
Wavenumber cm-1

2-(3-bromophenyl)-1H-imidazole

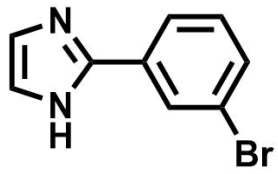

^{1}H NMR

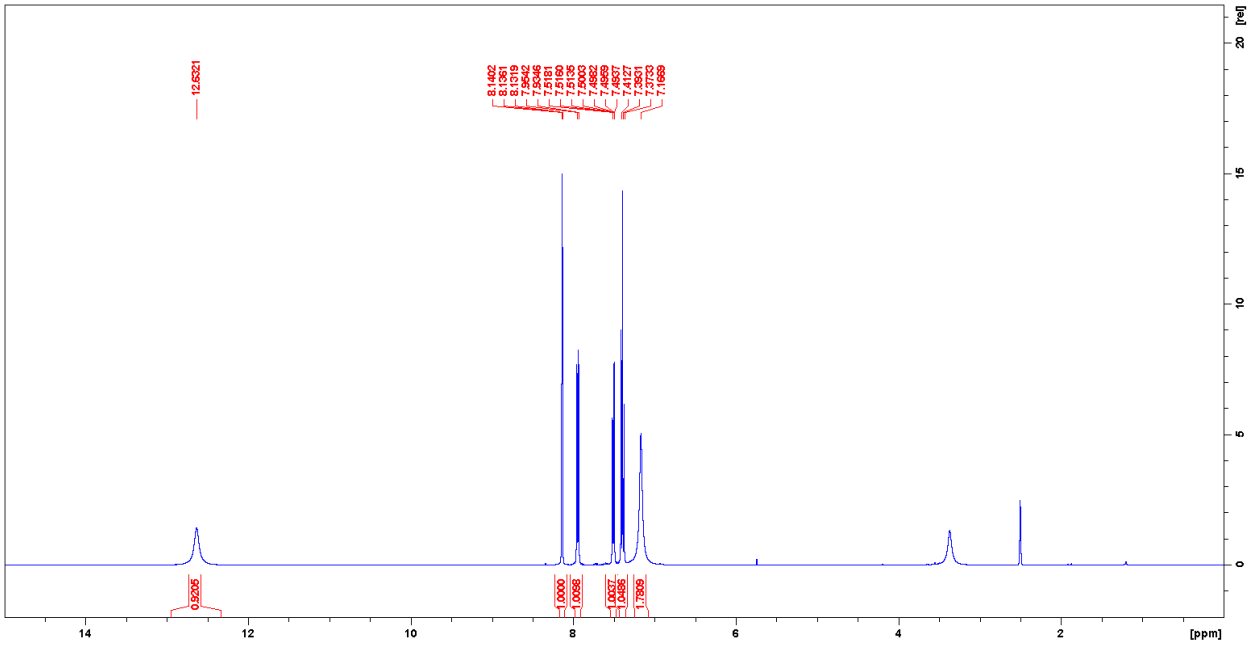

^{13}C NMR

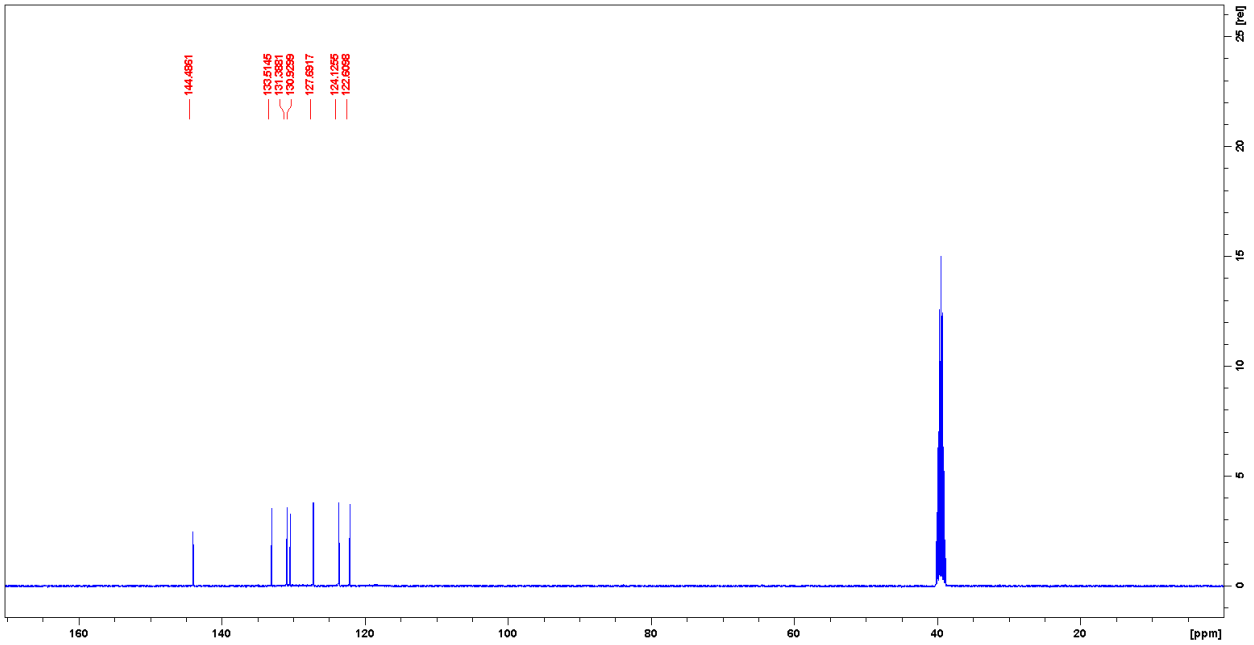

HRMS (ESI)

Elemental Composition Report **Page 1**

Single Mass Analysis
Tolerance = 5.0 PPM / DBE: min = -1.5, max = 50.0
Element prediction: Off
Number of isotope peaks used for i-FIT = 3

Monoisotopic Mass, Even Electron Ions
7 formula(e) evaluated with 1 results within limits (up to 50 closest results for each mass)
Elements Used:
C: 5-10 H: 5-10 N: 0-5 Br: 0-1

Sean
SMM_01_076 9 (0.222) AM (Top,4, Ar,10000.0,0.00,0.00); Cm (1:96)
1: TOF MS ES-
2.71e+007

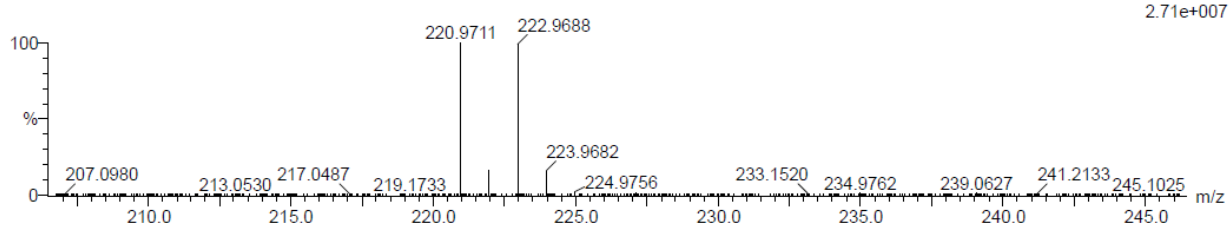

Minimum:				-1.5				
Maximum:		5.0	5.0	50.0				
Mass	Calc. Mass	mDa	PPM	DBE	i-FIT	Norm	Conf(%)	Formula
220.9711	220.9714	-0.3	-1.4	7.5	739.9	n/a	n/a	C9 H6 N2 Br

FTIR

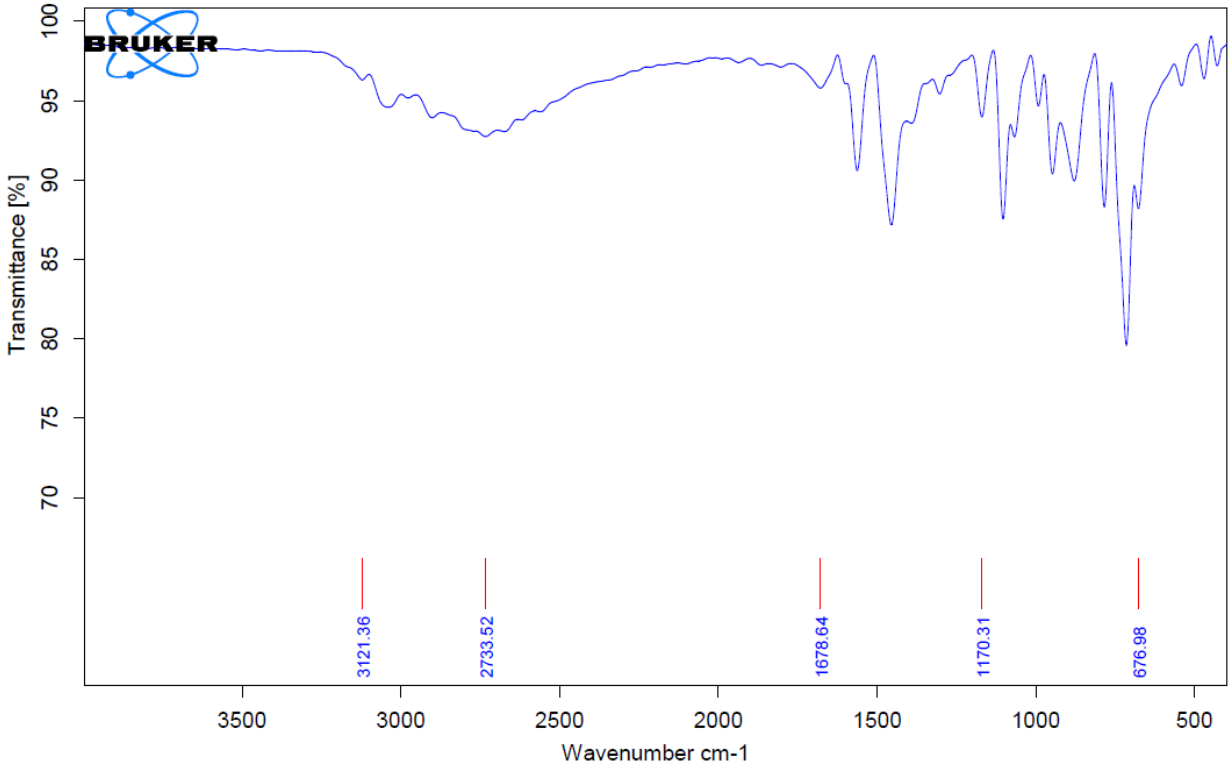
BRUKER
Transmittance [%]
100
95
90
85
80
75
70
3121.36
2733.52
1678.64
1170.31
676.98
3500
3000
2500
2000
1500
1000
500
Wavenumber cm-1

1-benzyl-2-(3-bromophenyl)-1H-imidazole (3.17)

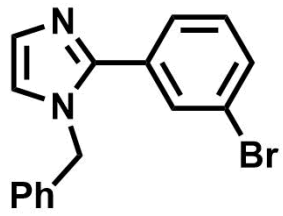

^{1}H NMR

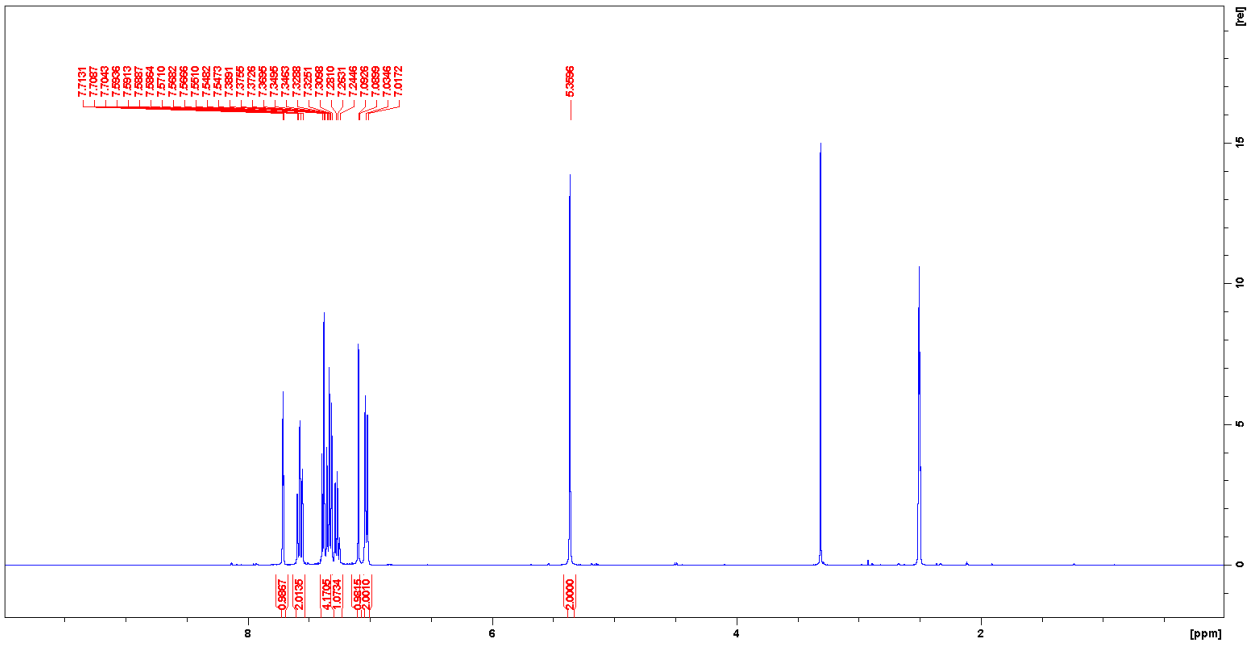

^{13}C NMR

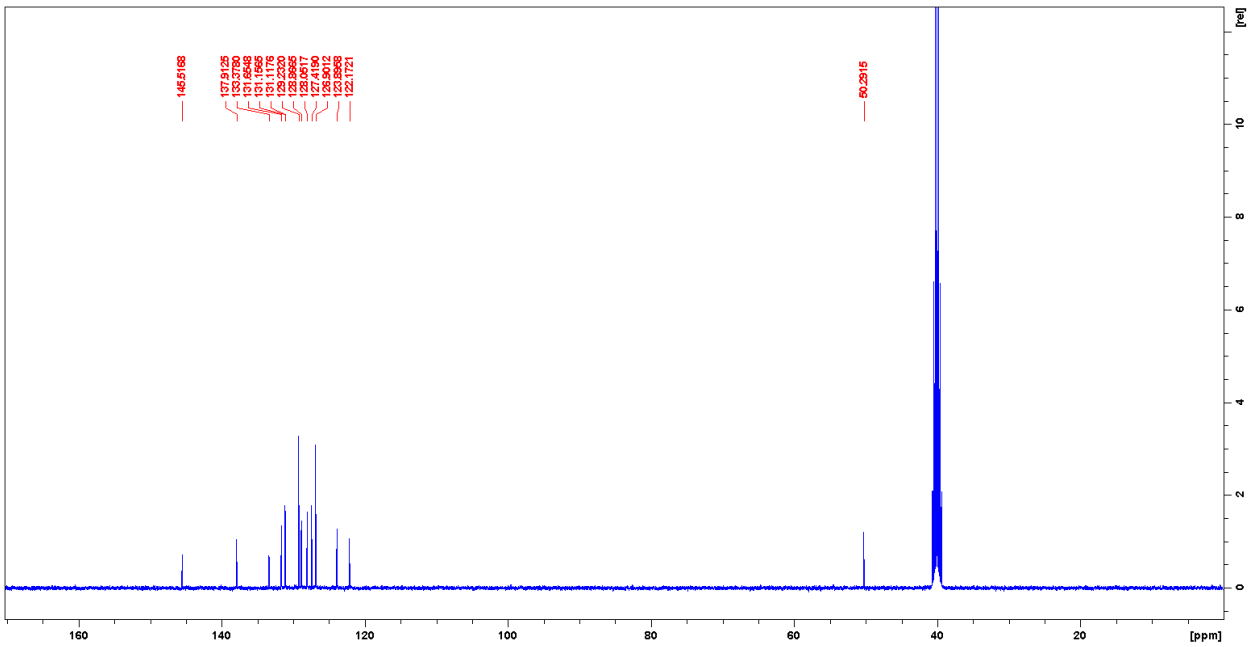

HRMS (ESI)

Elemental Composition Report **Page 1**

Single Mass Analysis
Tolerance = 5.0 PPM / DBE: min = -1.5, max = 50.0
Element prediction: Off
Number of isotope peaks used for i-FIT = 3

Monoisotopic Mass, Even Electron Ions
6 formula(e) evaluated with 1 results within limits (up to 50 closest results for each mass)
Elements Used:
C: 15-20 H: 10-15 N: 0-5 Br: 0-1

Sean
SMM_01_075 1 (0.060) AM (Top,4, Ar,10000.0,556.28,0.00); Cm (1:96)

1: TOF MS ES+
7.58e+006

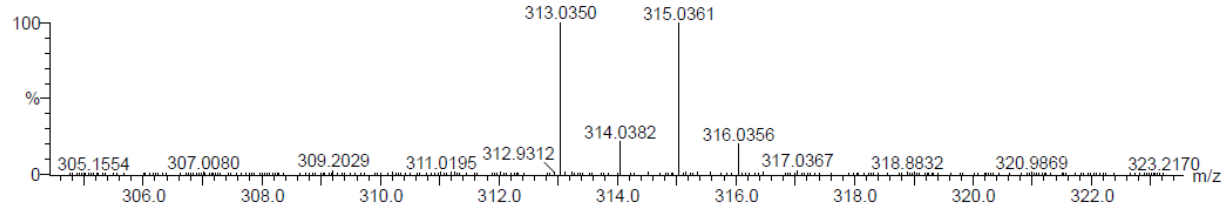

Minimum:				-1.5				
Maximum:		5.0	5.0	50.0				
Mass	Calc. Mass	mDa	PPM	DBE	i-FIT	Norm	Conf(%)	Formula
313.0350	313.0340	1.0	3.2	10.5	540.3	n/a	n/a	C16 H14 N2 Br

FTIR

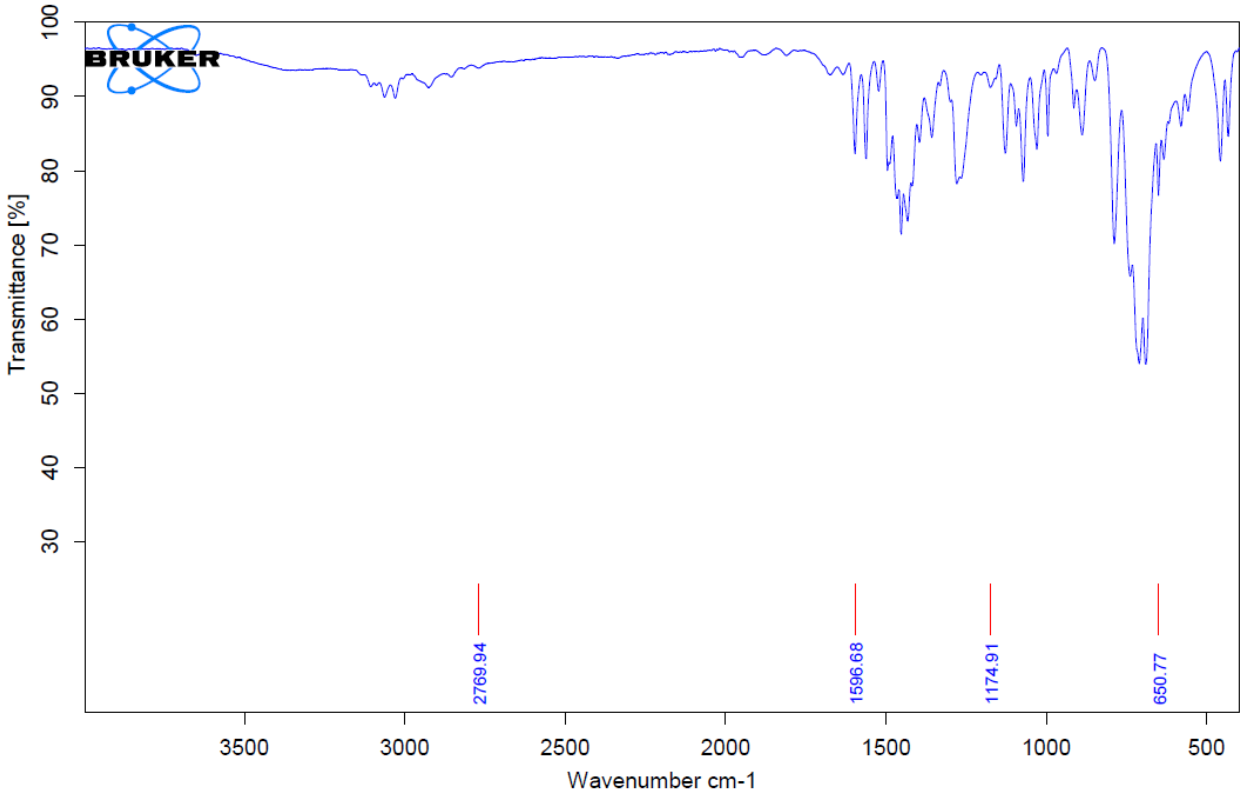
BRUKER
Transmittance [%]
100
90
80
70
60
50
40
30
2769.94
1596.68
1174.91
650.77
3500
3000
2500
2000
1500
1000
500
Wavenumber cm-1

dppf-$PdCl_2$ (3.8)

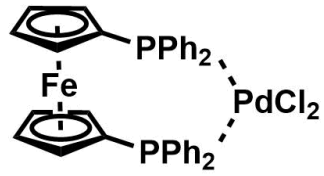

^{1}H NMR

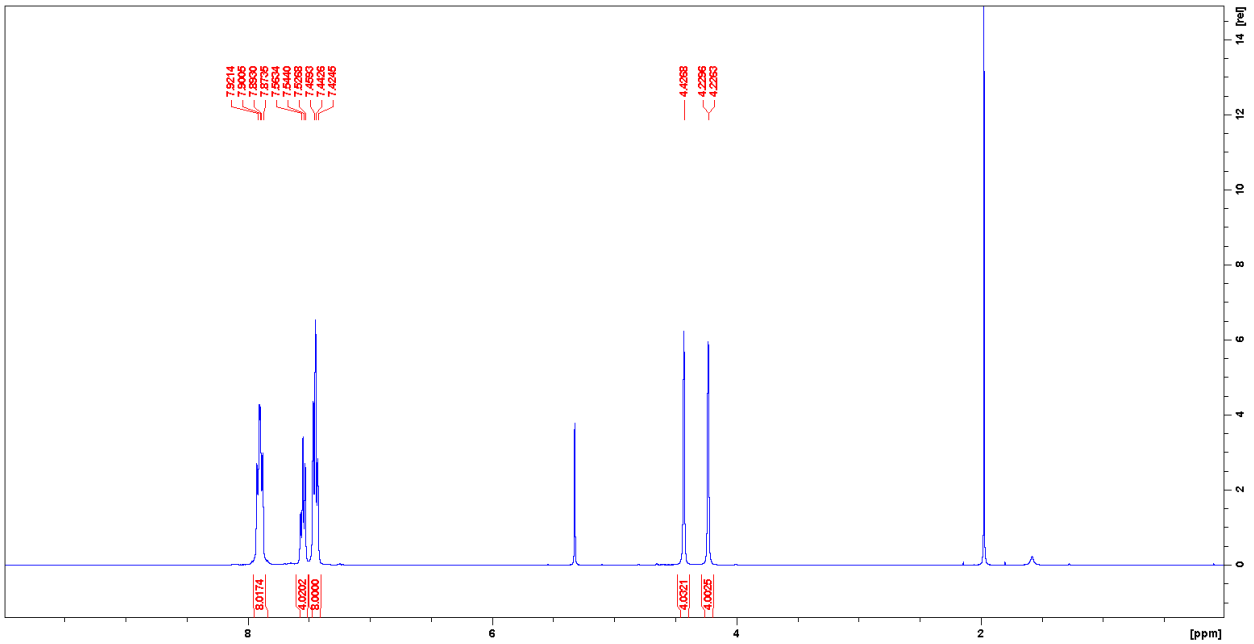

^{35}P NMR

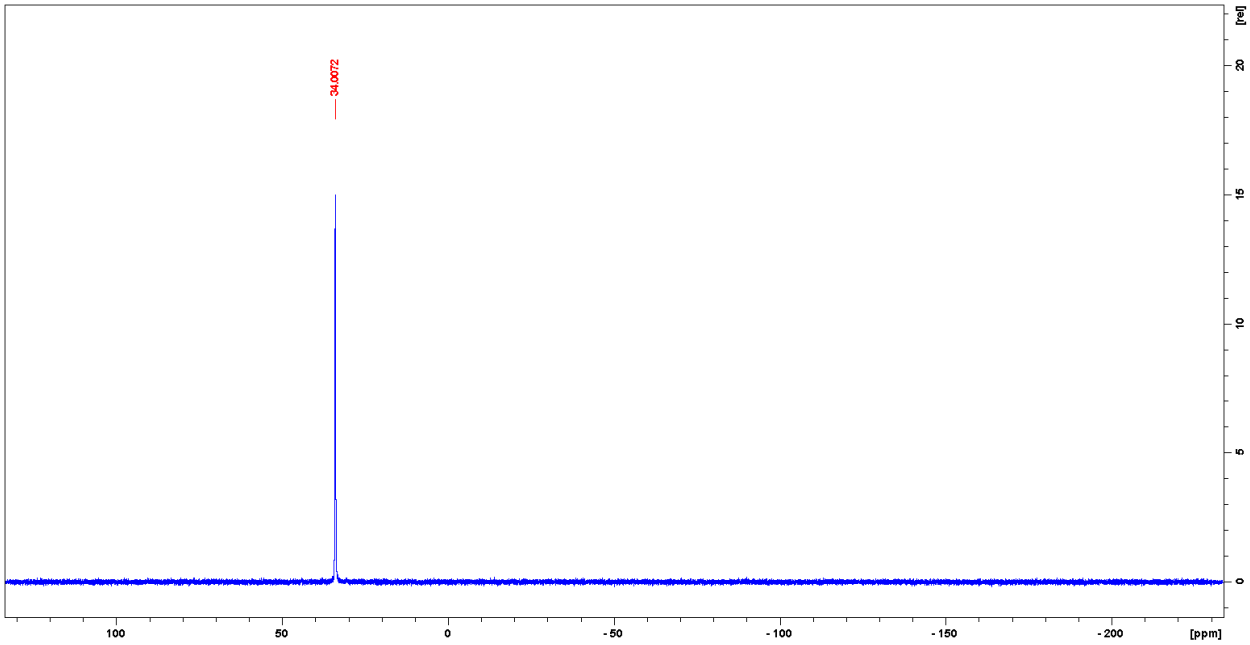
34.0072
[rel]
20
15
10
5
0
100
50
0
-50
-100
-150
-200
[ppm]

FTIR

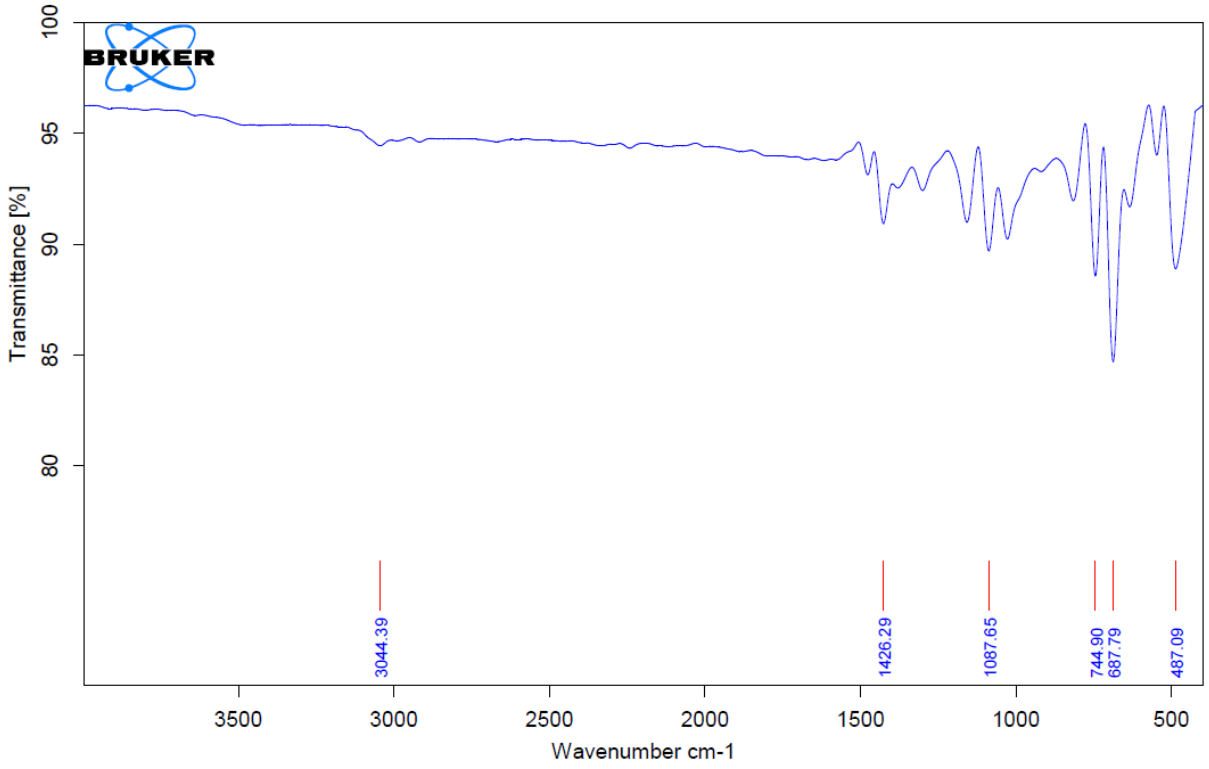
BRUKER
Transmittance [%]
100
95
90
85
80
3044.39
1426.29
1087.65
744.90
687.79
487.09
3500
3000
2500
2000
1500
1000
500
Wavenumber cm-1